An investigation into the role of TBX3 in breast carcinogenesis and its regulation by the TGF-β1 signalling pathway

by

JAROD ANG LI

Thesis presented for the Degree of

DOCTOR OF PHILOSOPHY

In the Department of Human Biology

Faculty of Health Science

UNIVERSITY OF CAPE TOWN

June 2014

DECLARATION

I, Jarod Ang Li, hereby declare that the work on which this thesis is based is my original work (except where acknowledgments indicate otherwise) and that neither the whole work nor any part of it has been, is being, or is to be submitted for another degree in this or any other University. I empower the University to reproduce for the purpose of research either the whole or any portion of the contents in any manner whatsoever.

June 2014

ACKNOWLEDGEMENTS

This thesis is dedicated to:

My supervisor Assoc. Prof. Sharon Prince
My family
The T-box lab
Sponsors
The nature

Special thanks to Deeya and Jade for proofreading

TABLE OF CONTENTS

LIST OF FIGURES AND TABLES

ABSTRACT

Cancer is the second leading cause of death among both men and women and accounts for 13% of total deaths worldwide. Enormous efforts have therefore been made to cope with this problem, but unfortunately limited success has been achieved with most of the current therapeutic strategies. The T-box family of developmentally important transcription factors plays a role in the genesis of cancer and shows much promise as a focus for targeted therapeutic approaches to treat cancer. For example, the T-box factor TBX3 is overexpressed in a number of cancers including breast cancer but the mechanism(s) responsible for this upregulation as well as the precise role of TBX3 in the progression of this disease still need to be elucidated. This study provides novel data that show that TBX3 is specifically involved in breast cancer cell proliferation and migration and that its upregulation by the TGF-β1 signalling pathway mediates the TGF-β1-regulated anti-proliferative and pro-migratory effects. Furthermore, this study demonstrates that TBX3 mediates the anti-proliferative function of TGF-β1 through repressing transcription of its homologue, TBX2, which allows for the de-repression of p21 and a G1 cell cycle arrest. The findings of the current study are of great significance as it identifies TBX3 as a potential target for the development of novel breast cancer therapeutics.

In order to ascertain the function of upregulated expression of TBX3, cell culture models were established in which TBX3 was either (1) stably silenced in an invasive breast ductal carcinoma cell line (MCF-7) which was previously shown to overexpress TBX3 or (2) overexpressed in a normal human breast epithelial cell line (MCF-12A). The resultant cells were then compared to control cells and tested for key characteristics of cancer. The data generated provide evidence that increased TBX3 levels inhibit breast epithelial cell proliferation in growth curve, BrdU incorporation and MTT assays. However, in vitro motility assays show that TBX3 may contribute to breast cancer progression by enhancing the migratory ability of these cells.

To identify the molecular mechanism(s) that upregulate TBX3 in breast epithelial cells, this study focused on the TGF-β1 signalling pathway because like TBX3, it plays an important role in mammary morphogenesis and is notoriously activated during breast cancer development. Indeed, TGF-β1 is shown to transcriptionally upregulate TBX3 protein and mRNA levels. Using luciferase reporter assays and both in vitro and in vivo DNA-binding assays this transcriptional activation is shown to be mediated by a co-operation between Smad3/4 and JunB through a Smad binding element in the *TBX3* proximal promoter. Furthermore, cell proliferation and migration assays demonstrate that TBX3 is key in mediating the anti-proliferative and pro-migratory roles of TGF-β1 in epithelial cells.

Finally, the question regarding which TBX3 target genes are responsible for its anti-proliferative effect downstream of TGF-β1 is explored. Previous data from our laboratory as well as that of others have showed that TBX2, the homologue of TBX3, functions as a pro-proliferative factor and it was hypothesized that in response to TGF-β1, TBX3 represses TBX2 in order to inhibit cell proliferation. Using luciferase reporter and DNA-binding assays, this study demonstrates that when the TGF-β1 pathway is stimulated in breast epithelial and melanoma cells, TBX2 expression is repressed through the direct binding of TBX3 to a half T-element in the *TBX2* promoter. Furthermore, using a combination of knockdown and overexpression studies and growth curve analyses the downregulation of TBX2 is shown to be required for the anti-proliferative effect of TGF-β1, primarily through allowing upregulation of p21.

Taken together, results from this study suggest that TBX3 plays an important role in the proliferation and migration of breast epithelial cells. Furthermore, this study provides compelling data that demonstrate that TBX3 is a key mediator of the anti-proliferative and pro-migratory roles of the TGF-β1 pathway. These findings are of great significance as they identify TBX3 as a potential target for the development of novel therapeutic interventions to treat breast cancer.

CHAPTER 1

LITERATURE REVIEW

1.1 Introduction

Cancer, or malignant neoplasm, is the leading cause of death worldwide and the number of cancer-related deaths is projected to double over the next 20-40 years with 26 million new cancer cases predicted to occur by 2030 (Thun *et al.*, 2010). Despite major advances in the field of cancer research, cancer continues to present a serious health problem because many cancers are not detected early and there are still no effective treatments for most cancers. To address this requires an understanding of the molecular mechanisms underpinning the disease because it will lead to the identification of early markers as well as novel targets in the development of anti-cancer therapies. At a molecular level the initiation and progression of cancer can be characterised, in part, by the deregulated expression of genes which often belong to networks of closely related signalling pathways that regulate normal cell processes. It is therefore not surprising that several components of signalling pathways including transcription factors have been identified as targets in the design of novel therapies.

Members of the T-box family of developmental transcription factors have emerged as potentially important players in the genesis of cancer. In particular, TBX2 and TBX3, play critical roles in embryonic development (Naiche *et al.*, 2005; Hoogaars *et al.*, 2007; Douglas and Papaioannou, 2013) and there is a rapidly growing body of evidence to suggest that they play key roles in the cancer process when they are overexpressed (Prince *et al.*, 2004a; Rowley *et al.*, 2004; Abrahams *et al.*, 2008; Davis *et al.*, 2008; Peres *et al.*, 2010; Mowla *et al.*, 2011; Ballim *et al.*, 2012). This review will provide a general overview of the roles and regulation of TBX2 and TBX3 in cancer genesis and will introduce key areas of research pertaining to this thesis.

1.2 The T-box gene family

The founder gene of the T-box family is Brachyury (or T) and investigations into its structure and function were seminal to the discovery of other T box genes. Brachyury was first identified in mouse in 1927 by Dobrovolskaia-Zavadskaia who observed that heterozygous mutations in the *Brachyury* gene resulted in mice with short and often kinked tails, hence the name T denoted for the gene family (Dobrovolskaia-Zavadskaia, 1927). In 1935, Chesley reported that mice with homozygous mutations of *Brachyury* die shortly after gastrulation (by embryonic day 10.5) with successfully initiated mesoderm formation of the anterior primitive streak but a complete loss of posterior mesoderm (Chesley, 1935). The main cause of this mesodermal abnormality was later found to be related to the role of Brachyury in cell adhesion and migration. Stem cells of homozygous mutant embryos showed compromised ability to migrate from the primitive streak and the accumulation of these cells eventually triggered cell death. This impaired normal mesoderm development and lead to allantois malformation which failed to connect to the chorion, thereby affecting the connection to the placenta and eventually resulting in the death of the embryo (Gluecksohn-Schoenheimer, 1938, 1944; Rashbass *et al.*, 1991; Wilson *et al.*, 1993, 1995). The T gene displays dosage sensitivity as illustrated by observations that its increased expression is required for the formation of the anteroposterior axis in the mouse embryo (MacMurray and Shin, 1988; Yanagisawa, 1990). This was confirmed by inter-crossing mice carrying an extra copy of wild-type T gene with mice carrying various T mutations (Stott *et al.*, 1993). The degree by which the tail length could be rescued directly correlated with the levels of T gene expression. The *Brachyury* gene was first cloned in 1990 and has been shown to act as a transcription factor with an N-terminal domain that confers DNA binding to a palindromic sequence T(G/C)ACACCTAGGTGTGAAATT with core sequence AGGTG (Herrmann *et al.*, 1990; Kispert *et al.*, 1995a). Two sets of alternatively arranged transactivation and repression domains have been identified in the C-terminal domain suggesting that Brachyury can function as either a transcriptional activator or repressor (Kispert *et al.*, 1995a). In 1992, the *Drosophila melanogaster omb* gene was found to encode a protein containing a 200 amino acid DNA binding sequence which was homologous to the DNA binding domain of

Brachyury (Pflugfelder *et al.*, 1992). Subsequently, Brachyury paralogues were identified in several species, including frog *Xenopus laevis* (Smith *et al.*, 1991), the zebrafish *Brachydanio rerio* (Schulte-Merker *et al.*, 1992), the chick (Kispert *et al.*, 1995b) and the ascidian *Halocynthia roretzi* (Yasuo and Satoh, 1993, 1994; Bollag *et al.*, 1994; Papaioannou and Silver, 1998). The collective name, the T-box gene family was then used to name this group of genes that encode proteins which share the highly conserved 200 amino acid core sequence. This sequence corresponds to their DNA binding domain called the T-box which is capable of recognising and binding a half-palindromic core sequence TCACACCT called the T element (Kispert and Herrmann, 1993; Kispert *et al.*, 1995a; Wilson and Conlon, 2002).

It is now well established that the T-box gene family encodes transcription factors that are highly conserved in evolution ranging from invertebrates to vertebrates (Wilson and Conlon, 2002). There are more than 50 protein members that have been assigned to the T-box gene family and 18 of them are found in humans. Genomic sequencing of a range of vertebrate and invertebrate species has suggested that the T-box gene family can be divided into five subfamilies referred to as *Brachyury*, *T-brain1*, *TBX1*, *TBX2* and *TBX6* according to their evolutionary backgrounds and expression patterns (Papaioannou, 2001; Wilson and Conlon, 2002). The *TBX2* subfamily, which includes the *TBX2*, *TBX3*, *TBX4* and *TBX5* genes, is of particular interest to this review. These genes arose from duplication and recombination of a two-gene cluster that was formed by unequal crossing over of an ancestral gene (Wilson and Conlon, 2002; Rowley *et al.*, 2004). While the DNA-binding domain of T-box proteins is located in their N-termini, their transcriptional regulatory domains are generally located in their C-termini (Tada and Smith, 2001; Wilson and Conlon, 2002; Rowley *et al.*, 2004). There is evidence to suggest that T-box proteins interact with co-factors which is anticipated to play an important role in regulating their distinct transcriptional activities on their downstream targets (Tada and Smith, 2001; Minguillon and Logan, 2003). For example, in vitro assays from different studies showed that Tbx2, Tbx5 and Tbx20 can directly interact with the cardiac homeobox protein Nkx2-5 which results in synergistic transcriptional effects (Bruneau *et*

al., 2001; Hiroi *et al.*, 2001; Habets *et al.*, 2002; Stennard *et al.*, 2005). Interestingly, recent findings have shown that while Tbx24 generally activates the zebrafish *mesp-b* gene in ripply1-deficient embryos, interaction of ripply1 with the T-domain of Tbx24 converts it into a repressor by recruiting the transcriptional co-repressor Groucho/TLE (Kawamura *et al.*, 2008).

Members of the T-box gene family are widely expressed during all stages of embryonic development ranging from gastrulation to organogenesis (Wilson and Conlon, 2002; Showell *et al.*, 2006). Consistent with this, T-box factors play critical roles in several developmental processes which are highlighted by the congenital birth defects observed when they are mutated (Naiche *et al.*, 2005). For example, the lack of TBX1 in humans leads to Di-George syndrome which is characterised by facial deformities, behavioural and learning difficulties and aplasia of the heart and thymus (Jerome and Papaioannou, 2001; Baldini, 2005). Mutations in human *TBX19* and *TBX22* give rise to adrenal insufficiency and X-linked cleft palate with ankyloglossia respectively (Braybrook *et al.*, 2001; Liu *et al.*, 2001b). Moreover, haploinsufficiency of TBX3 and TBX5 causes Ulnar-mammary syndrome (UMS) and Holt-Oram Syndrome respectively. UMS is characterised by forelimb abnormalities and malformations of the conduction system, apocrine glands, mammary glands, heart, dental and genital structures (Tada and Smith, 2001; Wilson and Conlon, 2002; Davenport *et al.*, 2003; Meneghini *et al.*, 2006; Hoogaars *et al.*, 2007; Kawakami *et al.*, 2007; Mesbah *et al.*, 2008). Patients with Holt-Oram syndrome exhibit upper limb malformations and congenital cardiac abnormalities including atrial or muscular ventricular septal defects (Basson *et al.*, 1999). Due to the focus of the current project, the following sections of this literature review will describe the structure of TBX2 and TBX3 as well as their function in embryonic development and their involvement in oncogenesis.

1.3 TBX2 and TBX3

1.3.1 Genes and proteins

As mentioned earlier, *TBX2* and *TBX3* both belong to the *TBX2* subfamily which includes the *TBX4* and *TBX5* genes that all originated from the same ancestral gene (Agulnik *et al.*, 1996). Based on branch length and locations on their phylogenetic tree, analysis reveals that *TBX2* and *TBX3* represent a cognate gene pair whereas *TBX4* and *TBX5* represent another (Agulnik *et al.*, 1996). It is proposed that at certain points along the vertebrate lineage, two gene clusters *(Tbx2/3* and *Tbx4/5*) were formed by duplicative unequal crossing over events. Each cluster then duplicated again to give rise to four separate genes, with *TBX2* and *TBX4* being located on chromosome 17q23 and *TBX3* and *TBX5* being located on chromosome 12q24 in humans (Campbell *et al.*, 1995; Agulnik *et al.*, 1996; Bamshad *et al.*, 1997). Human *TBX2* and *TBX3* share a high degree of homology with their murine counterparts. For instance, the T-box regions of the human and mouse *TBX2* gene share 90% similarity and 87% of nucleotides in the human and mouse *TBX3* cDNA sequence are identical (Law *et al.*, 1995; Bamshad *et al.*, 1997). In addition, TBX2 and TBX3 share ~95% identity in their T-box domain and ~70% identity in their N-termini. This suggests that besides having very similar DNA binding domains, they may also share functional similarities (Bamshad *et al.*, 1999).

The 3.378 kb *TBX2* transcript contains 7 exons which encodes a protein of 712 amino acids (**Fig. 1.1**). The T-box DNA binding domain is located between amino acids 106-289 in the N-terminus of the TBX2 protein. An arginine at position 122 has been shown to be conserved in all T-box proteins and is essential for DNA binding (Sinha *et al.*, 2000). Tbx2 was shown to bind the palindromic and half-site T-element as a monomer, with the four base pair GTGT motif thought to be important for binding (Carreira *et al.*, 1998; Sinha *et al.*, 2000). The structure of the *TBX3* gene is however more complex and interesting. The 743 amino acid TBX3 protein is encoded by 7 exons and an alternative splicing event in the intronic region between exons 2 and 3 of the *TBX3* gene, called exon 2a, produces a second transcript (*TBX3+2a*). Exon 2a contains an additional 60 bp, resulting in the addition of 20 amino acids to the TBX3+2a protein (**Fig. 1.2**) (Bamshad *et al.*, 1999). The

TBX3+2a transcript is otherwise identical to *TBX3*, spanning ~5.2 kb except that it gives rise to a protein with an extra 20 amino acids (LAFPSDHATWQGNYSFGTQT at 220-240) inserted into the middle of the T-box DNA binding domain (amino acids 105 – 285) (Bamshad *et al.*, 1999; Fan *et al.*, 2004). Whether this insertion disrupts the DNA-binding ability of the TBX3+2a protein or whether, compared to TBX3, it results in differential target gene regulation are unclear. Indeed, Fan et al. (2004) reported that the TBX3 and TBX3+2a isoforms have distinct cellular functions. They showed that while overexpressing TBX3 led to the immortalization of mouse embryonic fibroblast cells (MEFs), overexpression of TBX3+2a accelerated senescence in these cells. Furthermore, they demonstrated using in vitro DNA binding assays that TBX3, but not TBX3+2a, is able to bind the T-site (Fan *et al.*, 2004). While the results from the study by Fan et al. (2004) provided evidence that TBX3 and TBX3+2a are functionally distinct, this was challenged by Hoogaars et al. (2008) who showed equivalent binding affinity of these two isoforms to the consensus T-element, as well as to repress the T-site previously identified in the *Nppa* and *p21* promoter. Using transgenic mouse models they also showed that both isoforms were able to inhibit chamber differentiation during cardiac development and repress the expression of connexin 40 (Cx40) (Hoogaars *et al.*, 2008). Results from a recent study also suggest that during the maintenance of pluripotency, the two Tbx3 isoforms may both regulate *Nanog* but through different mechanisms (Zhao *et al.*, 2014). Taken together, these results suggest that the functions of TBX3 and TBX3+2a may vary depending on the specific cellular context.

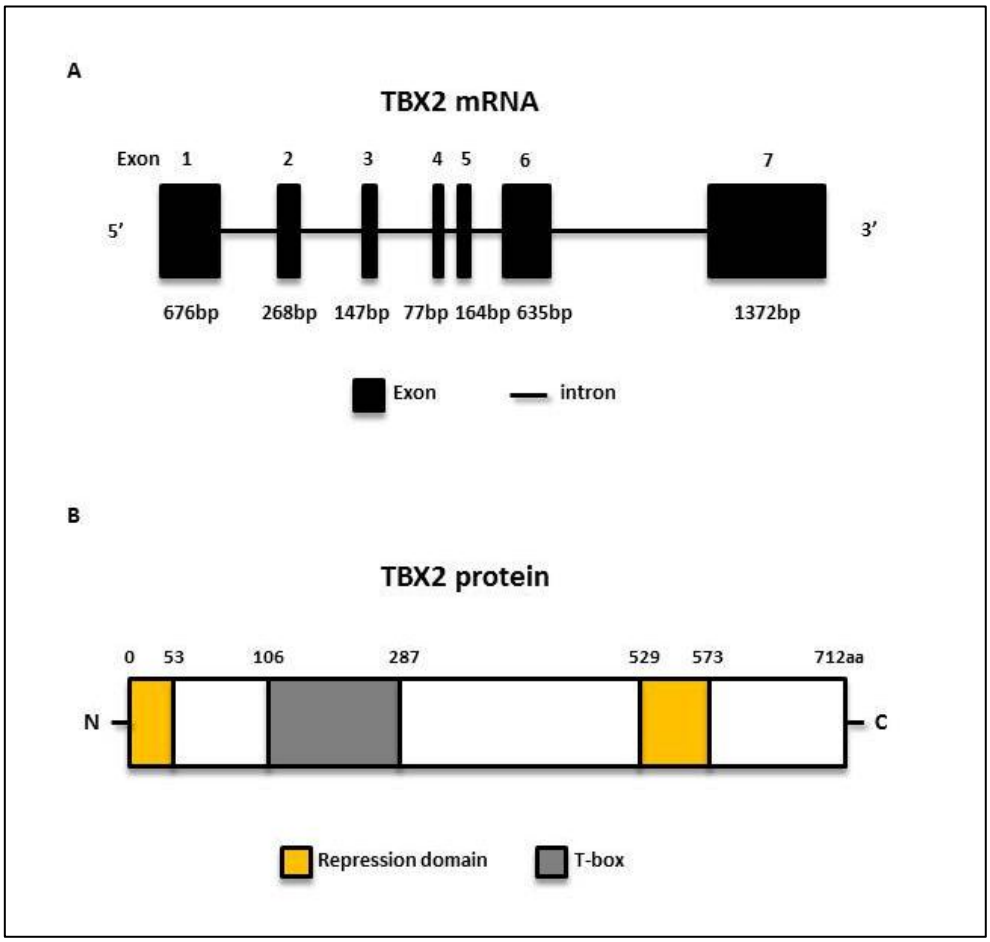

Figure 1.1 Schematic representations of human TBX2 mRNA and protein. (A) TBX2 mRNA depicting seven exons and their sizes. (B) TBX2 protein showing the two repression domains (yellow boxes) and the T-box DNA binding domain (grey box). The amino and carboxy termini are labelled N and C respectively.

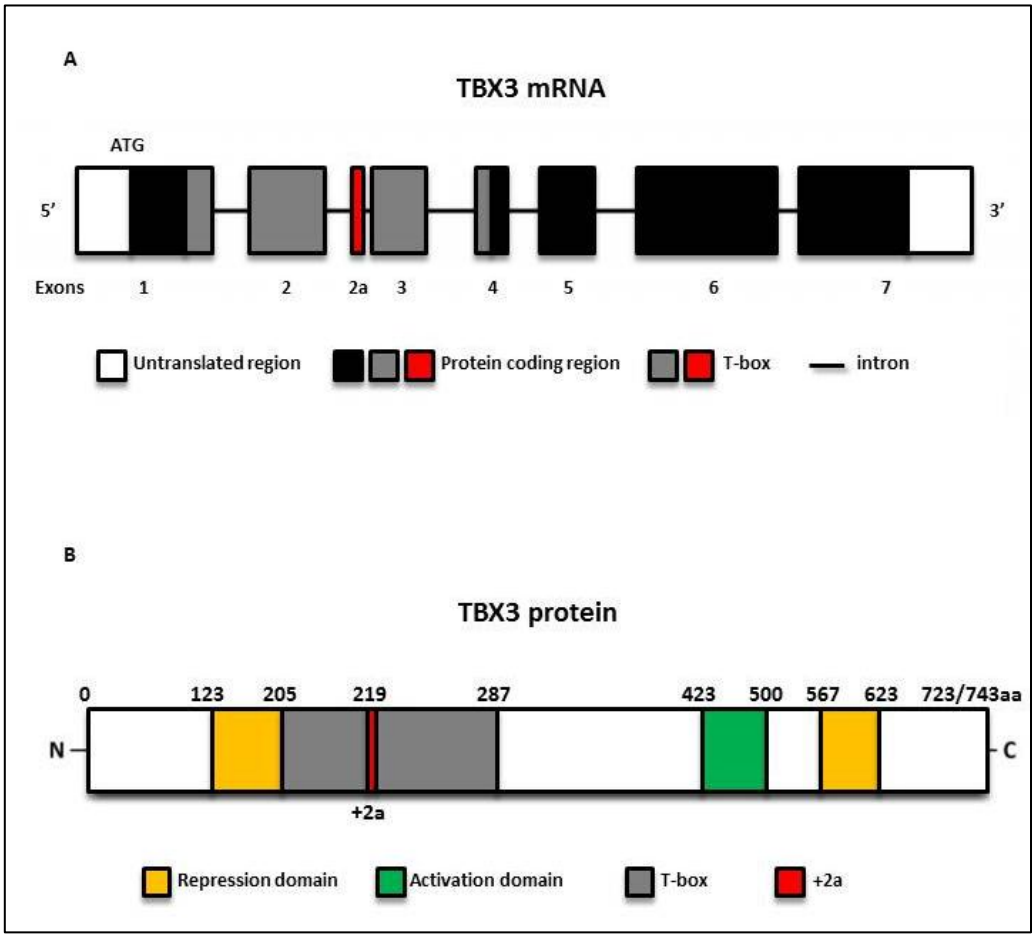

Figure 1.2 Schematic representation of human TBX3 mRNA and protein. (A) TBX3 mRNA depicting seven exons. In the TBX3+2a isoform, exon 2a is inserted in exon 2 and exon 3. (B) TBX3 protein. Repression domains (yellow boxes), T-box (grey boxes), activation domain (green box), additional 20 amino acids in TBX3+2a protein splice form (red box). The number of amino acid residues is shown under each box. The amino and carboxy termini of the protein are labelled N and C respectively.

Both TBX2 and TBX3 can bind the consensus T-element as monomers in vitro and they each contain two repression domains, one in their N-termini and one in their C-termini (Carreira *et al.*, 1998; Carlson *et al.*, 2001a; van den Boogaard *et al.*, 2012). Consistent with their high degree of homology, TBX2 and TBX3 regulate a few common targets such as the cyclin dependent kinase inhibitors $p14^{ARF}$/$p19^{ARF}$ (Jacobs *et al.*, 2000; Brummelkamp *et al.*, 2002a; Lingbeek *et al.*, 2002) and $p21^{WAF1/KIP/CIP1/SDI1/Cap20}$ (hereafter referred to as p21) (Prince *et al.*, 2004a; Hoogaars *et al.*, 2008), Nppa during heart development (Christoffels *et al.*, 2004; Hoogaars *et al.*, 2008) as well as the cell adhesion molecule E-cadherin (Rodriguez *et al.*, 2008; Wang *et al.*, 2012). There have also been reports that TBX3 represses the tumour suppressor PTEN (Burgucu *et al.*, 2012) and the

sodium channel genes Scn5a/Scn10a (van den Boogaard *et al.*, 2012) and that TBX2 transcriptionally represses the melanocyte specific enzyme, tyrosinase related protein 1 (TYRP-1) (Carreira *et al.*, 1998) and the breast tumour suppressor NDRG1 (Redmond *et al.*, 2010). These studies did not however check the effect of both TBX2 and TBX3 on these targets and therefore whether they are TBX2/3 specific is unknown. Interestingly, while TBX2 and TBX3 have been reported to function predominantly as transcriptional repressors, there is evidence to suggest that they may also function as activators. In vitro studies performed by Paxton et al. (2002) revealed that TBX2 has a weak activation domain located within its T-box region (Carlson *et al.*, 2001a; Paxton *et al.*, 2002) and a recent study confirmed that this may be physiologically relevant. Using a luciferase reporter assay Tbx2 was shown to directly activate *Tgfb2* expression through T-element binding during mouse outflow tract cushion development (Sakabe *et al.*, 2012). Carlson et al. (2001) performed experiments using a GAL4 fusion protein and mapped a putative activation domain at amino acids 423-500 of the TBX3 protein. It was only recent that this finding was shown to be physiologically relevant when TBX3 was shown to activate *Connexin43* (Boogerd *et al.*, 2011) and *Gata6* (Lu *et al.*, 2011) which are both important during heart development. Moreover, unpublished data from our laboratory show that TBX3 is able to directly bind and activate *COL1A2* and *ID1.* These findings suggest that TBX2 and TBX3 are able to function as activator or repressor but the mechanism(s) that enables them to switch between the two are unknown and deserves further investigations.

1.3.2 TBX2 and TBX3 in embryonic development

As mentioned above, there is a lot of information on the widespread expression and the important developmental roles of T-box factors during embryonic development (Reviewed by Naiche *et al*, 2005; Abrahams *et al*, 2008; Douglas & Papaioannou, 2013). The expression of both TBX2 and TBX3 has been observed in many human organs including the foetal lung and kidney, and adult kidney, heart, ovary, placenta, prostate, lung, spleen, testis and small intestine (Law *et al.*, 1995; Bamshad *et al.*, 1999). In addition, TBX3 expression has been observed in the human foetal spleen, liver and heart

as well as in adult thyroid, breast, bladder, liver, salivary gland, adrenal gland, thyroid, uterus and bladder (Bamshad *et al.*, 1999). The expression patterns of TBX2 and TBX3 in these organs may suggest that they play a role in their development and studies using mouse models have made important contributions to confirming this.

Mutations in a single copy of the human *TBX3* gene that accelerate protein decay or affects its ability to transcriptionally regulate its target genes results in Ulnar-mammary syndrome (UMS) (He *et al.*, 1999; Carlson *et al.*, 2001a; Coll *et al.*, 2002). UMS is an autosomal dominant disorder which is characterised by a range of congenital defects as described earlier (Tada and Smith, 2001; Wilson and Conlon, 2002; Davenport *et al.*, 2003; Meneghini *et al.*, 2006; Hoogaars *et al.*, 2007; Kawakami *et al.*, 2007; Mesbah *et al.*, 2008). It is worth noting that a number of tissues and organs where TBX3 is expressed are unaffected in individuals with UMS. This suggests that differential expression of TBX3 is required for different tissues which is consistent with observations that the severity of the UMS phenotype varies within and among families and depends on the degree of TBX3 deficiency (Bamshad *et al.*, 1999; Sasaki *et al.*, 2002; Wollnik *et al.*, 2002; Meneghini *et al.*, 2006; Frank *et al.*, 2013). It is however also possible that other T-box factors, for example TBX2, may compensate for TBX3 in such tissues and organs (Bamshad *et al.*, 1999). Interestingly, Frank et al. (2013) generated different truncated Tbx3 proteins and showed that in mouse models the deletion of the T-box encoding region does not necessarily lead to functionally null alleles but rather produces aberrant transcripts and proteins. The authors further suggested that as TBX3 may function as both repressor and activator, the mutant proteins that only possess one of these functional domains in the absence of the DNA binding domain may have significantly different and/or unexpected activities. UMS results in various degrees of mammary gland abnormalities from hypoplasia to complete aplasia of the mammary gland and areola (Bamshad *et al.*, 1997). Whereas no homozygous mutant patient has been identified, probably due to lethality, mouse models of UMS showed that homozygous *Tbx3* embryos have severe defects in mammary gland induction and limb development and die in utero by embryonic day (E) 11.5 (Davenport *et al.*, 2003). Unlike their human

counterparts, the heterozygous mice exhibited a relatively normal phenotype although a minor genital anomaly and ductal aplasia in mammary glands 1, 2 and 3 (MG1, MG2 and MG3) is observed in female mice (Davenport *et al.*, 2003; Jerome-Majewska *et al.*, 2005).

Frequent microdeletions of the long arm of chromosome 17 that results in haploinsufficiency of TBX2 and TBX4 have been shown to lead to a range of developmental abnormalities. This includes severe congenital microcephaly, heart defects (patent ductus arteriosis, atrial septal defects and pulmonary hypertension), mild facial dysmorphia, musculoskeletal abnormalities and anomalies of the hand and foot, particularly long, thin fingers and toes (Ballif *et al.*, 2010; Nimmakayalu *et al.*, 2011). Due to the loss of several other genes resulting from the above microdeletions, it is difficult to determine the exact impact of TBX2 deficiency on this phenotype. However, mouse Tbx2 null mutants also show a phenotype with heart defects (including abnormal formation of the atrioventricular canal and outflow tract), facial dysmorphia and digit IV duplication in the hindlimb (Harrelson *et al.*, 2004). Functional redundancy between Tbx2 and Tbx3 has been reported in Xenopus eye development (Takabatake *et al.*, 2002), in the atrioventricular canal and in mammalian secondary palate formation (Singh *et al.*, 2012). Moreover, individual loss of function of either of these proteins resulted in a delay of gastrulation movements in the Xenopus embryo (Weidgang *et al.*, 2013). It is however important to note that there are also studies that have illustrated that TBX2 and TBX3 may play distinct roles during embryogenesis. For example, mouse *Tbx2* homozygous mutant embryos display digit IV duplication in the hindlimb, whereas *Tbx3* homozygous embryos show abnormalities in digits IV and V of the forelimbs and severely reduced hindlimb development (Gibson-Brown *et al.*, 1996; Davenport *et al.*, 2003; Harrelson *et al.*, 2004).

Together, clinical reports and mouse studies from mutations in *Tbx2/TBX2* and *Tbx3/TBX3* have revealed the critical roles of TBX2 and TBX3 in, at the very least, the development of the heart, mammary glands and limbs. As the results of the current project have implications for the role and regulation of TBX3 in breast development and

cancer, the following section will focus on mammary gland development and what is known of the role of TBX2 and TBX3 in this process.

1.3.2.1 TBX2 and TBX3 in embryonic mammary gland development

Mammary gland development is a continuous biological remodelling process which begins during embryogenesis, continues after birth and through lactation and involution (Platonova *et al.*, 2007; Cowin *et al.*, 2010). Tbx2 and Tbx3 are the only members of the T-box family that have been detected in developing mammary glands (Douglas and Papaioannou, 2013). During mouse embryonic development, the first sign of mammogenesis becomes evident at E10.5 along the anteroposterior axis between fore and hind limb buds of each flank (**Fig. 1.3A**) (Veltmaat *et al.*, 2004). It is evidenced by the formation of a milk line which is an elevated bilateral ectodermal ridge and is defined by the expression of several markers in the canonical Wnt signalling pathway, especially Wnt10b (Chu *et al.*, 2004; Veltmaat *et al.*, 2004, 2006). The Wnt and fibroblast growth factor (FGF) signalling pathways, particularly FGF10, FGF8, FGFR1 and FGFR2B, play pivotal roles to induce and maintain the expression of TBX3 as early as E10.25 in a thin line overlapping the milk line (Eblaghie *et al.*, 2004a). During E10.5-E11.5, the underlying mesenchyme induces the thickened ectodermal cells along the milk line to resolve into a columnar and multilayered structure called the mammary placode (MP) (**Fig. 1.3B**) (Jerome-Majewska *et al.*, 2005). The expression of both Tbx2 and Tbx3 are detected at E10.5 in overlapping stripes along the ventro-lateral border between the developing limbs (Jerome-Majewska *et al.*, 2005). Tbx3 is one of the first markers which accumulates in the epithelium of MP1 and MP3 at E10.5 and in all 5 pairs of placodes at E11.5 and its ventral extension at this stage is antagonized by bone morphogenic protein 4 (Bmp4). Tbx2, however, remains only in the mesenchyme underlying the mammary line at E10.5 and E11.5 (Chapman *et al.*, 1996; Jerome-Majewska *et al.*, 2005; Cho *et al.*, 2006; Douglas and Papaioannou, 2013). The confined TBX3 expression, in a positive feed-back loop, induces FGF signalling, Wnt10b and its target gene *Lef1*, which later define the dorsal-ventral positioning of the milk line (Eblaghie *et al.*, 2004a; Cho *et al.*, 2006). At E12.5 and E13.5, all mammary buds express Tbx3 which seems to be critical for their

maintenance (Chapman *et al.*, 1996; Davenport *et al.*, 2003; Eblaghie *et al.*, 2004b; Jerome-Majewska *et al.*, 2005). In loss of function studies, $Tbx3^{+/-}$ mice show normal induction of all five placodes but fail to maintain the development of the three thoracic pairs of the future mammary glands. These compromised mammary glands exhibited reduced numbers of ductal trees in branching morphogenesis, especially in adult virgin females. The $Tbx3^{-/-}$ mice, however, fail to induce MPs and die during gestation due to both cardiac and yolk sac defects (Davenport *et al.*, 2003; Jerome-Majewska *et al.*, 2005; Frank *et al.*, 2012). At E18.5, both Tbx2 and Tbx3 are found in overlapping domains in the mammary mesenchyme underlying the nipple, with Tbx3 also expressed in the epithelium of the branching mammary ducts (Jerome-Majewska *et al.*, 2005). In postnatal female mammary glands, the Tbx3 transcript is detected at various stages of development including virgin, pregnancy, lactation and involution (Platonova *et al.*, 2007). The precise role(s) of TBX2 and TBX3 in late stage mammary gland development still remains elusive, as no mouse or human study has to date addressed this.

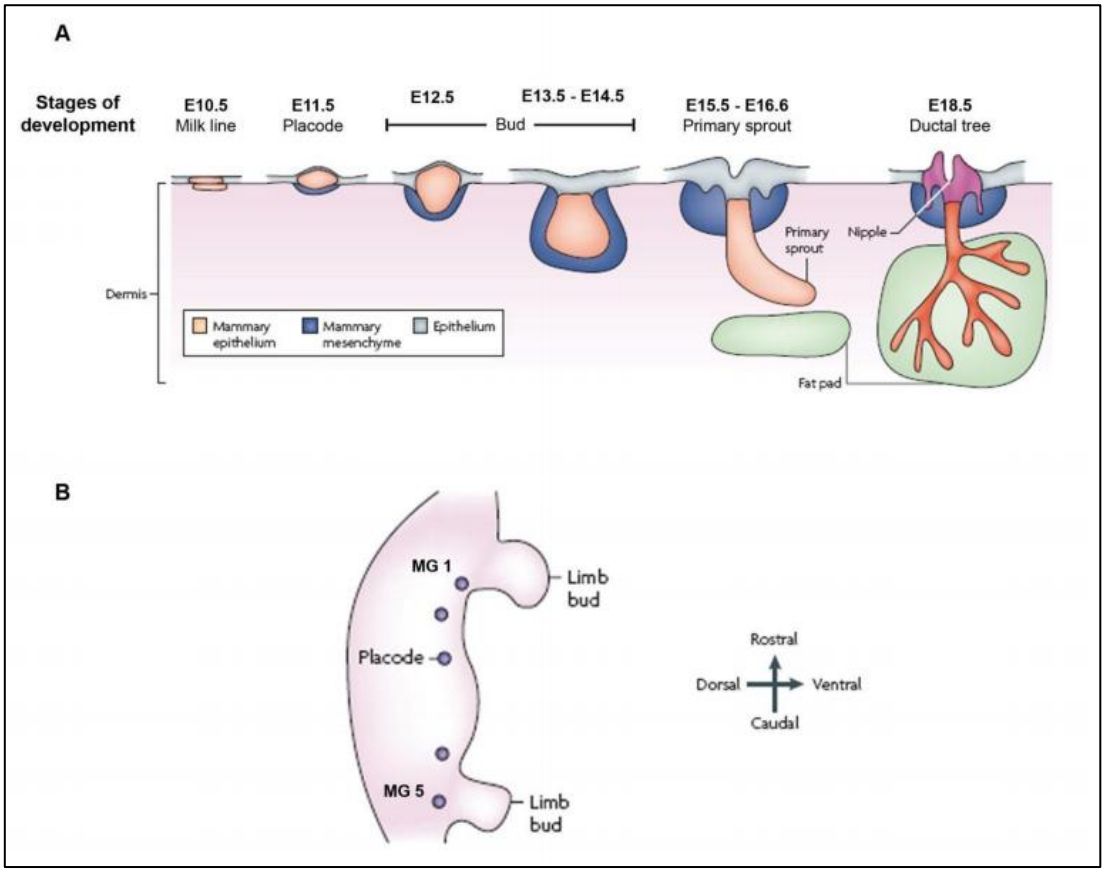

Figure 1.3 Embryonic development of the mammary glands. (A) Schematic diagram depicting the invagination of the mammary epithelium (orange) into the underlying mesenchyme (blue) and fat pad (light green) to form the embryonic rudimentary mammary glands through E10.5—E18.5. (B) Schematic depicting the position of the five mammary placodes along the lateral body wall at E11.5, with mammary gland 1 (MG1) found next to the forelimb and mammary gland 5 (MG5) next to the hindlimb on the ventral body wall of the embryo (Modified from Robinson, 2007).

While Tbx2 is expressed during mammary gland development, studies using heterozygous and homozygous mutant embryos showed no statistical differences in their mammary gland development, suggesting that Tbx2 may not be required for MP induction (Jerome-Majewska *et al.*, 2005). In comparison, Tbx3 homozygous mutant embryos failed to develop mammary buds, revealing the essential role of Tbx3 in this process (Davenport *et al.*, 2003). It is however worth noting that Tbx2, Tbx3 double heterozygotes exhibited a higher degree of ductal tree aplasia compared to the Tbx3 heterozygotes which suggests some contribution of Tbx2 to the formation of the ductal tree (Jerome-Majewska *et al.*, 2005).

1.3.2.2 TBX2 and TBX3 in embryonic stem cell biology

Pluripotent embryonic stem cells (ESCs) and induced pluripotent stem cells (iPSCs) are specialised progenitor cells which are characterised by the potential to continuously self-renew. They have the ability to maintain an undifferentiated state of pluripotency and have the potential to differentiate into all three germ layers (Hirai *et al.*, 2011). ESCs originate from the inner cell mass of the blastocyst, where Tbx3 is among the first T-box factors to be detected (Chapman *et al.*, 1996). Tbx3 has been found sufficient to maintain pluripotency of mouse ESCs (mESCs) by mediating LIF/STAT signalling (Niwa *et al.*, 2009). It also helps their reprogramming by direct binding and activation of the *OCT4* promoter and the loss of function of Tbx3 in mESCs abolishes self-renewal and induces differentiation (Han *et al.*, 2010). Moreover, levels of Tbx3 expression is highest in the undifferentiated mESCs and it blocks differentiation into mesoderm, ectoderm, trophectoderm and neural crest cells (Ivanova *et al.*, 2006; Lu *et al.*, 2011). In addition to Tbx3 playing a role as a repressor of specific cell fates, it also encourages differentiation

into extraembryonic endoderm (ExEn) by directly activating GATA6 expression (Lu *et al.*, 2011) and mediates Wnt signalling to induce a metastable primitive endoderm state that gives rise to visceral endoderm (Price *et al.*, 2013). The dual function of Tbx3 in sustaining pluripotency of undifferentiated mESC and promoting differentiation of ExEn suggests that the function of Tbx3 is intricate and may be intertwined with a number of signalling networks. In addition, Tbx3 has recently been found highly expressed in definitive endoderm progenitor cells and is involved in endoderm formation with the histone demethylase JMJD3 and EOMES (Cheng *et al.*, 2012; Kartikasari *et al.*, 2013). A recent study showed that Tbx3 directs ESC differentiation toward mesendoderm by transcriptionally regulating specific mesoderm and endoderm transcription factors (Weidgang *et al.*, 2013).

The mESCs isolated from blastocysts of the preimplanted embryo have been denoted as having a naïve state as they exhibit less 'mature' features than the 'primed' state of mouse epiblast stem cells (mEpiSC). These two sets of stem cells are distinct with respect to X chromosome inactivation and developmental potential and also differ with regard to colony morphology, growth dependent signalling and gene expression (Hanna *et al.*, 2010; Pera and Tam, 2010). Interestingly, while human ESCs (hESCs) and mESCs are both derived from the explanted blastocysts before implantation, hESCs show more biological similarities with the primed state mEpiSC. Moreover, the hESCs that have been treated with reprogramming factors to revert back to a more naïve state show higher expression of Tbx3 transcripts than the mEpiSC (Tesar *et al.*, 2007). In addition to the maintenance of the naïve state of ESCs during development, Tbx3 also improves the quality of iPSCs generated from mouse embryonic fibroblasts. With reprogramming factors Sox2, Oct4, and Klf4, it accelerates stem cell colony formation, expression of pluripotency markers and enhances germline contribution and transmission (Han *et al.*, 2010). Tbx3 can also improve the generation of porcine-induced pluripotent stem cells (piPSCs) when co-expressed with Oct4 (Pou5f1), Sox2, Klf4 and c-myc (Wang *et al.* 2013). ESCs and iPSCs sporadically enter a two-cell-like state (2C-state) that resembles the totipotent two-cell stage and expresses 2-cell genes including Zscan4, which is crucial for repair and

maintenance of telomeres and genomic stability (Macfarlan *et al.*, 2012; Surani and Tischler, 2012). Dan et al. (2013) showed that Tbx3 can activate *Zscan4* promoter activity by negatively regulating DNA methylation, suggesting a role for Tbx3 in telomere maintenance and the self-renewal of ESCs.

While there is limited information of Tbx2 in stem cell biology, microarray studies on somatic stem cell populations have revealed that Tbx2 gene expression is upregulated in hematopoietic stem cells (Park *et al.*, 2002) and the epithelial basal stem-cell like population (Rock *et al.*, 2009). However, further investigations are needed to confirm the role of Tbx2 in somatic stem cell populations.

1.3.3 TBX2 and TBX3 in cancer

In recent years, T-box factors have also been implicated in the progression of cancer. For example, Fernando et al. (2010) reported that in human pancreatic tumour cells, elevated levels of Brachyury induces epithelial-mesenchymal transition (EMT), a process allowing primary tumour cells to acquire a motile phenotype which promotes metastasis. In contrast, Brachyury can also function as a tumour suppressor as evidenced by the fact that its expression is reduced in non-small cell lung tumours compared to normal tissues due to epigenetic silencing (Park *et al.*, 2008). Similarly, T-bet (also known as TBX21) has been implicated as both a tumour promoting and tumour suppressor factor. T-bet was found overexpressed in a subset of estrogen receptor alpha positive (ERα+) breast cancers which was associated with a negative impact on sensitivity to hormonal therapy and prognosis (McCune *et al.*, 2010). In addition, a study by Stoicov et al. (2009) showed that T-bet knockout (KO) mice were protected from *Helicobacter felis*-induced gastric cancer. On the other hand, a clinicopathological study from Zhang et al. (2012) suggested a tumour suppressor role for T-bet in gastric cancers. The authors observed that the *T-bet* T-1993C polymorphism, which results in the repression of T-bet expression (Li *et al.*, 2011), correlated with increased risk of gastric cancer, especially with distant metastasis. Three other studies also revealed a tumour-suppressing role for T-bet and/or Eomes (also known as T-box brain protein 2) through a T cell-mediated adaptive

antitumour immunity (Atreya *et al.*, 2007; Zhu *et al.*, 2010; Chen *et al.*, 2013). Moreover, a tumour suppressing role has also been reported for Tbx1, TBX4 and TBX5. In many mouse skin tumours the expression of Tbx1 was found to be reduced and the re-expression of it significantly suppressed tumour growth in vivo and inhibited cell proliferation and anchorage-independent growth in cultured cells (Trempus *et al.*, 2011). Proteomic analysis in pancreatic ductal cell adenocarcinoma showed that low TBX4 expression correlates with increased metastasis and reduced patient survival rate (Qi *et al.*, 2008; Zong *et al.*, 2011). Similar to Brachyury, TBX5 has been found to be downregulated in colon cancer cell lines due to promoter methylation, and re-expression of TBX5 in these cells inhibited cell proliferation, migration and colony formation and induced apoptosis (Yu *et al.*, 2010). Importantly, the T-box factors most frequently implicated in carcinogenesis are TBX2 and TBX3, and so the rest of this review will examine the role of these two transcription factors in cancer.

In the last decade, the abnormal expression of TBX2 and TBX3 has been associated with a growing list of cancers including breast (Jacobs *et al.*, 2000; Sinclair *et al.*, 2002; Fan *et al.*, 2004; Yarosh *et al.*, 2008; Fillmore *et al.*, 2010), pancreatic (Mahlamäki *et al.*, 2002; Hansel *et al.*, 2004; Duo *et al.*, 2009), liver (Renard *et al.*, 2007), ovarian (Lomnytska *et al.*, 2006), gastric (Yamashita *et al.*, 2006), endometrial adenocarcinoma (Liu *et al.*, 2010), glioblastomas (Etcheverry *et al.*, 2010), colorectal (Han *et al.*, 2013), uterine cervical (Lyng *et al.*, 2006), bladder (Ito *et al.*, 2005; Kandimalla *et al.*, 2012) and melanoma (Hoek *et al.*, 2004; Vance *et al.*, 2005; Rodriguez *et al.*, 2008). Relevant to this thesis, *TBX2* is located on chromosome 17q22–q24, a region that is frequently amplified in many cancers including BRCA1/2-associated breast tumours (Bärlund *et al.*, 2000; Jacobs *et al.*, 2000; Sinclair *et al.*, 2002; Adem *et al.*, 2004) and of the many cancer types in which TBX3 is overexpressed, it has been most extensively assessed in cultured breast cancer subtypes and patient samples (Fan *et al.*, 2004; Lomnytska *et al.*, 2006; Yarosh *et al.*, 2008; Stephens *et al.*, 2012).

1.3.3.1 TBX2 and TBX3 in senescence, proliferation and apoptosis

Three early studies suggested that both TBX2 and TBX3 may directly contribute to cancer progression by showing that they are able to immortalize mouse embryonic fibroblasts (MEFs) and ST.*Hdh*^{Q111} striatal cells by bypassing senescence, one of the critical self-protection mechanisms against cancer (Jacobs *et al.*, 2000; Carlson *et al.*, 2001a; Brummelkamp *et al.*, 2002a; Hanahan and Weinberg, 2011). These groups and others further showed that the anti-senescence effect is due to TBX2 and TBX3 directly repressing mouse *p19*^{ARF} and human *p14*^{ARF} through a variant T-site in their initiators (Jacobs *et al.*, 2000; Carlson *et al.*, 2001a; Brummelkamp *et al.*, 2002a; Lingbeek *et al.*, 2002). The anti-senescence function of TBX2 was further investigated by Prince et al. (2004) and they found that the overexpression of TBX2 bypassed cell senescence in ST.*Hdh*^{Q111} striatal cells by binding and repressing the cyclin-dependent kinase inhibitor *p21* promoter via a T-element in its initiator region (Prince *et al.*, 2004a). In addition, the role of TBX2 in transformed cells was first investigated by Vance et al. (2005) who demonstrated that TBX2 is overexpressed in many melanoma cell lines. The authors further showed that high TBX2 levels maintain a high proliferation rate and allow these cells to escape senescence by repressing p21 in association with histone deacetylase 1 (HDAC1). Their data was further validated by inducibly expressing a dominant-negative Tbx2 in B16 mouse melanoma cells that led to senescence and elevated levels of p21 (Vance *et al.*, 2005). The anti-senescence effect of TBX2 has also been observed in human vertical growth phase melanoma when TBX2 expression was silenced by a shRNA approach (Peres *et al.*, 2010). In contrast, however, no anti-senescence function of TBX3 has yet been shown in transformed cells. Furthermore, whether TBX2 and TBX3 have distinct cell type-specific roles in regulating proliferation in transformed epithelial cells is not known.

In line with the pro-proliferative role of TBX2 in mouse and human melanoma cells, Peres et al. (2010) showed that the knockdown of TBX2 significantly reduced cell proliferation in the 501mel metastatic melanoma cell line (Vance *et al.*, 2005; Peres *et al.*, 2010). MCF-7 breast cancer cells also require TBX2 to drive proliferation (Peres et al., 2010;

Redmond *et al*, 2010) which was shown to result from TBX2 interacting with early growth response 1 (EGR1) to target and repress *N-myc downregulated gene 1* (*NDRG1*), a breast tumour suppressor. Some studies also suggest that Pax3 and Mitf, two potent pro-proliferative factors in melanomas upstream of TBX2, may activate TBX2 to promote cell proliferation (Carreira *et al.*, 2000, 2006; Liu *et al.*, 2013). There is also evidence that TBX3 may function to promote cell proliferation. For example, Ito et al. (2005) showed that reducing Tbx3 expression by an anti-sense approach in rat bladder carcinoma cells slowed down proliferation of these cells. Moreover, TBX3 was identified in an array-based search to be downstream of Wnt/β-catenin, a growth promoter, in the human hepatoma cell line HepG2 (Renard *et al.*, 2007). In the same study the authors employed a dnTBX3 approach and showed that TBX3 promotes cell proliferation of these cells. In contrast, silencing TBX3 was reported to increase cell proliferation in vertical growth phase (VGP) melanoma, metastatic melanoma and breast cancer cells suggesting an anti-proliferative role of TBX3 in transformed epithelial cells (Peres *et al.*, 2010). In summary, while there is consistent data supporting a role for TBX2 as a pro-proliferative factor, the data for TBX3 suggests that its role in proliferation may be cell-type and/or cell-context dependent.

In addition to the role of TBX2 in promoting cell proliferation, Davis et al. (2008) reported that ectopic expression of TBX2 in transformed fibroblasts and murine melanoma cells with low endogenous TBX2 levels induced several key features of genomic instability such as chromosome missegregation, chromosomal rearrangements and polyploidy. During cancer progression, tumour cells gradually acquire functional capabilities to enable them to survive, proliferate, invade and disseminate. The development of genomic instability is therefore critically important because it allows tumour cells to generate random mutations enabling them to adapt to unfavourable conditions (Hanahan and Weinberg, 2011). Davis et al. (2008) also demonstrated that the TBX2 overexpressing cells become more resistant to cisplatin treatment, a widely used chemotherapeutic agent. The cisplatin resistance conferred by endogenous overexpression of TBX2 in TBX2-driven cancers was soon confirmed by Wansleben et al.

(2013). The authors revealed a mechanism by which this occurs by showing that knocking down TBX2 sensitises the cells to cisplatin by disrupting the ATM-CHK2-p53 signalling pathway. Another study by Ismail & Bateman (2009) also reported that ectopic TBX2 expression in the p53-negative SW13 adrenocortical carcinoma cell line increased resistance to apoptotic stimuli, including doxorubicin, by upregulating apoptosis inhibitor cIAP2/BIRC3 and dampening UV–irradiation induced activation of caspase 3, 8 and 9 which are key mediators of apoptosis.

There is evidence that TBX3 may also contribute to the oncogenic process and to render cells resistant to anti-cancer drugs by enabling them to evade apoptosis. For example, it was reported that elevated Tbx3 levels protected primary MEFs against oncogene Myc-induced apoptosis (Carlson *et al.*, 2002) and that knocking down Tbx3 in rat bladder carcinoma cells triggered apoptosis (Ito *et al.*, 2005). Furthermore, two other studies showed that modulating TBX3 levels impacted on p53-dependent apoptosis induced by doxorubicin, a DNA damaging agent. One group found that TBX3 is a critical downstream mediator of β-catenin survival functions in human colon carcinoma and osteosarcoma cell lines and that overexpression of TBX3 in these cells conferred resistance to doxorubicin-induced apoptosis (Renard *et al.*, 2007). Another group showed that the suppression of TBX3 by the aqueous extract of *Fructus Ligustri Lucidi* sensitized the human colorectal carcinoma, DLD-1 cells, to doxorubicin-induced apoptosis (Zhang *et al.*, 2011). Moreover, in head and neck squamous carcinoma cell lines, TBX3 was also shown to protect against anoikis, a specific type of programmed cell death which is triggered by the loss of substrate in anchorage dependent cells (Humtsoe *et al.*, 2012). Together, these studies all point to the important role of TBX2 and TBX3 in anti-cancer drug resistance and the regulation of apoptosis, however, the detailed mechanisms behind this still remains to be further elucidated.

1.3.3.2 TBX2 and TBX3 in tumour formation, invasion and metastasis

The ability of cells to proliferate in the absence of a substrate is widely accepted as an important hallmark of cancer cells and is referred to as either substrate- or anchorage-

independent growth (Carney *et al.*, 1980). Anchorage-independent growth not only allows cancer cells to grow on top of one another to form tumours but also enables them to break away from a monolayer, favouring migration and metastasis. To date, both TBX2 and TBX3 have been implicated in promoting anchorage-independent growth. Using a soft agar assay, Ismail and Bateman (2009) demonstrated that the overexpression of TBX2 confers anchorage-independence on SW13 adrenocortical carcinoma cells. Renard et al. (2007) reported that siRNA-mediated Tbx3 depletion dramatically reduced the anchorage-independent growth of hepatoma and colon carcinoma cells and that injection of cells expressing mutant Tbx3 in nude mice significantly inhibited tumour formation. Using a shRNA approach, the same oncogenic roles were observed for TBX2 and TBX3 in melanoma cells (Peres *et al.*, 2010). As mentioned above, reduced Tbx3 expression also renders cells more susceptible to suspension-induced cell death (Humtsoe *et al.*, 2012).

Invasion and metastasis are essential mechanisms by which cancer cells escape the primary tumour mass and re-locate to form distant colonies. This dissemination of tumour cells is the ultimate cause of death in 90% of cancer patients (Hanahan *et al.*, 2000). A strong correlation has been observed between TBX3 mRNA expression and breast cancer metastasis (Chen *et al.*, 2009) and TBX3 expression was shown to correlate with ERα+ tumours and metastatic recurrence (Fillmore *et al.*, 2010). In line with these findings, Rodriguez et al. (2008) reported that TBX3 promotes melanoma invasiveness in vitro as siRNA-induced TBX3 depletion significantly reduced cell migration. Moreover, two studies from our laboratory showed similar results. We demonstrated that silencing TBX3 using shRNA reduced migration in both melanoma and breast cancer cells (Peres *et al.*, 2010) and that TBX3 could mediate PMA-induced breast cancer cell migration (Mowla *et al.*, 2011). Furthermore, a recent study from Wang et al. (2012) demonstrated that silencing *TBX2* led to reduced tumour cell migration and metastatic potential and a meta-analysis of *TBX2* expression in 1107 primary human breast tumours revealed that *TBX2* is highly expressed in metaplastic breast cancers with poor prognosis and is associated with shortened recurrence-free survival.

TBX3 and TBX2 have also recently been associated with epithelial-mesenchymal transition (EMT), an emerging interesting topic. It has been widely observed that EMT plays an essential role during development and is characterised by loss of epithelial cell junctions, apical-basal polarity and the development of a fibroblast-like motile phenotype (Thiery *et al.*, 2009; Heldin *et al.*, 2012; Humtsoe *et al.*, 2012). At a molecular level EMT is associated with downregulated expression of epithelial markers such as cytokeratin and E-cadherin and increased expression of mesenchymal markers such as N-cadherin, fibronectin and vimentin (Kalluri and Weinberg, 2009). EMT occurs in response to certain signalling stimuli and during cancer progression dysregulated signalling pathways can render a more motile phenotype to cancer cells and facilitate metastasis (Klymkowsky and Savagner, 2009; Thiery *et al.*, 2009). In vivo and in vitro studies in many cancer cell types have revealed the invasion suppressive role of E-cadherin (Jawhari *et al.*, 1997; Richmond *et al.*, 1997; Karatzas *et al.*, 1999; Karayiannakis *et al.*, 2001; Joo *et al.*, 2002). In many types of epithelial-derived cancers such as breast, ovarian and non-small cell lung carcinoma, loss of E-cadherin disrupts intercellular contacts and facilitates metastasis (Sulzer *et al.*, 1998; Onder *et al.*, 2008; Rodriguez *et al.*, 2008; Sawada *et al.*, 2008). The repression of the adhesion molecule E-cadherin has therefore been suggested as one of the critical contributors in the EMT-driven cell invasion (Thiery, 2002; Thiery *et al.*, 2009; Kallergi *et al.*, 2011).

Two studies reported that high TBX3 expression observed in many melanoma cell lines and squamous carcinoma correlates with a low E-cadherin expression (Rodriguez *et al.*, 2008; Humtsoe *et al.*, 2012). A recent study showed that Tbx3 knockdown partially reduces cell invasion in squamous carcinoma cells and *TBX3* was found to be one of the strongly upregulated genes in EMT-like cells and Snail-mediated EMT, suggesting that TBX3 promotes invasion in these cells as part of the EMT process (Humtsoe *et al.*, 2012). This is consistent with the report from Rodriguez et al. (2008) who showed that Tbx3 can directly bind and repress the *E-cadherin* promoter through a T-element in its initiator. Furthermore, they showed that silencing Tbx3 leads to increased E-cadherin mRNA and protein levels and conversely, ectopic Tbx3 expression results in reduced levels of

E-cadherin. Our group also showed that the silencing of TBX3 by shRNA, significantly increased *E-cadherin* mRNA levels in VGP and metastatic melanoma cells (Peres *et al.*, 2010). Moreover, Wang et al. (2012) demonstrated that TBX2 alone is able to induce EMT, with reduced expression of epithelial markers including E-cadherin, and promotes migration and invasiveness in mammary epithelial cells. They further showed that TBX2 directly binds and represses the activity of the proximal *E-cadherin* promoter which may contribute to the pro-metastatic activities of TBX2-driven EMT in breast cancer cells (Wang *et al.*, 2012). Together, while the detailed molecular mechanisms of how TBX3 and TBX2 promote invasion and metastasis remain largely to be elucidated, these findings suggest that TBX3 and TBX2 may have crucial roles in malignant tumour progression through inducing EMT and promoting cell invasiveness and that they may both serve as novel prognostic markers.

1.3.3.3 The regulation of TBX2 and TBX3 in cancer

Since the deregulation of TBX2 and TBX3 levels has devastating consequences on normal cell function which contributes to cancer, it is very important to understand how these proteins are regulated. However, only a few signalling pathways have been identified that regulate TBX2 and TBX3 gene expression in cancers.

PKC signalling pathway

The protein kinase C (PKC) family consists of serine/threonine-specific protein kinases which promote tumourigenesis by modulating cell proliferation, migration, apoptosis and survival (Griner and Kazanietz, 2007; Marengo *et al.*, 2011). Many studies which have investigated the role of the PKC pathway have employed the phorbol ester 12-O-tetradecanoylphorbol-13-acetate (TPA, also called PMA) which activates PKC isoforms by translocating them to specific cellular compartments (Parker *et al.*, 1987; Basu *et al.*, 1990; Marengo *et al.*, 2011). Though acting through different mechanisms, both TBX2 and TBX3 have been reported to be induced by TPA in a PKC-dependent manner (Teng *et al.*, 2009; Mowla *et al.*, 2011). Teng et al. (2009) demonstrated that TBX2 is transcriptionally activated by TPA-activated PKC signalling in normal and

transformed embryonic fibroblasts. The authors show that this occurs through activation of the mitogen- and stress-activated kinase 1 (MSK1), a protein that phosphorylates histone H3, resulting in chromatin remodelling of the TBX2 promoter which enhances binding and transcriptional activation by Sp1. A study by Mowla et al. (2011) showed that activation of the TPA induced PKC signalling pathway led to the upregulation of TBX3 mRNA and protein levels via the activator protein-1 (AP-1) transcription factors c-Jun and JunB. They further show that these factors transcriptionally activate TBX3 through binding a non-consensus TPA response element. Using in vitro motility assays, this PKC regulated activation of TBX3 was shown to promote cell migration of MCF-7 human breast cancer cells, suggesting a mechanism by which TBX3 may contribute to metastasis. Taken together these studies revealed that, while TBX2 and TBX3 share a high degree of homology, they may be regulated by different mechanisms in the same signalling pathway.

PI3K signalling pathway

The phosphatidylinositol-3-kinase (PI3K) signalling pathway has also been shown to regulate both TBX2 and TBX3. This pathway has been implicated in tumourigenesis for its potent contribution to cancer cell growth, cell cycle regulation, adhesion, survival and metastasis and thus has been suggested as a drug target in the treatment of certain human cancers (Roymans and Slegers, 2001; Courtney *et al.*, 2010). Upon activation by growth factor signals, PI3K phosphorylate inositol lipids in the plasma membrane, leading to the recruitment of serine/threonine kinase Akt (also known as protein kinase B) which in turn conducts a series of downstream regulatory activities (Fry, 2001; Osaki *et al.*, 2004; Hemmings and Restuccia, 2012). TBX2 levels were shown to be upregulated in p53-negative SW13 adrenal carcinoma cells by growth factor FGF4 in a PI3K-dependent manner and this upregulation was abrogated when the phosphorylation of Akt was inhibited (Ismail and Bateman, 2009). Moreover, Niwa et al. (2009) investigated the pluripotency of mESCs and showed that TBX3 expression is positively regulated by the cytokine leukaemia inhibitory factor (LIF), an ESC self-renewal factor, via the PI3K-Akt pathway. Unpublished data from our laboratory have also demonstrated

that TBX3 is phosphorylated by AKT in advanced melanoma and that this leads to increased TBX3 protein stability, nuclear localisation, transcriptional activity and that it mediates Akt-induced melanoma cell migration.

Wnt/β-catenin signalling pathway

The Wnt/β-catenin signalling pathway serves as a critical mediator for both embryogenesis and adult tissue maintenance by regulating cell fate, proliferation and differentiation (Logan and Nusse, 2004). It is therefore not surprising that deregulated Wnt/β-catenin signalling gives rise to many human degenerative diseases and cancers, especially the promotion of liver tumourigenesis (Kondo *et al.*, 1999; Inagawa *et al.*, 2002; Thorgeirsson and Grisham, 2002; Goodall *et al.*, 2004; Logan and Nusse, 2004). The Wnt/β-catenin signalling pathway has been implicated in the activation of both TBX2 and TBX3. For example, Verhoeven et al. (2011) showed that in response to Wnt/β-catenin signalling Tbx2 is activated by the bone morphogenetic proteins 2 and 4 during heart patterning. In addition, the inhibition of β-catenin degradation by treating pancreatic cancer cells with lithium chloride induced TBX2 mRNA and protein expression (Chen *et al.*, 2008a). Moreover, an array-based search revealed that high TBX3 levels were associated with a mutant active form of β-catenin in both human and mouse hepatocellular carcinomas and human hepatoblastomas (Renard *et al.*, 2007). In the same study it was demonstrated that TBX3 can be upregulated by co-operative binding of β-catenin with its co-activator T-cell factor (Tcf) to a Tcf-binding element on the *TBX3* promoter. The authors further showed that TBX3 mediates β-catenin functions in hepatocellular carcinoma proliferation and survival.

FGF signalling pathway

The estrogen/FGF signalling pathway has been demonstrated to regulate Tbx3 expression in the expansion of breast cancer stem cells (breast CSC) (Fillmore *et al.*, 2010). This drug-resistant subpopulation of breast cancer cells, which can be isolated from primary tumours or cell culture, drives the long process of cancer progression and is usually associated with high tumour recurrence (Fillmore and Kuperwasser, 2008).

Fillmore et al. (2010) observed that oestrogen treatment of ERα+ MCF-7 cells led to Tbx3 expression being induced by paracrine FGF9/FGFR3 signalling. Their group also showed that the FGF/Tbx3 signalling is conserved in ERα− SUM149, SUM159 and BT-20 breast cancer cell lines and that the knockdown of Tbx3 mRNA in these cells significantly reduced the number of CSCs and mammosphere forming ability. These data suggest that FGF/Tbx3 signalling plays a critical role in enhancing breast cancer tumourigenesis through expanding the breast CSC population and is consistent with their findings that chemotherapy-resistant breast tumour cell lines generally have high Tbx3 levels (Fillmore *et al.*, 2010).

Retinoic acid signalling pathway

All-trans retinoic acid and its derivatives are used as anti-cancer agents and compromised retinoic acid (RA) signalling is often found early in tumourigenesis, including breast cancer (Tang and Gudas, 2011; Garattini *et al.*, 2012). Besides the regulation of TBX1 and TBX5 by RA during development, a few studies have suggested that RA may also be able to regulate TBX2 and TBX3 (Liberatore *et al.*, 2000; Boskovic and Niles, 2004; Roberts *et al.*, 2005; Ballim *et al.*, 2012; Sakabe *et al.*, 2012). For example, Boskovic & Niles (2004) showed that RA upregulated Tbx2 transcriptionally in B16 mouse melanoma cells by directly binding a degenerate retinoic acid response element (RARE) between -186 bp and -163 bp in the *Tbx2* promoter region. In contrast, a recent study revealed that during murine outflow tract development, ectopic RA expression represses Tbx2 transcription via direct binding to a highly conserved RARE located 210 bp downstream of the *Tbx2* transcriptional start site (Sakabe *et al.*, 2012). A study from our laboratory also revealed that in human melanoma cell lines RA is a direct transcriptional activator of TBX3 through its direct binding to a degenerate RARE half site at −87 bp (Ballim *et al.*, 2012). This study also showed that the RA-induced TBX3 expression correlates with decreased cell proliferation and a knockdown of TBX3 expression by a shRNA approach significantly reduced the growth-inhibitory effect of RA. Taken together these results suggest that TBX3 partly mediates the RA-regulated inhibition of cell proliferation in the human melanoma cell lines tested (Ballim *et al.*,

2012).

DNA damage stress signalling pathway

The DNA damage repair pathway is frequently altered in cancer cells and a study performed in our laboratory showed that Tbx2 mRNA and protein levels are upregulated by UVC-induced DNA damage in MCF-7 cells (Abrahams *et al.*, 2008; Bouwman and Jonkers, 2012). In response to UV treatment the p38 MAP kinase was activated and phosphorylated Tbx2 on serine residues 336, 623 and 675. This phosphorylation not only increased Tbx2 protein stability and nuclear localisation, but it also enhanced the ability of Tbx2 to repress its target gene *p21.* This may provide an explanation for how TBX2 may disrupt cell cycle control to favour tumourigenesis.

1.6 Overview of the transforming growth factor β (TGF-β) superfamily

The transforming growth factor β (TGF-β) superfamily comprises a multitude of dimeric polypeptide growth factors which have been identified in a wide variety of species including at least 30 in mammals. According to their sequence similarities and unique manner of signal transduction, these ligands are divided into two functional groups: (1) the TGF-β-like group which includes TGF-βs, Activins and Nodals and some Growth and Differentiation Factors (GDFs) and (2) the Bone Morphogenetic Proteins (BMP)-like group consisting of BMPs, most GDFs and Anti-Müllerian Hormone (AMH) (Weiss and Attisano, 2012). In humans, three isoforms of TGF-β have been described, namely TGF-β1, TGF-β2 and TGF-β3. Each isoform is encoded by a distinct but highly conserved gene in mammals, giving them unique and overlapping features in terms of spatial expression and biological functions. Besides the essential roles of the TGF-β superfamily in regulating fundamental cellular processes such as proliferation, apoptosis, adhesion and migration, they also have critical functions throughout the entire development of multicellular organisms. For example, during early development, Nodal signalling and BMP morphogen gradients have essential roles in germ layer formation, determination of the left/right axis and body patterning. In addition, several mouse studies suggest that the haploinsufficiency of TGF-β superfamily members or the malfunctioning of their

receptors in late developmental stages leads to defects in cardiac, kidney, bone, liver, gastrointestinal tract and gonad development (Affolter and Basler, 2007; Gordon and Blobe, 2008; Mizutani and Bier, 2008; Schier, 2009; Wu and Hill, 2009; Zakin and De Robertis, 2010). Disruption of TGF-β signalling is therefore detrimental to human health and mutations in mediators of this pathway have been associated with the pathogenesis of cancer and a range of autoimmune, muscle, cardiovascular and skeletal diseases (Gordon and Blobe, 2008; Moses and Barcellos-Hoff, 2011).

1.4.1 TGF-β1/Smad signalling pathway

The most well defined TGF-β1 signalling cascade is the canonical Smad signalling pathway (Feng and Derynck, 2005) (**Fig. 1.4**). On the cell surface, TGF-β1 signals through "type I" and "type II" receptors, also referred to as TGFβRI and TGFβRII respectively, which are structurally similar but differ slightly in their amino acid sequences. The complex formed by the binding of TGF-β1 to TGFβRII recruits and phosphorylates the TGFβRI, which in turn phosphorylates Smad2 and Smad3 (receptor-activated Smads, also known as R-Smads) to release them from the TGFβRI. The phosphorylated Smad2/3 can form a complex with Smad4 (common-Smad, also known as Co-Smad), and translocate to the nucleus where they bind target genes at a consensus Smad-binding-element (SBE) with the sequence 5'-GTCTAGAC-3' (Massagué *et al.*, 2005). While the TGF-β1 signalling pathway has mostly been associated with transcriptional activation there is also evidence that it transcriptionally represses target genes. Both R-Smads and Co-Smads can bind to DNA, however Smad2 has a small insert which interferes with its DNA binding β-hairpin (Shi *et al.*, 1998). Several GC-rich regions have also been identified as alternate binding sites for Smad proteins, suggesting that 'GNCN' may be a degenerate SBE. Interestingly, the affinity of Smads for a single SBE is low and most natural promoters regulated by Smads therefore possess multiple SBEs or the Smads physically interact with sequence-specific transcription factors as partners to ensure high-affinity binding (**Fig. 1.4**) (Feng and Derynck, 2005; Massagué *et al.*, 2005). Previous reports and recent chromatin immunoprecipitation (ChIP) sequencing results revealed that the diverse range of SBEs and the transcriptional outcome of Smad signalling are highly

dependent on associated spatially and temporally available co-factors (Chen *et al.*, 2008b; Morikawa *et al.*, 2011; Mullen *et al.*, 2011). Furthermore, the amplitude of their transcriptional activity also depends on the involvement of co-activators or co-repressors which will be discussed below.

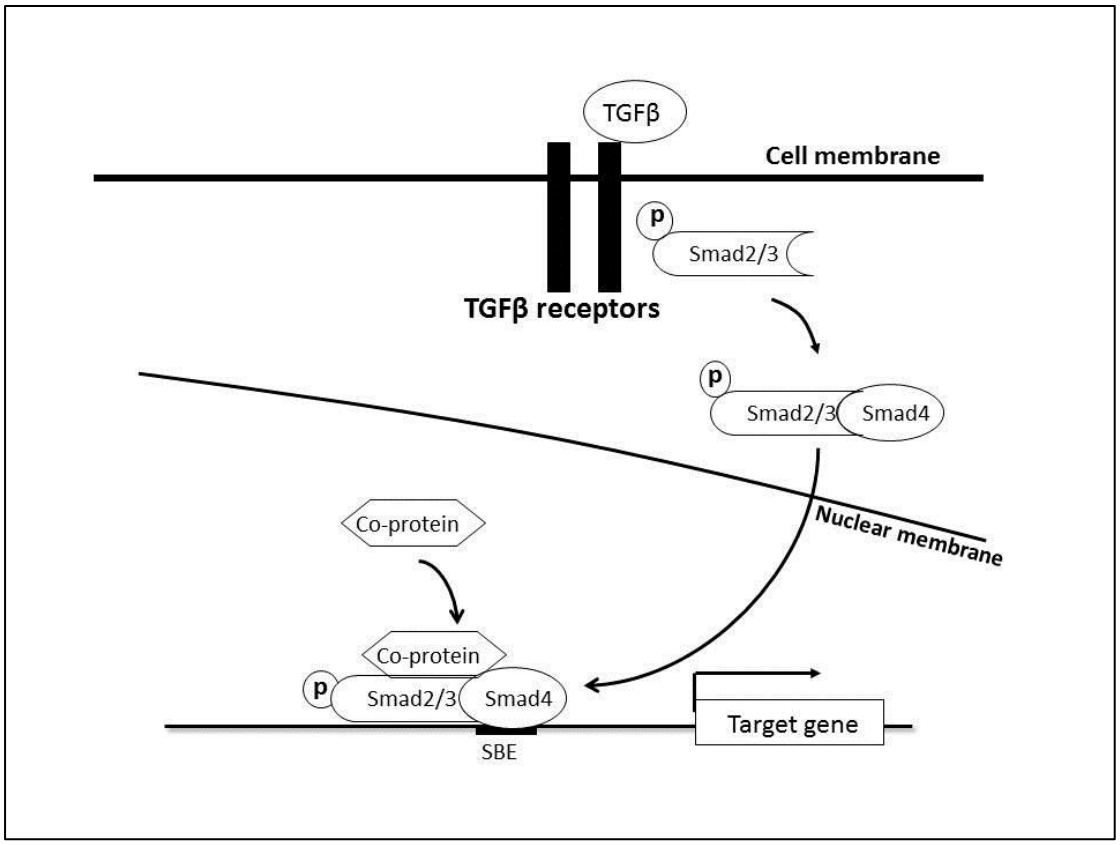

Figure 1.4 Schematic representation of the canonical TGF-β1/Smad signalling pathway.

1.4.2 Transcription factor-related TGF-β1/Smad regulation of gene expression

TGF-β1 induced transcriptional activation is generally based on the co-operation of Smad proteins with sequence-specific DNA binding transcription factors at the promoter of target genes. However, Smad proteins alone can also activate some early response genes. For example, the AP-1 family member JunB can be directly activated by Smad proteins in an immediate response to TGF-β1 signalling via multiple SBEs in the JunB promoter (Jonk, 1998). Similarly, the Id1 gene is also activated by Smad3/4 from as early as 0.5 hours after TGF-β1 treatment (Liang *et al.*, 2009). In most cases the co-operation between activated Smad proteins and other sequence-specific DNA binding transcription factors

have a synergistic activating effect. For example, activated Smad2/3 and Smad4 form a complex with FoXO proteins and bind to adjacent multiple SBEs and the FoXO binding element on the distal *p21* promoter (Seoane *et al.*, 2004). A similar mechanism has been reported for the binding and activation of the Smad2/3/4/Sp1 complex on the $p15^{Ink4b}$ (hereafter referred to as p15) promoter (Feng *et al.*, 2000). Interestingly, the proximal region of the *p21* promoter can also be bound by the Smad3/4/Sp1 complex, suggesting that a single promoter can have multiple Smad complexes bound at different locations. However, in this case, the binding of Smads to the proximal region is not essential for the activation of the *p21* promoter, but it enhances the activation by Sp1 (Pardali *et al.*, 2000). A similar mechanism operates when GATA-3 recruits Smad3 to the GATA-specific DNA binding site on the *IL-5* promoter upon TGF-β1 stimulation. The complex which is formed activates *IL-5* independent of Smad3 binding to DNA (Blokzijl *et al.*, 2002). In line with the fact that Smad3 can form complexes with AP-1 factors, several reports demonstrate a co-operative activation between Smad proteins and AP-1 factors on artificial as well as c-Jun and COL7A1 promoters (Zhang *et al.*, 1998; Liberati *et al.*, 1999; Wong *et al.*, 1999; Verrecchia *et al.*, 2001). In addition to the SBE and transcription factor binding sites on the promoter, a recent study using ChIP-on-chip technology revealed a novel SBE located within the first intronic region of the *p21* gene, forming a unique cis-regulating region together with Ets1 and AP-1/AP-2 transcription factors (Koinuma *et al.*, 2009).

In addition to sequence-specific transcription factors, Smads can also recruit co-activators to the protein/DNA complex to further enhance Smad-mediated activation. Such co-activators include CBP/p300, ARC and the Mediator complex which increase transcription by bringing the Smad-interacting transcription factors closer to the RNA polymerase II complex, thereby bridging upstream transcription factors with the general transcription machinery (Arias, 1996; Kato *et al.*, 2002; Soutourina *et al.*, 2011). The histone acetyltransferase activity of CBP/p300 also allows chromatin restructuring which improves accessibility of genes such as Id1 for transcription (Liang *et al.*, 2009). Other co-activators, such as ZEB1, augment transcription by promoting Smad-CBP/p300

interaction (Postigo, 2003).

While much less is known about TGF-β1 driven gene repression, several studies have reported on its repressive ability and the underlying roles in cellular activities. Some mechanisms of repression involve the prevention of transcriptional activation of target genes. For example, in response to TGF-β1, the activated Smad3 binds to MyoD thereby interfering with its heterodimerisation with E12 and E47 and hence with DNA binding. This results in decreased binding of the complex to E-box response elements on MyoD target genes responsible for myogenic differentiation (Liu *et al.*, 2001a). In addition, upon TGF-β1 signalling, the cytoplasmic Smad3 can form a repressive complex with both E2F-4 or E2F-5 and p107, a RB pocket protein known to recruit HDAC. Smad4 then leads the complex into the nucleus to bind to a unique TGF-β1 inhibitory element (TIE) on the *c-myc* promoter which overlaps with a consensus E2F site, and exerts repressive activity. (Chen *et al.*, 2001, 2002; Yagi *et al.*, 2002; Frederick *et al.*, 2004). Similarly, the repression of the osteocalcin promoter also depends on the recruitment of HDAC to the promoter by Smad3 (Kang *et al.*, 2005). TGF-β1 has also been shown to promote target gene repression through upregulation of a repressor. For example, in TGF-β1 induced repression of Id1, ATF3, a dominant negative regulator of basic helix-loop-helix (bHLH) transcription factors that are implicated in cell proliferation and tumourigenesis, is first promptly upregulated by TGF-β1. The activated ATF3 in turn interacts with Smad3 to repress Id1 expression through binding to the Id1 promoter (Kang *et al.*, 2003).

1.4.3 TGF-β1/Smad signalling pathway in cancer

TGF-β1 signalling has been widely reported to have a dual role in the progression of cancer. As shown in **Figure 1.5** while it acts as a tumour suppressor and inhibits cell proliferation during the early stages of carcinogenesis, it promotes migration and metastasis in the late stages of the disease (Imamura *et al.*, 2012).

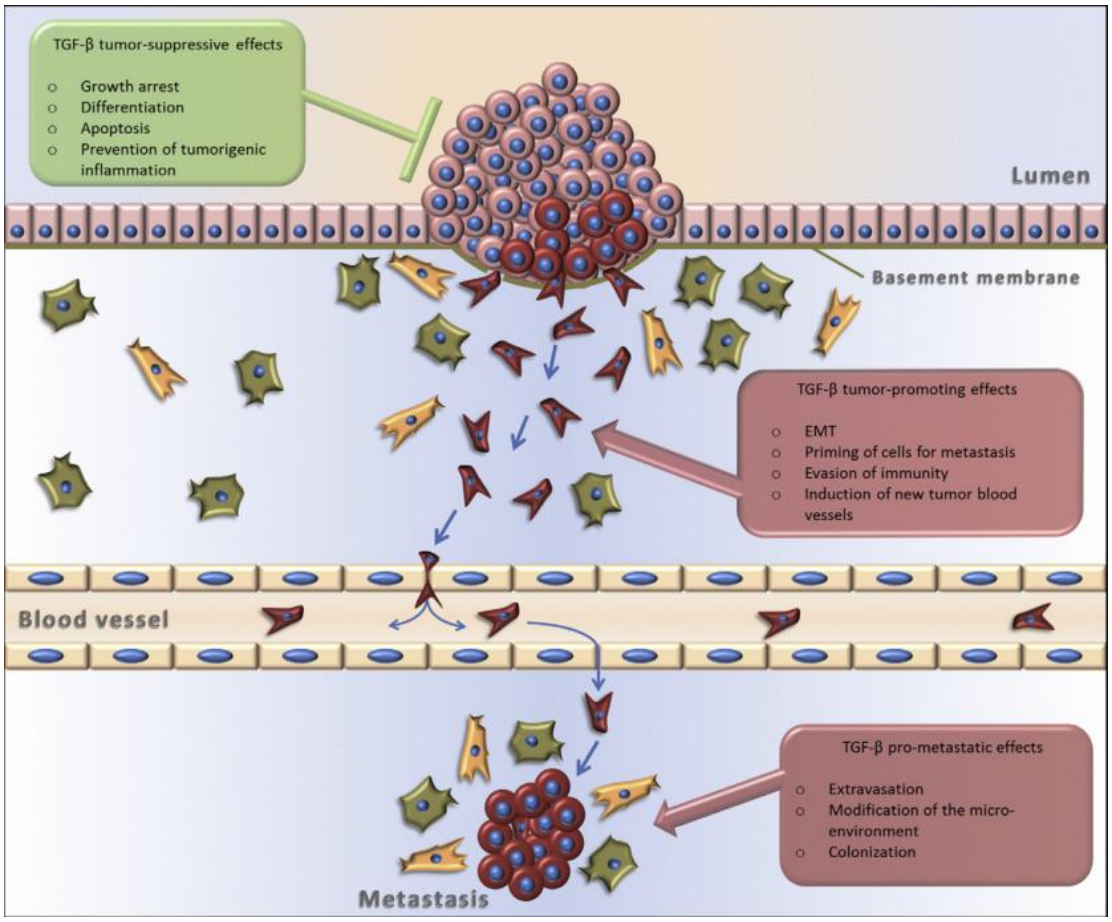

Figure 1.5 Role of TGF-β1 signalling in cancer progression (Figure from Heldin *et al.*, 2012).

1.4.3.1 Tumour suppressor activity of TGF-β1 in early stages of carcinogenesis

TGF-β1 generally functions as a tumour suppressor by inhibiting cell proliferation, differentiation, apoptosis and preventing tumourigenic inflammation (**Fig. 1.5**) (Heldin *et al.*, 2012). Due to the interest of the current project, the following sections of this literature review will focus on the mechanism by which TGF-β1 inhibits cell proliferation and promotes apoptosis.

In the cellular context of rapidly growing cells such as epithelial cells, there is a delicate balance of homeostasis between the gain and loss of cells. This is a self-protective mechanism against tumour formation and TGF-β1 plays an important proliferation inhibitory role in this process which was first described in breast epithelial cells (Pierce *et al.*, 1993). To date, there has been a significant body of research studying

TGF-β1-induced proliferation inhibition which in general, it exerts by inducing cell cycle arrest.

During normal cell cycle progression the cyclin dependent kinases, together with their cyclin binding partners, drive the transition through G1/S and G2/M. In epithelial cells, the anti-proliferative effect of TGF-β1 has been attributed to a G0/G1 cell cycle arrest which is primarily caused by upregulating the expression of the cyclin dependent kinase (Cdk) inhibitory proteins p15 and p21, which are potent inhibitors of cyclin D–Cdk4/6 and cyclin E/A–Cdk2 complexes respectively (Reynisdóttir *et al.*, 1995) (**Fig. 1.6**). One mechanism by which p15 and p21 is activated involves a Smad-mediated mechanism in co-operation with FoXO proteins, Sp1 and AP-1 transcription factors as described above. Another mechanism involves inhibiting the ability of c-myc to repress the *p15* and *p21* promoters by interfering with the interaction of c-myc and Myc-interacting zinc-finger protein 1 (Miz1) (Claassen and Hann, 2000; Seoane *et al.*, 2001; Staller *et al.*, 2001; Feng *et al.*, 2002; Wu *et al.*, 2003). Once induced, p15 inhibits cdk4 resulting in the release of $p27^{Kip1}$ (hereafter referred to as p27) which together with Smad-activated p21 inhibit cdk2 kinase activity (Reynisdóttir *et al.*, 1995; Jahn *et al.*, 2012). The reduced kinase activity of cdk2 and cdk4 slows down cell cycle progression and therefore inhibits proliferation (**Fig. 1.6**).

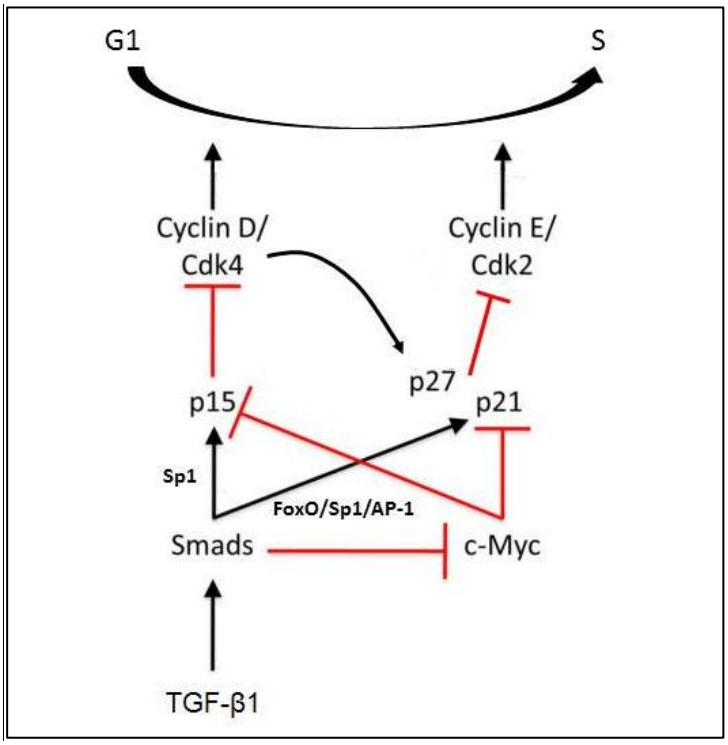

Figure 1.6 Fundamental mechanisms of TGF-β1-induced proliferation inhibition.

(Adapted from Jahn *et al.*, 2012)

Apoptosis is a process of programmed cell death that has critical roles in development, cellular homeostasis, immune reactions and many diseases including cancer, AIDS and several neurodegenerative disorders (Elmore, 2007). The two main apoptotic pathways are the death receptor pathway and the mitochondrial pathway, which lead to the activation of caspase 8 or 9 and the apoptosis executioner caspase-3 (Elmore, 2007). TGF-β1 has been implicated in a few pro-apoptotic events. For example, early studies revealed that TGF-β1 can elicit apoptosis by inducing oxidative stress in fetal hepatocytes (Alvarez, 1996) or by activating p38, a stress-responsive mitogen-activated protein kinase, in mouse primary hepatocytes (Yoo *et al.*, 2003). A pioneer study that linked TGFβ to the apoptotic machinery showed that the death-associated protein Daxx, which associates with the Fas receptor in the death receptor pathway, physically interacts with the cytoplasmic domain of the TGFβRII (Perlman *et al.*, 2001; Kim *et al.*, 2004). Besides the death receptor pathway, mitochondria play an essential role in triggering cell death as the release of cytochrome c from mitochondria into the cytoplasm accounts for the activation of the apoptotic programme (Wang and Youle, 2009). Larisch et al. (2000)

described that in rat prostate carcinoma cells, ARTS (apoptotic-related protein in the TGF-β1 signalling pathway), a septin-like protein, translocates from the mitochondria to the nucleus in response to TGF-β1 pro-apoptotic stimuli. The authors proposed that ARTS is a mitochondrial factor that regulates the activation of cytochrome c.

In addition to the above mechanisms, Smad proteins also play an important role in TGF-β1-induced apoptosis. For instance, Jang et al. (2002) connected Smads to mitochondrial-based pro-apoptotic events by showing that in response to TGF-β1, Smad2, 3 and 4 activate death-associated protein kinase (DAP-kinase) which mediates the release of cytochrome c from mitochondria and the dissipation of the mitochondrial membrane potential. It was also shown that the AP-1 family members JunD and FosB are induced by TGF-β1 and co-operate with Smad proteins to participate in TGF-β1 mediated apoptosis (Yamamura *et al.*, 2000). Furthermore, the Smad-dependent upregulation of inositol phosphatase SHIP (Src homology 2 (SH2) domain-containing 5' inositol phosphatase), an important regulator of phospholipid metabolism, leads to inhibition of PKB (protein kinase B)/Akt phosphorylation and cell survival (Valderrama-Carvajal *et al.*, 2002). It was later found that the sensitivity of TGF-β1-induced apoptosis is determined by PKB/Akt modulated phosphorylation of Smad3 (Conery *et al.*, 2004; Remy *et al.*, 2004).

Other findings linking TGF-β1 to apoptosis include observations that its stimulation lead to changes in expression levels or cellular localizations of core components of the cell death machinery such as both the pro- and anti-apoptotic members of the Bcl-2 family (Saltzman *et al.*, 1998; Yamamoto *et al.*, 1998; Wildey *et al.*, 2003) and the activation of caspase proteases (Chen and Chang, 1997; Schiffer *et al.*, 2001; Tótth *et al.*, 2001). These core components, together with all the other signalling that the cell receives, further determine the cell fate although the exact mechanism of TGF-β1 triggered apoptotic responses still remains to be further elucidated (Elmore, 2007).

1.4.3.2 TGF-β1 promotes late stage tumour progression

1.4.3.2.1 Evading the TGF-β1 anti-proliferative effect

In several cancers, including many breast cancers, the anti-proliferative effect of TGF-β1 is lost to facilitate the progression of malignancies (Bierie and Moses, 2006). Although it varies between different cancer types, the mechanisms behind this process generally involve somatic mutations in components of the TGF-β1 signalling cascade as well as altered expression of key cell cycle regulators. For example, early stage cancer cells lose the TGF-β1 governed anti-proliferative effect through alterations in the activity of TGFβRI and TGFβRII which may occur at both genetic and epigenetic levels.

In the early 90s, the TGFβRII was reported as a colorectal cancer tumour suppressor as its coding sequence was found to be mutated in the majority of sporadic and hereditary colorectal cancers with microsatellite instability (MSI). The mutations are caused by a deletion or insertion of adenines in a polyadenine repeat, resulting in a truncated inactive form of TGFβRII (Markowitz *et al.*, 1995; Parsons *et al.*, 1995; Grady *et al.*, 1999). Inactivated TGFβRII has also been observed frequently in gastric cancers and gliomas with MSI (Chung *et al.*, 1996; Izumoto *et al.*, 1997) and in some endometrial cancers with a frameshift mutation (Parekh *et al.*, 2002). Furthermore, the downregulation of TGFβRII expression has also been reported in breast, lung and prostate cancers (Jakowlew, 2006). While mutations in TGFβRI are less common, some cases have been reported in breast, ovarian, head and neck cancers and T-cell lymphomas (Jakowlew, 2006).

Other mechanisms that were reported to impair normal TGFβRII functioning in cancers include epigenetic modification of the gene which reduces the accessibility of the DNA for transcription. For example, histone methylation and acetylation/deacetylation were shown to result in chromatin remodelling of the *TGFβRII* leading to its expression being downregulated in breast, lung, ovarian and pancreatic cancers (Osada *et al.*, 2005; Hinshelwood *et al.*, 2007; Yamashita *et al.*, 2008). In addition, CpG methylation of the *TGFβRII* promoter was also implicated as the cause of gene silencing in human B-cell lymphoma cell lines (Chen *et al.*, 2007). Interestingly, later studies using several different

lung cancer cell lines suggested that epigenetic silencing of *TGFβRII* may be due to the combined effect of both histone deacetylase and methyltransferase to maintain the nucleosome in a compact form (Osada *et al.*, 2005; Chowdhury *et al.*, 2009).

The ablation of TGF-β1 induced proliferation inhibition can also be caused by aberrant Smad activity which impairs TGF-β1 signal transduction. In pancreatic and colon cancers, Smad2 and Smad4 have frequently been found to be mutated or deleted on chromosome 18q21 (Eppert *et al.*, 1996; Hahn *et al.*, 1996; Thiagalingam *et al.*, 1996). Although mutations in Smad3 have not been reported, its expression is reduced in human gastric cancers which do not respond to TGF-β1 anti-proliferative signals (Han *et al.*, 2004). The loss of Smad3 expression has also been marked as a specific feature of paediatric T-cell acute lymphoblastic leukaemia (Wolfraim *et al.*, 2004). In addition to the negative impact of deregulated c-myc on Smad proteins, several other mechanisms have been identified that inactivate the transcriptional activities of Smad3 and Smad4 and consequently preventing their ability to inhibit proliferation. For example, the widely expressed pro-proliferative transcription factor, serum response factor (SRF), interferes with the binding of Smad3 to DNA and its overexpression reduced TGF-β1-induced expression of p15 and p21 (Lee *et al.*, 2007). Similarly BCL6, a transcriptional co-repressor, can also physically interact with Smad3 and Smad4, disrupting the Smad/p300 complex and repressing Smad4 activity in B-cell lymphoma (Wang *et al.*, 2008a).

Smad7, an inhibitory Smad (I-Smad), also plays an important role in inhibiting TGFβ1 anti-proliferative signals in many cancer types. Its overexpression has been reported in 50% of human pancreatic cancers and stable transfection of a Smad7 expression vector in COLO-357 pancreatic cancer cells completely abrogated TGF-β1-mediated suppression of proliferation (Kleeff *et al.*, 1999). Smad7 was originally reported to exert its repressive activity by associating with TGFβRI, and inhibiting its phosphorylation of Smad2 and Smad3 which disrupts complex formation with Smad4 and subsequent nuclear translocation (Hayashi *et al.*, 1997). Another study using the COLO-357 pancreatic cancer

cell line also revealed Smad2/3 independent mechanisms by which Smad7 represses TGF-β1-mediated inhibition of proliferation. These mechanisms include interfering with TGF-β-mediated repression of cyclin A and B1, inhibition of cdk1 and cdk2 and upregulation of p27 (Boyer Arnold and Korc, 2005). Smad7 also functionally inactivates retinoblastoma protein (RB) and reverses the repression of E2F activity by TGF-β1 (Boyer Arnold and Korc, 2005).

c-Ski is a co-repressor of Smad proteins which renders cells resistant to inhibition of proliferation by interfering with the binding of the Smad/p300 complex to DNA and recruiting HDAC to inhibit transactivation of a number of anti-proliferative TGF-β1 target genes (Akiyoshi *et al.*, 1999; Sun *et al.*, 1999). The amplification of Ski is a negative prognostic marker of colorectal cancer and elevated expression of Ski correlates clinically with the progression of oesophageal squamous cell carcinoma (Buess *et al.*; Fukuchi *et al.*, 2004). Together with Ski, a highly homologous and structurally similar protein SnoN, has also been implicated in the progression of primary cutaneous melanoma (Boone *et al.*, 2009). Its repressive action is achieved through binding to Smad2 and Smad4 and inactivating their transcriptional activity by recruiting N-CoR, another co-repressor (Stroschein, 1999).

The appropriate regulation of key cell cycle proteins is important in the execution of the anti-proliferative effects of TGF-β1. As mentioned above, TGF-β1 suppresses proliferation by upregulating Cdki proteins p15, p21 and p27 and downregulating cyclins A, B1, D1 and E (Barlat *et al.*, 1993; Ralph *et al.*, 1993; Reddy *et al.*, 1994; Satterwhite *et al.*, 1994; Feng *et al.*, 1995; Ko *et al.*, 1995; Robson *et al.*, 1999; Xie *et al.*, 2003; Hu *et al.*, 2007). Anything that interferes with complex formation between cdk/cyclin/cdki would have a negative impact on the ability of TGF-β to suppress the proliferation of certain cell types. For example, ectopic expression of c-myc abrogates TGF-β1 activated expression of p15 and p21 and consequently inhibits the TGF-β1-induced anti-proliferative effect (Claassen and Hann, 2000; Feng *et al.*, 2002). Several early studies also reported on the overexpression of cyclin D and cyclin E in a few mammary epithelial cell lines, primary

keratinocytes and several hepatocellular carcinoma cell lines which are resistant to TGF-β1-induced inhibition of proliferation and the reduction of cyclin D in one of these studies partially rescued the resistance (Sgambato *et al.*, 1997; Martinez *et al.*, 2000; Jong *et al.*, 2002). Furthermore, the constitutive expression of cdk4 in mink lung epithelial cells renders them refractory to TGF-β1 and mammary tumours and mink lung epithelial cells that are engineered to stably express a cyclin D1-Cdk2 fusion protein are also resistant to TGF-β1 induced inhibition of proliferation (Ewen *et al.*, 1993; Chytil *et al.*, 2004; Corsino *et al.*, 2007)

1.4.3.2.2 TGF-β1 induced EMT in cancer migration and metastasis

A hallmark of malignant tumours is their ability to metastasize to distant organs through a complex series of steps which include: EMT, cell migration, invasion, and intravasation and extravasation from the circulatory system (Hanahan *et al.*, 2000; Hanahan and Weinberg, 2011). There is considerable evidence to suggest that the overexpression of TGF-β1 is linked to tumour progression and the involvement of TGF-β1 in cancer metastasis has been extensively studied. High levels of circulating TGF-β1 have been reported in the plasma of patients with breast, lung, colon and liver cancer and correlate with high death rates (Anscher *et al.*, 1993; Levy and Hill, 2006). Immuno-staining has also shown that elevated TGF-β1 levels are associated with a higher rate of metastasis and shortened time to relapse in many epithelial cancers. In fact, cancer patients with positive staining of TGF-β1, TGFβRI and TGFβRII have the poorest five year survival statistics (Takanami *et al.*, 1997).

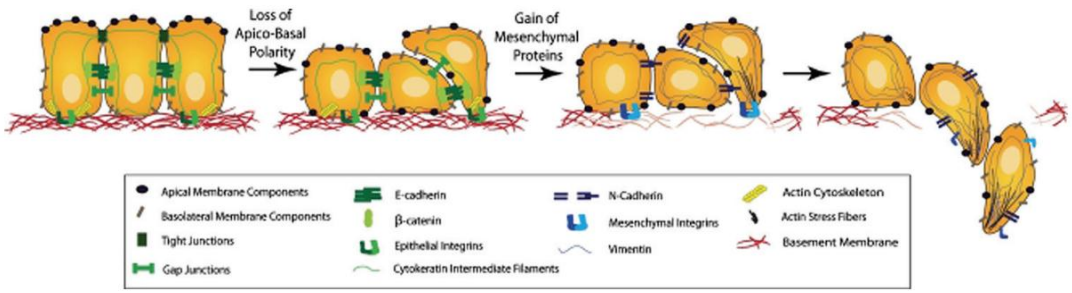

Figure 1.7 Schematic representation of cells undergoing EMT.

(Figure from Talbot *et al*., 2012)

As mentioned earlier, EMT plays an important role in metastasis and the mechanism by which TGF-β1 promotes cancer cell migration is through its ability to induce EMT. As shown in **figure 1.7** during EMT, the extracellular matrix is restructured and cell adhesion molecules are modified, resulting in a loss of cobblestone-like epithelial characteristics and an acquisition of a fibroblastic-like mesenchymal phenotype (Guarino, 2007; Heldin *et al.*, 2012). This process facilitates the transformation of epithelial tumour cells into a malignant metastatic phenotype and enables the invasion of the tumour cells into lymph or blood vessels (Thiery *et al.*, 2009). An early in vivo study using TGF-β1 transgenic mice showed that TGF-β1 promoted the development of invasive spindle skin carcinoma with significantly increased malignant conversion rate (Cui *et al.*, 1996). Another study demonstrated that the expression of TGF-β1 in papillomas causes a loss of the invasion suppressor E-cadherin in the cell membrane and rapid metastasis (Weeks *et al.*, 2001). In contrast with the invasion suppressive role of E-cadherin, N-cadherin generally functions as a potent invasion promoter (Hazan *et al.*, 2000; Cavallaro, 2004; De Wever *et al.*, 2004; Derycke and Bracke, 2004; Nakajima *et al.*, 2004; Deramaudt *et al.*, 2006) and TGF-β1-induced EMT has been linked with a transition from E-cadherin to N-cadherin. For example, Nakajima et al. (2004) observed a significant correlation between TGF-β1, N-cadherin and vimentin in metastatic liver tumours and TGF-β1 treatment of pancreatic cancer cells upregulated N-cadherin and vimentin but inhibited the expression of E-cadherin. Diamond et al. (2008) further demonstrated that TGF-β1 increased the migration of oral keratinocytes by upregulating the expression of N-cadherin. These findings were supported by Araki et al. (2011) who reported a strong association between a high E-cadherin/N-cadherin ratio and 5-year survival rate, and vice versa, of patients with extrahepatic cholangiocarcinoma.

TGF-β1 can induce EMT through transcriptional or post-transcriptional regulation of a group of transcription factors which repress E-cadherin (Miyazono, 2009; Heldin *et al.*, 2012). For example, Smad-mediated expression of high mobility group A2 (HMGA2) has been found responsible for the induction of Snail, Slug and Twist which are known to be important repressors of E-cadherin (Thuault *et al.*, 2006, 2008; Tan *et al.*, 2012).

Interestingly, TGF-β1-induced Smad proteins can also co-operate with factors in other pathways to mediate EMT. It has been reported that TGF-β1 co-operates with oncogenic H-Ras in both the MAPK and PI3K pathways to activate the *Snail* promoter (Peinado *et al.*, 2003), and this co-operation is enhanced by the activation of the transcription factor *NF*-κB (Huber *et al.*, 2004). Moreover, a ChIP-sequencing study of proteins immunoprecipitated with ATF3, a known activator of Snail, Slug and Twist, revealed its co-operation with Smad2/3 (Yin *et al.*, 2010). TGF-β1-induced EMT can also occur through Smad-independent mechanisms which include epigenetic regulation, miRNA regulation, differential splicing and regulation of mRNA translation (Heldin *et al.*, 2012). Due to the focus of this thesis these mechanisms will not to be discussed in any detail.

1.5 Aims of this study

The T-box transcription factors, TBX2 and TBX3, play critical roles in embryonic development and their deregulated expression has been implicated in a growing list of cancers including breast cancer and melanoma. This study aims to elucidate the role of the over-expression of TBX3 in breast cancer and to investigate the regulation of TBX2 and TBX3 by the TGF-β1 signalling pathway. Based on the literature, as well as unpublished data from our laboratory, the specific aims of this study were:

1. To silence TBX3 in breast cancer cells that express high levels of this protein using a shRNA approach and to determine whether, at the very least, some features of the transformed phenotype could be reversed.
2. To overexpress TBX3 in “normal” breast epithelial cells and to establish if a transformed phenotype could be induced.
3. To investigate the effect of the TGF-β1 signalling pathway on TBX3 expression in breast epithelial cells and its possible function downstream of this pathway.
4. To investigate a TBX3 target gene that mediates its role in the TGF-β1 signalling pathway.

CHAPTER 2

MATERIALS AND METHODS

2.1 Plasmids and DNA constructs

All constructs used in this study were prepared according to standard techniques (Sambrook *et al*, 1989). The pSuper.neo/GFP vectors, containing either a shTBX3- or a scrambled shControl- sequence were previously cloned by Dr Emily Davis and are available in the Prince laboratory. The human TBX3 promoter luciferase reporter constructs have been described previously (Abrahams *et al.*, 2008). The pCMV-JunB expression vector was generously provided by Dr. Michael Birrer (National Cancer Institute, National Institutes of Health, Bethesda, MD, USA) and the pCMV-Smad3 and pCMV-Smad4 expression vectors were from Dr RikDerynck (University of California at San Francisco, CA, USA). The human *TBX2* promoter luciferase reporter constructs have been described previously (Teng *et al.*, 2008). The pcDNA 3.1(+) containing the full-length human *TBX2* cDNA was supplied by Prof. van Lohuize (Antoni van Leeuwenhoek hospital, Amsterdam, The Netherlands). The *TBX2* cDNA was then excised and the vector re-ligated to generate the pcDNA3.1 (+) empty vector, into which the human *TBX3* cDNA was cloned using the NheI and BamHI sites. The pRc/CMV containing the full-length human p21 cDNA was purchased from Addgene (plasmid # 20814) and was provided by Dr William Kaelin (Adams *et al.*, 1996). The *p21* cDNA was then excised by using HindIII and XbaI and the vector re-ligated to generate the pRc/CMV empty vector.

The *TBX3* N-terminal construct was constructed by Mrs Aretha Cooper. Briefly, the C-terminal portion of the pCMV-TBX3 construct was excised: 1X Reaction buffer, 2 µg DNA template, 10 U BglII and 10 U SpeI in a total volume of 50 µl and incubated for 90 minute (min) at 37 ^{o}C. Blunt ends were created using 1 X buffer B, 5 U of T4 DNA polymerase (Promega, USA) per µg of DNA and dNTP mix and incubated for 5 min at

37 ^{o}C followed by heat inactivation at 75^{o}C for 10 min. Product was isolated by running through 0.8% agarose gel and purified using QIAquick PCR purification kit according to manufacturer's instruction (Qiagen, USA). The blunt ends were re-ligated using DNA ligase, 1 X ligation buffer (Promega, WI, USA) and 100 ng DNA in a total volume of 20 µl. The product construct was tested by diagnosis digestion.

2.1.1 Site-directed mutagenesis (SDM)

The TBX3 DNA binding domain mutant (R133G) construct was produced by Dr Jade Peres. Briefly, point mutations were introduced into the pCMV-TBX3 cDNA by site-directed mutagenesis using appropriate primer pairs containing the desired mutations (see table 2.1). Standard polymerase chain reaction (PCR) mix contained: 1X Reaction buffer, 50 ng DNA template, 400 nM forward primer, 400 nM reverse primer, 200 nM dNTP mix (Promega, Madison, WI USA), 4 µl Dimethyl Sulphoxide (DMSO) (Sigma, St. Louis, MO, USA), 3 Units Pfu DNA polymerase (Promega, Madison, WI, USA) in a total volume of 50 µl. The parameters for PCR amplification were 1 min at 95^{o}C for 1 cycle; 45 second (sec) at 95^{o}C, 1 min at 55^{o}C and 14 min at 73^{o}C for 17 cycles. PCR was performed on an Applied Biosystems 2720 Thermal cycler. The PCR products were assessed by agarose gel electrophoresis to confirm successful amplification. The synthesised DNA containing the mutation was selected for by digesting the methylated, non-mutated parental DNA template with 1 µl DpnI (10U/µl) endonuclease for 1 hour (hr) at 37^{o}C. XL1-Blue supercompetent cells were transformed with 5 µl of the DpnI digested DNA as follows: incubation on ice for 30 min, heat shock at 42^{o}C for 1 min and incubation on ice for 2 min. To each transformation reaction 0.3 ml of Luria broth (LB) (see **Appendix, section 6.1**) was added and then incubated for 2 hrs at 37^{o}C with shaking at 225-250 rpm. Following incubation, the entire volume of each transformation reaction was plated onto LB Ampicillin (100 µg/ml) agar plates. Plates were incubated at 37^{o}C for at least 16 hrs and a selection of colonies was expanded by mini-prep culture. DNA constructs extracted from these mini-preps were screened for the presence of desired mutation by sequencing and a single verified mutant construct was amplified by maxiprep.

Point mutations were introduced into the pGL3basic-TBX3 promoter luciferase constructs containing 141 bp of the 5' regulatory region of the human *TBX3* gene by site-directed mutagenesis using appropriate primer pairs containing the desired mutations (see **Table 2.1**). Point mutations were introduced into the pGL3basic-TBX2 promoter luciferase constructs containing 218 bp of the 5' regulatory region of the human *TBX2* gene by site-directed mutagenesis using appropriate primer pairs containing the desired mutations (see **Table 2.1**).

The PCR were performed using 5 µl KAPA HiFi Hot Start Ready Mix 2X (KAPA Biosystems, South Africa), 300 nM forward primer, 300 nM reverse primer, 10 ng DNA template in a total volume of 10 µl. The parameters for PCR amplification were 2 min at 95^{o}C for 1 cycle; 20 sec at 98^{o}C, 15 sec at 63^{o}C and 3 min at 72^{o}C for 17 cycles; 5 min at 72^{o}C. PCR was performed on an Applied Biosystems 2720 Thermal cycler (Life Technologies Corporation, USA). The PCR products were purified using a PCR purification kit (Qiagen, USA) and assessed by agarose gel electrophoresis to confirm successful amplification. The synthesised DNA containing the mutation was selected for by digesting the methylated, non-mutated parental DNA template with 1 µl Dpn I (10U/µl) (Promega, USA) endonuclease for 1 hour (h) at 37°C. Dpn I was heat inactivated at 80°C for 20 min and Escherichia coli (E.coli) DH5α competent cells were transformed with 10 µl of the Dpn I digested DNA by firstly incubating on ice for 30 min, heat pulsing at 42°C for 45 sec and incubation for 2 min on ice. To each transformation reaction 0.3 ml of LB was added and then incubated for 1 hr at 37°C with shaking at 225-250 rpm. Following incubation, the entire volume of each transformation reaction was plated onto LB Ampicillin (100 µg/ml) agar plates. Plates were inverted and incubated at 37°C for at least 16 hrs. To confirm successful transformation of the mutated plasmid DNA, the presence of the mutation was verified by sequencing.

Table 2.1 Sequence of primers used to generate mutant *TBX2* or *TBX3* promoter constructs by site-directed mutagenesis.

Mutant	Template	Forward primer
AP1 (−86/−69)	*TBX3* (141 bp) WT promoter	5′-GGTCCGAAAG**g**GT**ag**AAGAGC**Ctc**T**ag**AGAGGCCTCCGGC-3′
SBE (−67/−58)	*TBX3* (141 bp) WT promoter	5′-GCCAATCAAG**A**a**G**C**t**T**t**C**G**GCTCCCCGC-3′
T-element (-186 bp)	*TBX2* (218 bp) WT promoter	5′-GCTGAGGCTTC**C**a**A**a**A**a**C**TTCTCCCAGGCC-3′
pCMV *TBX3* DNA Binding Domain Mutant	WT *TBX3* cDNA full length	5′ CATTACCAAGTCGGGA**g**GG**g**GAATGTTTCCTCCATTTAAAG 3′

*Primer sequences corresponding to the wild type template are represented in uppercase. Mutations are depicted in bold lower case. Putative AP-1 binding sites are highlighted in yellow; putative SBEs are highlighted in green and T-element binding sites are highlighted in blue.

2.2 Cell culture

The normal human breast epithelial MCF-12A cells were maintained in complete media consisting of DMEM/Ham's F12 supplemented with 10% FBS, 100 U/ml penicillin, 0.1 µg/ml cholera toxin (Gibco/BRL), 0.5 µg/ml hydrocortisone (Sigma), 10 µg/ml insulin (Sigma), 20 ng/ml EGF (Sigma) and 5% horse serum (Gibco/BRL). HT-1080 human fibrosarcoma, WI38 human embryonic lung fibroblasts, HEK293T cells and human keratinocyte HaCaT cells were maintained in DMEM (Dulbecco's modified Eagle's medium) supplemented with 10% (v/v) FBS (fetal bovine serum), 200 U/ml penicillin and 100 µg/ml streptomycin. B16 mouse melanoma and MCF-7 breast adenocarcinoma cells were maintained in RPMI 1640 medium supplemented with 10% (v/v) FBS (fetal bovine serum), 200 U/ml penicillin and 100 µg/ml streptomycin. All cell lines were maintained in a 5% CO_2 humidified incubator at 37^{o}C. Media was replaced every 2-3 days and cells

routinely subjected to mycoplasma tests. Only mycoplasma free cells were used in experiments.

2.2.1 Mycoplasma test

Cells grown on sterile coverslips with antibiotic-free medium for 24 hrs were fixed in fixing solution (25% glacial acetic acid; 75% methanol) for 5 sec, washed with water and repeated and air-dried at room temperature (RT) for 5 min. DNA was then stained with Hoechst 33258 (0.5 µg/ml) for 30 sec, washed with water and mounted on a slide with mounting fluid (see **Appendix, section 6.2**). The cells were viewed immediately by fluorescence microscopy using the DAPI filter. Mycoplasma negative cells stained positive with Hoechst 33258 only in the nucleus, while cells infected with mycoplasma showed staining in both the nucleus and the cytoplasm.

2.2.2 Transfections

Prior to performing transfections, the concentration and quality of all DNA constructs were assessed using a NanoDrop ND-1000 spectrophotometer (Agilent Technologies, Boeblingen, Germany) and confirmed by agarose gel electrophoresis. Four different transfection reagents were used:

1. FuGENE HD (Roche, Germany): Cells were transfected using a 3:1 ratio according to the manufacturer's instructions. Cells were plated at 1.5 X 10^5 cells per 35 mm dish (1 X 10^4 cells per well of 12 well plate) 1 day before transfection. Three microlitres (2 µl for 12 well plate) of the transfection reagent was added to 97 µl (48 µl for 12 well plate) serum-free media (without antibiotic) and incubated at room temperature for 5 min. The diluted transfection reagent was then added to the DNA, mixed and incubated at room temperature for a further 15 min. The transfection reagent: DNA complex was added dropwise to the cells and incubated for thirty hours at 37°C.

   MCF-7 shctrl and shTBX3 cell lines: MCF-7 cells at 70% confluency in 35mm dishes were transfected with 1 µg of pSuper.neo/GFP-shctrl or pSuper.neo/GFP-shTBX3 vectors.

   TGF-β1 activates TBX3: MCF-12A cells were co-transfected with 400 ng of a

TBX3-luciferase reporter plasmid plus 40 ng of the JunB or 30 ng each of the Smad3 and Smad4 expression plasmids or corresponding amounts of an empty-vector plasmid.

p21 overexpression: MCF-12A-TBX2 cells 24-well plate were transfected with 150 ng of pRc/CMV-p21 or pRc/CMV.

2. X-tremeGENE HP (Roche, Germany): Operations were the same as for FuGENE HD except cells were transfected using a 2:1 ratio.

   MCF-12A EC and TBX2 overexpressing cell lines: MCF-12A cells at 70% confluency in 35mm dishes were transfected with 1 µl of pcDNA3.1 (+) or pcDNA3.1 (+)-TBX2 vectors.

   TBX3 represses TBX2: MCF-12A cells were co-transfected with 400 ng of a TBX2-luciferase reporter plasmids plus 100 ng of the pCMV-TBX3 expression plasmids or corresponding amounts of an empty-vector plasmid.

3. Lipofectamine™ LTX with PLUS™ (Invitrogen, USA): HEK 293 cells at a density of 70% in 10 cm dish were switched to 0.5% serum medium before transfection. 3.5 µg linearized Adeno-X-TBX3 vector was diluted in 720 µl serum-free medium and mixed with 20 µl PLUS reagent and incubated at RT for 5 min. 30 µl Lipofectamine LTX was then added to the mixture and incubated for 30 min. The whole mixture was then added directly to the cells and the dishes were incubated at 37^{o}C for 6 hrs before the medium was replaced with normal growth medium.

4. HiPerFect®: Transient knockdown of JunB, Smad4, TBX3 or p21 expression in MCF-12A cells was achieved by siRNA that specifically targets *JunB*, *Smad4, TBX3* or *p21* mRNA (siJunB, siSmad4, siTBX3 or sip21). Cells at 60% confluency in each well of 24 well plate (6 well plate) were washed twice with 1X PBS and replaced with 400 µl (1.9 ml) serum-starved medium (for TGF-β1 treated experiments) or complete medium. 30 nM of siJunB (sc-35726, Santa Cruz Biotechnology, USA) or siSmad4 (SI00076041, Qiagen, USA) or 50 nM of siTBX3 (SI00083503, Qiagen, USA) or 25 nM of sip21 (Dharmacon siRNA, ONTARGETplus SMARTpool, CDKN1A L-003471-00-0005, Thermo Fisher Scientific., Lafayette, CO, USA) or a control (non-silencing) siRNA (Qiagen, USA) was diluted in 100 µl serum-free, antibiotic-free medium. Three

microlitres (6µl) of HiPerFect was added directly to the diluted siRNA solution, incubated at RT for 5 min and added to cells. Numbers in bracket indicate amount used for 6 well plate for RNA analysis.

2.2.3 Generation of stable cell lines in which TBX3 was knocked down

The MCF-7 breast cancer cells have been shown to over-express TBX3 and were thus selected to generate stable cell lines knocking down TBX3 (Fan *et al.*, 2004). Cells were stably transfected with the pSuper.neo/GFP vector, containing either a *TBX3*-(constructed by Dr Jade Peres) or a scrambled control- sequence. Stable transfectants were selected for with 400 µg/ml G-418 antibiotic (Promega, USA) (as described below) 48 hrs post transfection and individual clones selected. Among subcloned cell lines, those chosen for subsequent analysis were: MCF-7 shTBX3(2) and MCF-7 shTBX3(8) and expressing the shTBX2 construct while MCF-7 shcontrol(5) expressed the shcontrol construct.

2.2.4 Generation of adenoviral inducible adeno-TBX3 virus

The adeno-TBX3 virus was generated using Adeno-X Tet-off expression system 1 (Clontech, USA) according to manufacturer's instructions. The system was a kind gift from Dr Luiz (International Centre for Genetic Engineering and Biotechnology, University of Cape Town, SA). Briefly, both of pcDNA3.1 (+)–TBX3 and pTRE-Shuttle 2 vectors were restriction digested using Promega reagents: RE 1 x buffer B, 5 µg BSA, 5 U NheI, 5 U XbaI, 15 µg plasmid DNA in a total volume of 50 µl, incubated at 37^{o}C overnight (O/N). The digested vectors were ligated using Promega reagents as follows: 100 ng pTRE-Shuttle 2 vector, 20 ng pcDNA3.1 (+) –TBX3 vector, Ligase 1X buffer, 0.5 U T4 DNA ligase in a total volume of 5 µl, incubated at RT for 3 hrs and transformed into DH5α supercompetent cells as described above. Agar plates containing 50 µg/ml kanamycin were incubated at 37^{o}C O/N. The successful ligation was confirmed by restriction enzyme digestion. To subclone the expression cassette into the Adeno-X genome, the recombinant pTRE-Shuttle2-TBX3 vector was further digested using the provided I-Ceu and PI-Sce I enzymes, purified and ligated using provided reagents as instructed. To destruct

non-recombinant Adeno-X DNA construct, the ligation product was restriction digested using provided Swa I enzyme as instructed. The successfully ligated Adeno-X-TBX3 vector was transformed into DH5α supercompetent cells as described. Agar plates containing 100 µg/ml ampicillin were incubated at 37^{o}C O/N. The successful ligation was confirmed by restriction enzyme digestion and linearized by Pac I restriction enzyme digestion as instructed. Pac I digested Adeno-X-TBX3 was transfected into low passage HEK 293 cells using Lipofectamine™ LTX and PLUS™ Reagents (Cat. no. 15338-100, Invitrogen, USA) according to manufacturer's instructions. The cytopathic effect (CPE) was observed within two weeks. Cells and medium were transferred to 15 ml centrifuge tube and centrifuged at 1500 g for 5 min at RT. Cell pellet was resuspended in 500 µl PBS. Cells were then lysed with 3 consecutive freeze-thaw cycles between 37^{o}C and liquid nitrogen bath, centrifuged and cell debris discarded. To obtain high-titre stocks, HEK293 cells were transduced with cell lysate and cells exhibiting CPE were lysed and virus purified using Adeno-X Maxi Purification kit (Clontech, USA). The viral titre was determined by end-point assay according to manufacturer's instructions. Briefly, 1X10^{4} HEK 293 cells were plated in 96-well plate 24 prior to transfection with a serial dilution (10^{-3}-10^{-10}) of the purified virus and incubated at 37^{o}C. Wells were examined for CPE and the viral titre was calculated as: Titre (pfu/ml) = $10^{(x+0.8)}$, x=the sum of the fraction of CPE-positive wells. The MCF-12A cells were infected with multiplicity of infection (M.O.I.) of 50 pfu/cell.

2.2.5 Generation of lentiviral inducible MCF-12A cell line

The MCF-12A cells were stably transduced using a tetracycline inducible third generation lentiviral system expressing short hairpin TBX3 RNA (shTBX3) alongside constitutively expressed enhanced green fluorescent protein (eGFP). The system was a kind gift from Dr Marc Weinberg (University of Witswatersrand, Johannesburg, SA), who designed and cloned the shTBX3 sequence into the pHIV7-TetRIRESeGFP (Aagaard *et al.*, 2007) lentiviral vector (pTIG-shTBX3) (see **Appendix, section 6.3**). The third generation lentiviral system consists of key components of the HIV7 virus contained 1 lentiviral vector and 3 packaging plasmids that produce proteins which package the lentiviral vector into replication-deficient infectious particles that deliver the lentiviral vector into

target cells where it integrates into the genome.

2.2.5.1 Infectious particle production

Lentivirus infectious particles were produced by transfecting HEK293T cells using the calcium phosphate method. Early passage HEK293T cells plated in 5 x 10 cm tissue culture dishes were grown to 50-60% confluency in medium containing antibiotic. For transfection, 65 µg of pTIG-shTBX3 lentiviral vector was combined with 18.75 µg pVSV-G (pLP), 15 µg pRSV-Rev (pLP1) and 18.75 µg pRRE (pLP2) packaging vectors (Invitrogen) made up to 1.25 ml with sterile water, to which an equal volume (1.25 ml) of 0.5 M CaCl2 was added and mixed well. An equal volume (2.5 ml) of HBS2X (see **Appendix, section 6.4**) was placed in a separate 50 ml sterile conical tube and continuously agitated by bubbling with a pipette aid while adding the DNA solution directly to the liquid in dropwise fashion. After 20 min incubation at RT, 1 ml of the DNA mix was added per 10 cm dish of HEK293T cells and incubated at 37°C, 5% CO_2 overnight. The next day, medium was removed from the cells and replaced with 8 ml complete medium and incubated for another 24 hrs. The following day, virus-containing medium was collected and fresh medium added to the cells for a second round of virus collection. The collected medium was centrifuged at 2000 x g at 4°C for 7 min to pellet cell debris, and then filtered through a 0.45 µM disposable filter to remove any particulate matter. Virus was concentrated by ultracentrifugation at 25 000 rpm at 4°C for 2 hrs in a (SW 55 Ti, Beckman Coulter) swing bucket rotor using a (OptimaTML-80 XP, Beckman Coulter) ultracentrifuge and the viral pellets resuspended in total of 80 µl sterile PBS per 20 ml of virus-containing medium (250 fold concentration). Virus concentrates were stored as 10 µl aliquots at -80°C.

2.2.5.2 Infectious particle transduction of target cell lines

The lenti-MCF-12A cells were produced by transducing the parental MCF-12A cell line using virus concentrate. Cells were grown to 50% confluency in a 6 cm dish and medium was replaced with 6 ml of fresh medium and 30 µl of virus concentrate, along with 8 µg/ml polybrene (Hexadimethrine bromide) (Sigma, St Louis, USA) and returned to 37°C

O/N. The next day medium was replaced with fresh to remove the polybrene. Successful transduction was monitored by cells expressing GFP 48 – 96 hrs after infection, using an Axiovert fluorescent microscope (Zeiss, Germany) and a pure population was obtained by fluorescence activated cell sorting (FACS) for GFP expression using a FACSVantage SE (Becton Dickinson) cell sorter. Tetracycline induction of knockdown transcripts was achieved by treating the cells with 1 µg/ml doxycycline hyclate (Sigma, St Louis, USA) and effective knockdown assessed by western blot analysis with appropriate antibodies.

2.2.6 Generation of MCF-12A cell lines in which TBX2 was stably overexpressed

To generate stably transfected cell lines, MCF-12A cells at 70% confluency were transfected with either the empty expression vector pcDNA3.1 (+) or with this vector containing the full length human TBX2 cDNA (Lingbeek *et al.*, 2002) using X-tremeGENE HP (Roche, Germany). Transfected cells were selected by 400 µg/ml G-418 antibiotic for 10 days and were pooled for further analysis.

2.2.7 G-418 selection

To determine the effective concentration of antibiotic for each cell line, untransfected cells were seeded in a 6-well plate so that cells were approximately 60% confluent on the first day of treatment. Cells were treated with concentrations of G-418, ranging from 0 – 800 µg/ml and monitored daily. The lowest concentration which resulted in complete cell death after approximately 10 days was selected. Four hundred µg/ml G-418 was chosen for MCF-7 cells.

2.3 Cell treatments

2.3.1 TGF-β1 treatment

Equally plated cells were serum starved for at least 16 hrs and were treated with either 5ng/ml rhTGF-β1 (R&D systems, MN, USA), diluted in 4mM HCl, 1mg/ml BSA, or vehicle.

2.3.2 Actinomycin D treatment and Cycloheximide treatment

For transcription inhibitor experiments, cells were treated with 5 µg/ml Actinomycin D

(Sigma) or vehicle DMSO for control 1 hr prior to TGF-β1 treatment. For inhibition of de novo protein synthesis experiments, cells were pre-treated with 30 μg/ml cycloheximide (Sigma) or vehicle DMSO for control for 1 hr prior to TGF-β1 treatment. All inhibitors were added in the dark.

2.4 Western blot analysis

Cells were harvested on ice by scraping with a 1 ml plunger in RIPA buffer (see **Appendix, section 6.5**). Whole cell extracts were incubated on ice for a minimum of 30 min, centrifuged at 12,000 g for 20 min at 4°C and the supernatants recovered. Protein concentrations were determined using the BCA assay (Pierce, Rockford, IL, USA), according to the manufacturer's instructions with bovine serum albumin as the standard. Equal amounts of protein were loaded and separated on 8-10% SDS-polyacrylamide gels (see **Appendix, section 6.5**) and transferred to Hybond ECL nitrocellulose membrane (Amersham, Biosciences, USA). Membranes were blocked for 1 hr at RT with PBS containing 5% non-fat dry milk and probed with appropriate primary antibodies O/N at 4°C with shaking. Membranes were washed in PBS containing 0.1% Tween 20 (PBS/T) and incubated with peroxidase-conjugated anti-mouse or anti-rabbit (BioRad, Hercules, CA, USA) or anti-goat antibody (1:5000) (Santa Cruz Biotechnology, CA, USA). Membranes were again washed in PBS/T and visualised by enhanced chemiluminescence (Pierce, Rockford, IL, USA). The primary antibodies and appropriate dilutions were: rabbit polyclonal anti-JunB (sc-73, Santa Cruz Biotechnology, CA, USA), goat polyclonal anti-Smad2/3 (sc-6202, Santa Cruz Biotechnology, CA, USA), rabbit polyclonal anti-Smad4 (sc-7154, Santa Cruz Biotechnology, CA, USA), goat polyclonal anti-TBX2 (1:1000) (sc-17880, Santa Cruz Biotechnology, CA, USA), rabbit polyclonal anti-TBX3 (1:250) (42-4800, Invitrogen, USA) and rabbit polyclonal anti-p38 (1:5000) (Sigma, Missouri, USA). To analyse the membrane with a primary antibody targeted towards a different protein, bound primary antibody was removed as follows: membranes were rinsed with PBS/T, stripped in stripping buffer (see **Appendix, section 6.5**) for 30 min at 50°C and washed twice with PBS/T. If necessary, the expression of proteins was quantified as the densitometry value analysed by UN-SCAN-IT gel 6.1

software and normalised to the appropriate loading control.

2.5 Quantitative real-time PCR (qRT-PCR)

Total RNA was extracted from cells using the High Pure RNA Isolation Kit (Roche). Reverse transcription of RNA (1 µg) was performed according to the manufacturer's instructions using the InProm-II^{TM} reverse transcription system (A3800; Promega, USA). Using 1 µl of cDNA, PCR was conducted with the SensiMix Lite Kit (Quantace QT 405-05, USA) according to the manufacturer's protocol. Real-time PCR was performed on a LightCycler Version 4 (Roche, Basle, Switzerland) using the following parameters: denaturation (15 min at 95°C), annealing and amplification at 35 cycles (15 s at 94^{o}C; 20 s at 55^{o}C; 20 s at 72°C), melting temperature (15 s at 65°C), and a cooling step (30 s at 40°C). Each DNA sample was quantified in duplicate, and a negative control without cDNA template was run with every assay to assess the overall specificity. Melting curve analyses were carried out to ensure product specificity, and data were analysed using the $2^{-\Delta\Delta Ct}$ method. Relative mRNA expression levels were normalized to glucuronidase beta (GUSB) for each reaction with PCR efficiency correction calculated using the formula Ratio = $E_{target}CP_{target}$(control – sample)/$E_{ref}CP_{ref}$(control – sample), where E is the real-time PCR efficiency and CP is the crossing point. Primers used to amplify the human *TBX3* (QT00022484) and *GUSB* (QT00046046) were purchased from Qiagen.

Total RNA was extracted from cells using the RNeasy Plus Mini kit (Qiagen, USA). The quality and concentration of RNA was determined by spectrophotometry. Only samples exhibiting an A260/A280 ratio equal to or above 1.8 were selected and stored at -80°C for further applications. Reverse transcription of RNA was performed according to the manufacturer's instructions using the InProm-IITMreverse transcription system (Promega A3800). Briefly, 1 µg of RNA was combined with 0.5 µg of Oligo (dT)15 primer in a 5 µl volume and denatured at 70°C for 5 min, chilled on ice and combined with reverse transcription reaction mix (1X ImProm-IITMReaction buffer, 3 mM MgCl2, 0.5 mM dNTP mix, 20 units RNasin® ribonuclease inhibitor and 1 µl of ImProm-IITMreverse transcriptase) to a final volume of 20 µl. After a brief annealing at 25°C for 5 min, the

reactions were incubated at 42°C for 1 hr, followed by a 15 min incubation at 70°C to inactivate the reverse transcriptase prior to PCR. Quantitative real time PCR was conducted with the Sensimix lite kit (Quantace QT 405-05, USA). PCR reactions containing 1X Sensimix Lite, 1X SYBR Green, 0.75 µl Enzyme mix and 1.5 µl of combined forward and reverse primers (Quantitect real-time PCR primers, Qiagen) per 9 µl reaction were made up as a master mix and aliquoted into glass capillaries, with 1 µl of cDNA added to give a final reaction volume of 10 µl. The capillaries were sealed, centrifuged at 522500 rpm for 30 sec and placed in the LightCycler Version 3 (Roche, Switzerland). PCR cycle parameters were: denaturation (15 min at 95°C), annealing and amplification at 35 cycles (5 sec at 95°C; 3 sec at 55°C; 5 sec at 72°C), melting temperature (15 sec at 65°C) and a cooling step (30 sec at 40°C). Each DNA sample was quantified in duplicate and a negative control without cDNA template was run with every assay to assess the overall specificity. Melting curve analyses was carried out to ensure product specificity and data was analyzed using the 2-ΔΔCtmethod. Relative mRNA expression levels were normalized to glucuronidase beta (*GUSB*) for each reaction with PCR efficiency correction calculated using the formula Ratio = (Etarget)CPtarget(control – sample)/(Eref)CPref(control – sample) ; E: real-time PCR efficiency, CP: crossing-point. Primers used to amplify the human *TBX2* (QT00091266), *TBX3* (QT00022484) and *GUSB* (QT00046046) cDNAs were purchased from Qiagen, USA. The Microsoft Excel programme was used to calculate the standard deviation and statistically significant differences between samples using the Student t test. P values of <0.05 were considered statistically relevant.

2.6 Cell proliferation assays

2.6.1 Growth curves

Cell counts, using a haemocytometer, were determined as described previously (Prince *et al.*, 2003). Cells were seeded in triplicate in a 12-well plate at a density of 1 X 10^4 cells/well for the MCF-7 shctrl and shTBX3 cell lines. Cells were collected by trypsinisation and counted on a haemocytometer at 2-3 day intervals.

2.6.2 5-bromo-2-deoxyuridine (BrdU) incorporation assay

Cells were seeded on glass coverslips in 35 mm tissue culture dishes at a density of 4 X 10^4 cells/ml and allowed to adhere. The cells were then incubated in medium containing 10 µM BrdU for 3 hrs followed by fixing with Carnoy's Fixative (see **Appendix, section 6.6**) at -20°C for 20 min. For immunostaining, the cultures were incubated in 2N hydrochloric acid at 37°C for 1 hr, neutralised in 0.1 M borate buffer (see **Appendix, section 6.6**), rinsed with 1 X PBS containing 0.05% Tween-20 (1XPBS/T) and incubated in 1 X PBS/T with 5% swine serum for 30 min at 37°C. BrdU was detected with the anti-BrdU mouse monoclonal antibody (6 µg/ml, Roche, Germany) for 30 min at 37°C, followed by a secondary IgG coupled to Alexa 488 (1:1000, Molecular Probes, USA) for 30 min at 37°C. Cells were washed with 1 X PBS/T, incubated with 1 µg/ml DAPI (4',6-diamidino-2-phenylindole) (Sigma, USA) diluted in 1 X PBS for 10 min at RT in the dark, washed again, mounted onto slides and visualised by fluorescence microscopy using an Axiovert fluorescent microscope (Zeiss, Germany)**.**

2.6.3 MTT (3-(4,5-dimethylthiazol-2-yl)-2,5-diphenyltetrazolium bromide) assay

To determine cell growth using the methylthiazol tetrazolium (MTT) Cell Proliferation Kit, cells were seeded in quadruplicate in a 96-well plate (1000 cells/well) and cell viability determined according to the manufacturer's instructions. Briefly, 24 hrs prior to harvesting 10 µl of pre-warmed MTT labelling reagent was added to each well and 4 hrs later 100 µl of pre-warmed solubilisation solution was added to the cells. The spectrophotometrical absorbance of the samples was determined at a wavelength of 595 nm using a 96-well plate reader, with the absorbance of the medium only control being subtracted from the samples. Cell proliferation was determined over 10 days.

2.7 Transformation assays

2.7.1 Growth factor dependence assay

For the growth factor-dependence assay, cell proliferation was compared in medium containing either 2% or 10% FBS, using short-term growth assays as described in section 2.6.1 above.

2.7.2 Soft agar assay

For soft agar assays, 35 mm tissue culture dishes were coated with a 1% agar/medium layer to prevent cells from attaching to the bottom of the dish. Dishes were incubated at 4°C O/N to allow the agar to solidify. Cells were resuspended in 0.35% agar/medium slurry and plated on top of the 1% agar/medium layer at a concentration of 5000 cells per 35mm dish. In order to prevent the agar/medium slurry from desiccation, 1 ml of fresh medium was added per dish. The dishes were incubated at 37°C in the presence of 5% CO_2 for 30 days and a few drops of fresh medium was added twice a week. Cell viability was determined by O/N incubation with p-iodonitrotetrazolium-chloride (Sigma, USA), which forms a purple formazan dye when reduced. Pictures were taken using a non-phase contrast lens (Sony cybershot, DSC-T20). Higher magnification images were taken using an Axiovert fluorescent microscope (Zeiss, Germany) (10x magnification).

2.7.3 Cell migration assays

Two methods were utilised to determine cell migratory ability, namely: two-dimensional in vitro scratch motility assay and transwell cell motility assay, which will be described below.

2.7.3.1 Cell scratch motility assay

Cells were grown to confluence in 35 mm tissue culture dishes. A linear wound was made by scratching through the monolayer using a sterile 200 µl pipette tip. To remove cell debris, the growth medium was replaced, and to prevent cell proliferation Mitomycin C (Sigma, USA) was added at a final concentration of 10 µg/ml. Several markings were made along the edges of the scratch line which were used as reference points and the wound widths measured at the time of the scratching (0 hr) and thereafter at 1 – 2 hrs intervals. To induce migration in the MCF-7 cells, 12-O-tetradecanoyl-phorbol-13-acetate (TPA) was added at a final concentration of 10 nM. TPA induces migration in poorly migrating cell lines, including MCF-7 cells, by downregulating protein kinase C, a factor which suppresses cell migration (Jackson *et al.*, 2005). Pictures were taken using a phase contrast microscope and migration distances were measured using Axio software (Zeiss,

Germany). The difference in width represents the distance migrated in µm.

2.7.3.2 Transwell migration assay

$1x10^5$ serum starved cells were plated on the upper section of transwell chamber in 500 µl medium containing 1% FCS. Transwells were then placed on well of 12-well plate filled with 1 ml medium containing 10% FCS which was served as chemo-attractant. Each condition is carried out in triplicate and there is a well designated for total cell control. To encourage cell migration, TPA was added to all wells at a final conc. 100 nM. Plates were covered with foil and incubated at 37 ^oC for 24 hrs. The upper section of each triplicate well was wiped cleaned by a sterile ear bud to get rid of the cells that had not migrated through the membrane. The remaining cells and cells from total cell control wells were fixed in methanol and stained by crystal violet by dipping the wells into appropriate solutions and rinsed twice by sterile water. The wells were then dried O/N in the hood before the stains on the wells was washed off using 150 µl 50% acetic acid solution. The stain solution was then transferred to 96-well plate and the spectrophotometrical absorbance of the samples was determined at a wavelength of 595 nm using a 96-well plate reader.

2.8 Luciferase assays

Cells were transfected as described (see 2.2.2), cultured for 40 hrs and extracts were then assayed for firefly luciferase activity using the dual luciferase assay system (Promega, Madison, WI, USA) according to the manufacturer's instructions. Briefly, cells cultured in a 35 mm dish were lysed using 1 X lysis buffer (Promega, Madison, WI, USA) and subjected to freeze-thaw cycle O/N. On the next day, the cell lysate was briefly pulsed by bench top picofuge at RT and the supernatant was immediately assayed for firefly luciferase reporter activity using the dual luciferase assay system (Promega, USA). Luciferase activities were measured using the Luminoskan Ascent luminometer (Thermo Labsystems, Franklin, MA, USA). Firefly luciferase values were expressed relative to (a) empty-vector control or (b) untreated samples as compared to TGF-β1 treated. All transfections were performed in duplicate and at least three independent experiments

were done to confirm reproducibility. The Microsoft Excel programme was used to calculate the standard deviation and statistically significant differences between samples using the Student t test. P values of <0.05 were considered statistically relevant.

2.9 Immunofluorescence microscopy

MCF-12A or HaCaT cells grown on glass coverslip slides 3 hrs or 12 hrs after TGF-β1 treatment were washed with phosphate-buffered saline (PBS) and fixed with 4% paraformaldehyde for 10 min at room temperature. After three PBS washes, cells were then permeablised in 0.2% Triton X-100 in PBS for 5 min at room temperature, followed by a 1 hr incubation in blocking buffer (5% swine serum in PBS) at RT and incubated with rabbit TBX3 polyclonal antibody (42-4800, Zymed, Invitrogen, USA) at a dilution of 1:25 in blocking buffer at 4°C O/N in a humidifying chamber. Cells were washed in PBS and incubated with the appropriate secondary antibody coupled to Cy3 (Jackson ImmunoResearch, USA) at 1:1000 dilution for 2 hrs at RT in the dark. Cells were again washed in PBS and the DNA was stained by incubating the cells with 1 µg/ml DAPI (4',6-diamidino-2-phenylindole) (Sigma, USA) diluted in PBS for 5 min at RT in the dark. Cells were washed, the coverslips mounted onto glass slides with mounting medium (80% glycerol in water containing anti-fade (n-Propyl gallate) (Sigma, USA)) to prevent the signal fading and the cells visualised by fluorescence microscopy using an Axiovert fluorescent microscope (Zeiss, Germany). Negative controls were as for above, but the primary antibody was excluded.

2.10 siRNA sequences and transfection

The Cells were transfected with siRNAs using HiPerFect (Qiagen, USA) according to manufacturer's instructions. Treatment started 24 hrs post transfection. The anti-Smad4 siRNA (SI00076041), anti-TBX3 siRNA (SI00083503) and a control (non-silencing) siRNA were purchased from Qiagen (USA) and the anti-JunB siRNA (sc-35726) was purchased from Santa Cruz (USA).

2.11 Chromatin immunoprecipitation (ChIP) assays

ChIP assays were carried out as previously described (Prince *et al.*, 2004b). Briefly, 15cm dishes containing 80% confluent MCF-12A cells treated with TGF-β1 for 3 hrs were fixed in 1% formaldehyde at RT for 10 min, to crosslink proteins to DNA. The reaction was quenched with 125 mM glycine for 5 min at room RT. Cells were span down at 1600 rpm for 5min at 4°C and resuspended in 15 ml chilled 1 X PBS and span and resuspended in 1.5 ml 1XPBS. Cells were pelleted at 1500 x g at 4°C for 5 min, washed once in PBS, once in buffer 1 (see **Appendix, section 6.7**) and once in buffer 2 (see **Appendix, section 6.7**) , prior to lysis in 500 µl lysis buffer (see **Appendix, section 6.7**) plus protease inhibitors. Samples were sonicated to obtain fragments between 300 bp to 500 bp and span at 13 000 rpm for 10 min at 4°C and cell debris discarded. For each sample, 330 µl of sonicated cell lysate was diluted with immunoprecipitation buffer (see **Appendix, section 6.7**) plus protease inhibitors to a final volume of 1.5 ml and pre-cleared three times with Protein A/G PLUS-Agarose beads (sc-2003, Santa Cruz Biotechnology, USA) rotating at 4°C for 1 hr each time. Protein-bound DNA was immunoprecipitated using Protein A/G PLUS-Agarose beads and 5 µg of antibody against JunB (sc-73) or Smad4 (sc-7154) or TBX3 (sc-17871) or IgG (negative control, sc-2027, Santa Cruz Biotechnology, USA) with 1% of the supernatant volume reserved as input. Samples were rotated at 4°C O/N, followed by incubation with 50 µl of protein A/G beads rotating at 4°C for 3 hrs. Samples were span down and beads were sequentially washed twice for 10 min rotating at 4°C in 500 µl wash buffers 1-4 (see **Appendix, section 6.7**). The beads were collected and incubated in 100µl Extraction buffer (see **Appendix, section 6.7**) for 15 min at RT, span at 2000 x g for 1 min and supernatant saved. The extraction was repeated with another 100 µl to yield 200 µl supernatant in total. The input sample was made up to 200 µl with extraction buffer and all samples were incubated at 65°C in the heating block O/N to reverse the crosslink between DNA and proteins. The immunoprecipitated DNA was purified using the PCR purification kit (Qiagen, USA) and analysed by qRT-PCR using a primer pair amplifying the region spanning the AP1 binding site or SBE at position -80 bp of *TBX3* promoter or a T-element at -187 bp on *TBX2* promoter or a non-specific promoter region (GAPDH, Qiagen, USA). Crossing values (Ct) of precipitated DNA were

normalized against the Ct values of IgG. qRT-PCR was perform same as described in section 2.5. Primer pairs specific for the *TBX3* promoter: (5'-CTAGAGGCGACTCTGTGCGC-3' and 5'-CGCTTTCGGACCAATTGTGTTGC-3'), or for the *TBX2* promoter: (5'-TGGCCTGAGCTGTCAAAAC-3' and 5'-GCGCGACTGGTTAGATCTTG-3'), or a non-specific region in the *GAPDH* gene: (5'-CAGCCAGACGAGGACACA-3' and 5'-CCTTTCTGGGATTGCCTTTC -3'). Fold enrichment was determined using the ΔΔCt method: Fold enrichment= $2^{-(\Delta Ct1-\Delta Ct2)}$, where ΔCt1 is the ChIP of interest and ΔCt2 is the IgG. Statistical differences were determined using a student T-test. Significance was accepted at $p< 0.05$.

2.12 Non-radioactive Electromobility shift assay (EMSA)

Nuclear extracts from 3hr TGF-β1 treated MCF-12A cells were prepared as previously described (Smith *et al.*, 2011). Briefly, cells from sub-confluent 15 cm dishes were washed twice with 1X PBS, trypsinised, span down at 1500 rpm for 5 min at 4^{o}C. Cell pellet was 1 ml ice cold 1 X PBS, span down and resuspended in 800 µl ice cold 1 X PBS and span down at 3000 g for 30 s at 4^{o}C. The pellet was resuspended in 5 cell volumes of cold cell buffer 1 (see **Appendix, section 6.8**), incubated on ice for 15 min and was added with 0.3% volume 10% Triton-x100, incubated on ice for 5 min and span down for 4 min at 3000 g at 4^{o}C. Cell pellet was resuspended in equal volumes of buffer 2 (see **Appendix, section 6.8**) with protein inhibitors and DTT (5 mM final conc.) Protein concentration was assayed by BCA assay (Pierce, USA). The biotin labelling of DNA oligo was performed using the DNA 3' end Biotinylation kit (Pierce) according to manufacturer's instructions. Briefly, the labelling reaction was made with: 1X TdT Reaction Buffer, 100 nM Unlabeled Control Oligo (single stranded), 0.5 µM Biotin-11-UTP and 0.2 U/µl diluted TdT in a total volume of 50 µl and incubated at 37°C for 30 min. The reaction was stopped with 2.5 µl 0.2M EDTA. The labelled DNA oligo was purified using 50 µl chloroform:isoamyl alcohol and the top aqueous phase was collected. To anneal the labelled oligos, complementary strands were mixed and heated at 90°C and slowly cooled down to RT.

For EMSA assay, protein-oligo binding reactions were prepared with 15 µg nuclear

extract, 4 µl 5 x incubation buffer (see **Appendix, section 6.8**), 1 µl poly dI/dC (1 µg/µl), 1 µl DTT (10 mM) and unlabeled wild type (5'-GCCAATCAAGAGGCCTCCGGCTCCCCGC-3') or mutant competitor (5'-GCCAATCAAGAAGCTTTCGGCTCCCCGC-3') to a final volume of 20 µl. The full reaction volume was loaded onto a pre-electrophoresed 8% native polyacrylamide gel, electrophoresed at 200 V for 1 hr and transferred on nylon membrane at 380 mA for 30 min. DNA was cross linked to the membrane using a UV Stratalinker 1800 apparatus (Stratagene) and processed for chemiluminescence detection using the LightShift Chemiluminescent EMSA Kit (Pierce) according to manufacturer's instructions. Signals were visualized with a UVP biospectrum imaging system (visionworks LS software).

2.13 DNA affinity immunoblot (DAI) assay

Biotinylated DNA oligos and nuclear extract were prepared as described for EMSA. Biotinylated probes were immobilized on 100 µg of Dynabeads Streptavidin (Dynal Invitrogen, USA) according to the manufacturer's instruction. For each DNA-binding reaction, 40 µg nuclear extract was incubated with 1 µg bound biotinylated DNA probe in 200 µl binding buffer (see **Appendix, section 6.9**) at 4°C for 30 min with gentle rotation. The beads were extensively washed with binding buffer and boiled in 25 µl of 2 × protein loading buffer (see **Appendix, section 6.9**) to release proteins bound to the oligo. Proteins bound to the biotinylated probes were analyzed by SDS–PAGE, followed by immunoblotting using rabbit polyclonal anti-JunB (sc-73) or anti-Smad4 (C-19) antibodies or anti-TBX3 (sc-17871) (Santa Cruz Biotechnology, Santa Cruz, CA).

2.14 Flow Cytometry

Cells were collected by trypsinisation, washed twice with PBS, resuspended in 2 ml of cold PBS and counted on a haemocytometer to determine the volume of Propidium Iodide solution (see **Appendix, section 6.10**) that will be added. Cells were fixed in 8 ml of 70% cold ethanol for at least 30 min at -20°C. Fixed cells were collected by centrifugation at 1500 rpm for 5 min at RT, washed twice with PBS and centrifuged at 6000 rpm for 1 min at RT. Before flow cytometry analyses, the samples were treated with

RNase A (50 µg/ml) for 15 min at 37°C and immediately stained for 30 min at RT with PI solution, to yield a final concentration of 1 X 10^6 cells/ml. A minimum of 50 000 cells/sample were subjected to analysis using a Beckman Coulter FACSCalibur flow cytometer (Beckman Coulter, USA). Cell cycle profiles were analysed using the Modfit LT™ (Verity Software House, USA) Software.

CHAPTER 3

RESULTS

Introduction

TBX3 is overexpressed in a slew of cancers including a subset of breast cancer cell lines and tumours (Fan *et al.*, 2004; Hansel *et al.*, 2004; Lomnytska *et al.*, 2006; Renard *et al.*, 2007; Rodriguez *et al.*, 2008; Yarosh *et al.*, 2008; Fillmore *et al.*, 2010). However, at the time that this project started, it was unclear whether this aberrant expression was causative or consequential to cancer formation. Furthermore, the mechanism(s) responsible for upregulating TBX3 and the targets that mediate TBX3's role in breast cancer were poorly understood. The current study therefore aimed to address these questions by first establishing both TBX3 knock down and overexpressing cell culture models and investigating the effects of altering TBX3 levels on key features of tumourigenesis including cell proliferation, migration and anchorage independence. Secondly, the regulation of TBX3 by TGF-β1 signalling pathway implicated in breast cancer was investigated. Finally, the TBX3 homologue, TBX2, is shown to be downstream of TBX3 in inducing the anti-proliferative effect of TGF-β1 and a full characterisation of this regulation is described.

3.1 *Establishment and characterisation of a human breast cancer cell culture model in which TBX3 expression was stably knocked down*

3.1.1 Establishment of MCF-7 cell lines in which TBX3 was stably silenced

A good way to understand the function of a protein is to knock out or knock down its gene expression and to study the consequences on cellular functions. Silencing a specific gene can be achieved by using RNA interference (RNAi) approaches which include short interfering (si)RNA and short hairpin (sh)RNA. While both of these two approaches specifically target homologous mRNAs for degradation (Hannon, 2002; Dykxhoorn *et al.*,

2003), the siRNA only transiently knocks down the expression of targeted genes but shRNAs work in a more sustained manner because it gets integrated into the host genomic DNA. The shRNA approach was therefore employed in order to study the long-term effects of knocking down TBX3 in the MCF-7 breast cancer cell line.

The MCF-7 breast cancer cells were stably transfected with the pSuper.neo/GFP (Oligoengine) expression vector containing a shRNA sequence that target *TBX3* or a non-specific control sequence (these constructs are described in Peres et al., 2010). The cells were treated with G-418 (400 µg/ml) for a minimum of 10 days to select for successfully transfected Neomycin-resistant clones. The knock down of TBX3 expression was monitored and verified by qRT-PCR and western blot analysis (**Fig. 3.1**). As the TBX3 knock down cell lines shTBX3(2) and shTBX3(8) showed significant reduction of TBX3 mRNA and protein levels compared to the control cell line shctrl(5), these cell lines were used for further analyses. Expression of p38 was used as a measure of equal loading throughout this study because although its activity is modulated by phosphorylation, total levels of this protein remain unchanged in response to stimuli (Raingeaud *et al.*, 1995).

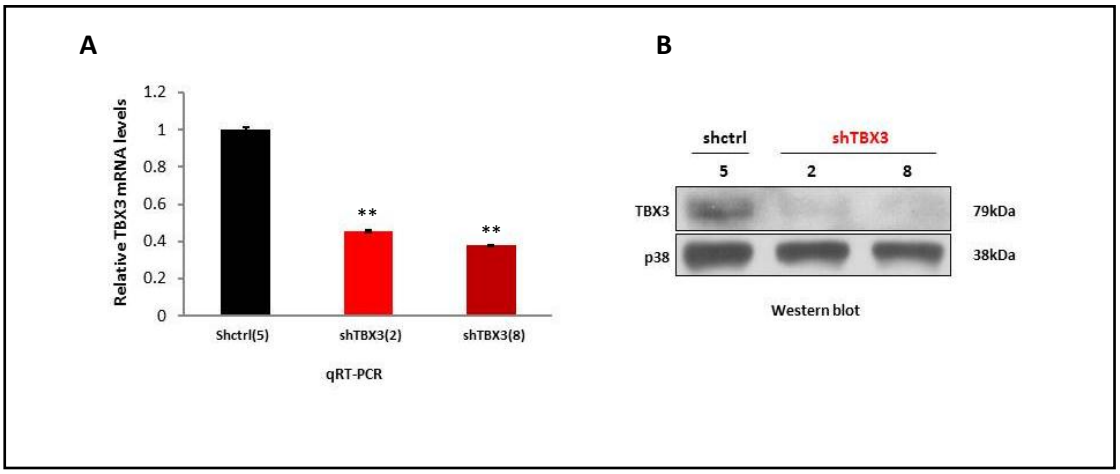

Figure 3.1 Establishment of MCF-7 breast cancer cell lines in which TBX3 was stably silenced. Cells were stably transfected with the pSuper.neo/GFP (Oligoengine) expression vector containing either a *TBX3* specific siRNA sequence (MCF-7 shTBX3) or a non-specific, scrambled control sequence (MCF-7 shctrl). (A) qRT-PCR was performed on reverse transcribed RNA using primers specific to *TBX3* and mRNA levels were normalised to *GUSB* and expressed relative to shctrl(5) mRNA. The result of one qRT-PCR experiment is shown which is representative of two independent experiments, each performed in duplicate. A Microsoft Excel student t-test was performed to calculate statistical significance (**p<0.001). Error bars represent standard deviation. (B) Protein extracts harvested from the indicated cell lines were subjected to western blotting using an anti-TBX3 antibody and p38 was used as a loading control.

3.1.2 Knocking down TBX3 in MCF-7 breast cancer cells results in an increase in substrate dependent and substrate independent proliferation and a decrease in expression of key cell cycle regulators

A critical trait of cancer cells involves their ability to bypass senescence and sustain uncontrolled proliferation (Hanahan and Weinberg, 2000). While expanding the cell lines, it was observed that the MCF-7 shTBX3 cells were growing more rapidly than the shctrl cells. To confirm this, MCF-7 shTBX3 and shctrl cells were cultured in standard medium containing 10% serum and their growth rate compared by counting cells using a haemocytometer over a 9 day period. Indeed, the shTBX3(2) and shTBX3(8) cells started to significantly outnumber the shctrl cells from day 7 (**Fig. 3.2A**).

As growth factor independence is another trait acquired by transformed cells (Hanahan *et al.*, 2000), the impact of knocking down TBX3 expression on the proliferative ability of the MCF-7 breast cancer cells cultured in medium containing low (2%) serum was investigated. While the shTBX3 cell lines still maintained a higher growth rate compared

to the shctrl cells in low serum (**Fig. 3.2B)**, the growth rate of the cells cultured in 2% serum was reduced in general compared to the cells cultured in 10% serum (compare cell numbers in **Fig. 3.2A** and **B**). Taken together, these results suggest that silencing TBX3 expression increases cell proliferation in a growth factor independent manner.

To investigate whether the positive effect of knocking down TBX3 on cell proliferation was due to an altered expression of key negative regulators of the cell cycle, the levels of p53, p21 and $p14^{ARF}$ were checked by western blot analyses. As **figure 3.2C** shows, the expression of these factors was largely reduced in shTBX3 cells compared to the shctrl cells. This suggests that the increase in the proliferative ability observed when TBX3 was silenced in MCF-7 cells resulted from the repression of these factors. Interestingly, however, this is not consistent with previous reports showing that TBX3 transcriptionally represses $p14^{ARF}$ and p21 (Brummelkamp *et al.*, 2002b; Hoogaars *et al.*, 2008). As these factors can also be repressed by TBX2, which has been implicated as a TBX3 target (Prince *et al*, 2004; Jacobs *et al*, 2000; Lingbeek *et al*, 2002; Rodriguez *et al*, 2008), it was speculated that the reduced levels of these key cell cycle regulators resulted from an enhanced expression of TBX2. However, western blot results do not support this hypothesis suggesting that their decreased expression is caused by factors other than TBX2 (**Fig. 3.2C**).

Cancer cells acquire the ability to proliferate independently of a substrate in order to form tumours (Hanahan *et al.*, 2000; Hanahan and Weinberg, 2011). To determine whether TBX3 is required for anchorage independent growth, the ability of shctrl and shTBX3 cells to form colonies in suspension was next investigated using soft agar assays. MCF-7 shctrl(5) and shTBX3(8) cells were suspended in 0.35% soft agar and plated on top of a 0.5% agar-medium layer and the colonies formed were monitored after 30 days. **Figure 3.2D** shows that unlike the shctrl(5) cells that formed predominantly small colonies, the shTBX3(8) cells formed considerably larger viable colonies. Taken together, these results suggest that TBX3 impacts negatively on both substrate-dependent and substrate independent cell proliferation.

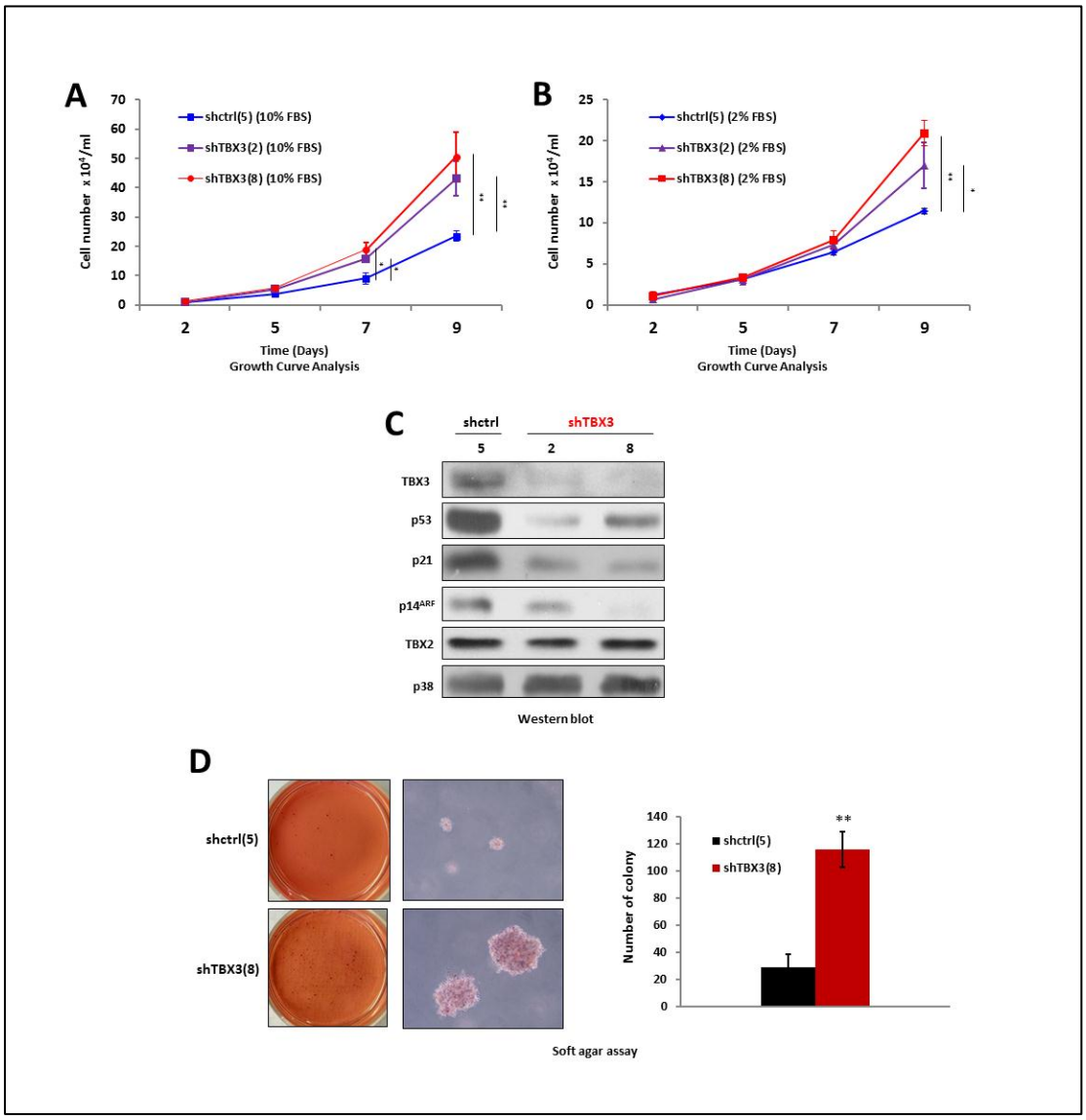

Figure 3.2 Silencing TBX3 increases the proliferation rate of MCF-7 cells and leads to a decrease in key cell cycle regulators. (A) Cells were seeded in triplicate at a density of 1 X 10^4 cells per well of a 12-well plate and were grown in medium containing 10% fetal bovine serum (FBS). Growth curve assays were performed over a 9 day period and cells harvested by trypsinisation and counted on a haemocytometer. (B) Cells were seeded as in (A) in medium containing 2% FBS. Growth curve assays were performed as described for (A). The results shown in A and B are representative of three independent experiments. A Microsoft Excel student t-test was performed to calculate statistical significance (*p<0.05; **p<0.001); error bars, SD. (C) Protein extracts harvested from the indicated cell lines were analysed on 10-15% SDS-PAGE and by western blotting using antibodies to indicated proteins. p38 was used as a loading control. (D) 5000 cells were resuspended in 0.35% agar-medium slurry and plated on top of a 0.5% agar-medium layer and allowed to proliferate for 30 days. Cell growth was assessed by staining with p-iodinitrotetrazolium chloride to indicate viable populations. Whole dishes were photographed and micrographs were captured at 10x magnification (left) and the number of colonies of shctrl and shTBX3 cell lines tested. The result of one soft agar assay is shown which is representative of three independent experiments, each performed in duplicate.

3.1.3 Silencing TBX3 in MCF-7 breast cancer cells inhibits cell migration

While transformed cells acquire the ability to migrate and invade adjacent tissue this has been reported to be mutually exclusive to their ability to proliferate which is referred to as the migration-proliferation dichotomy (Fedotov & Iomin, 2007). The effect of knocking down TBX3 on the migratory ability of MCF-7 breast cancer cells was therefore investigated using a two-dimensional *in vitro* scratch cell motility assay. As MCF-7 cells have poor invasive ability, their migration was induced in the experiment by the addition of 12-O-tetradecanoylphorbol-13-acetate (TPA), a chemical that activates the protein kinase C pathway (Parker *et al.*, 1987; Basu *et al.*, 1990). Briefly, cells were grown to confluence and a linear wound was made by scratching the cell monolayer. To exclude the effect of cell proliferation on the results, cells were treated with mitomycin C, a *de novo* proliferation inhibitor, before TPA treatment. As **figure 3.3A** shows, the shTBX3 cells had a significantly reduced migration rate compared to that of the shctrl cells. These results were confirmed by a three-dimensional transwell assay. Briefly, serum starved cells were plated on a transwell membrane of an upper transwell chamber in medium containing 1% FBS and a lower transwell chamber contained medium with 10% FBS which served as chemo-attractant. TPA and mitomycin C were added to both transwell chambers at a final concentration of 100 nM and 10 μg/ml respectively. The number of cells that migrated through the transwell membrane was counted and calculated as a percentage of total cells originally plated. As can be seen in **figure 3.3B**, significantly fewer shTBX3(8) cells were able to migrate through the membrane compared to shctrl cells. These results are consistent with previous reports demonstrating a pro-migratory role for TBX3 (Rodriguez *et al.*, 2008).

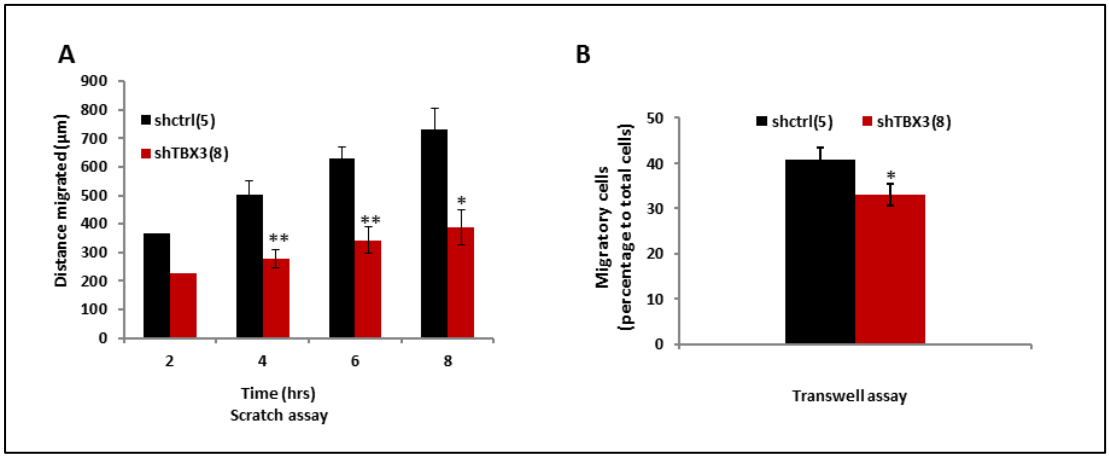

Figure 3.3 Knocking down TBX3 in MCF-7 cells reduces migration. (A) Cell migration was measured using a two-dimensional in vitro scratch motility assay. Cells were grown to confluence and a linear wound was made by scratching through the monolayer using a sterile 200 µl pipette tip. TPA (10 nM) and mitomycin C (10 µg/ml) were added to induce cell migration and prevent cell proliferation respectively. The distance migrated between pre-marked points along the scratch was measured using AxioVision 4.8 software (Zeiss, Germany) at 2 hr intervals over an 8 hr period. (B) Cell migration was measured using a transwell motility assay. $1x10^5$ serum starved shctrl(5) and shTBX3(8) cells were plated in a transwell insert (upper compartment) in 1% FBS serum media which was placed over a lower chamber containing 10% FBS serum media which serves as chemo-attractant. After 24 hr the cells that migrated through the membrane were stained and dried. The stain was then dissolved and measured with a spectrophotometer. Microsoft Excel student t-test was performed to calculate statistical significance (*$p<0.05$; **$p<0.001$); error bars, SD. The results shown for (A) and (B) are representative of three independent experiments which were performed in triplicate.

3.2 *Establishment and characterisation of normal human breast epithelial cells transiently overexpressing* TBX3

3.2.1 Overexpressing TBX3 in normal breast epithelial cells inhibits cell growth and promotes migration.

The above results showed that knocking down TBX3 in MCF-7 breast cancer cells resulted in increased proliferation and reduced migration. Because these experiments were performed in an already transformed cell line, the question arose as to whether the overexpression of TBX3 in normal breast epithelial cells is sufficient to inhibit cell proliferation while promoting migration. To this end, TBX3 was transiently overexpressed in “normal” human MCF-12A breast epithelial cells using an inducible adenovirus tet-off system. Briefly, the human TBX3 cDNA was cloned into the vector component of an

Adeno-X Tet-off system 1 and the adeno-TBX3 virus was produced in human embryo kidney HEK293 cells and purified. To overexpress TBX3, the MCF-12A cells were transduced with adeno-TBX3 virus and the control cells were transduced with adeno-TBX3 but were treated with Doxycyclin (Dox) to inhibit the viral-promoter-driven transcription of *TBX3*. As can be seen in **figure 3.4A**, compared to the untransduced (adeno-TBX3$^-$/Dox$^-$) and adeno-TBX3$^+$/Dox$^+$ control cells, the adeno-TBX3 virus transduction of MCF-12A cells significantly increased the expression of TBX3.

The 5-bromo-2-deoxyuridine (BrdU) incorporation assay was performed to determine the effect of overexpressing TBX3 on the ability of MCF-12A breast epithelial cells to proliferate. Briefly, equal numbers of TBX3-overexpressing and control MCF-12A cells were plated and pulsed with BrdU, an analogue of thymidine for 3 hrs. BrdU gets incorporated into the newly synthesized DNA in place of thymidine and can be detected by immunofluorescence with an antibody to BrdU. **Figure 3.4B** shows the total number of BrdU positive nuclei as a percentage of the total number of cells from 10 fields of view for each cell line. A significant reduction in BrdU-positive cells was observed in the TBX3-overexpressing cells compared to the control cell lines, suggesting that the overexpression of TBX3 in MCF-12A cells leads to an inhibition of cell proliferation. Consistent with the TBX3 knock down data, TBX3 overexpression was accompanied by an increase in p21 levels but interestingly, it correlated with a decrease in TBX2 levels (**Fig. 3.4C**).

When the impact of TBX3 overexpression on migratory ability was assessed using a scratch motility assay, the results show that the TBX3 overexpressing cells migrated significantly faster (**Fig. 3.4D**). Together, these findings show that TBX3 impacts negatively on cell proliferation but promotes cell migration of “normal” MCF-12A breast epithelial cells. This supports the findings of the TBX3 knock down data shown above.

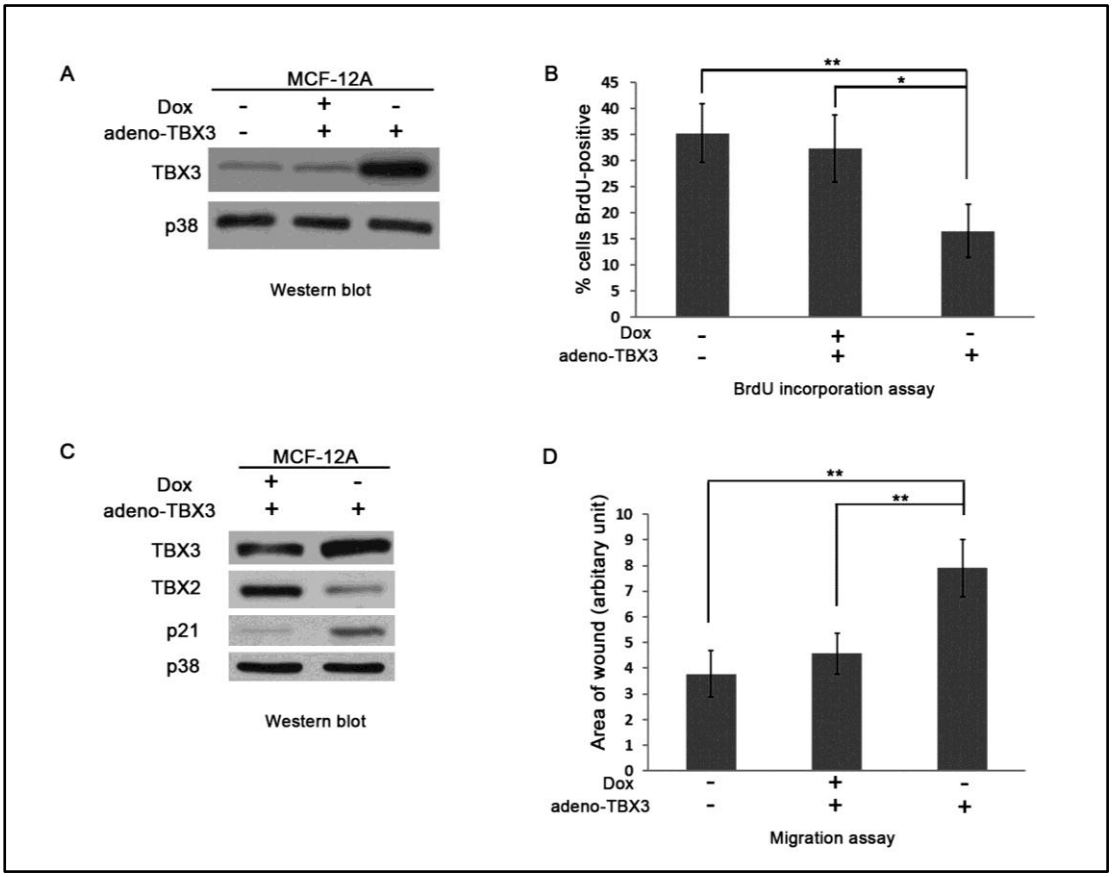

Figure 3.4 TBX3 overexpression inhibits cell proliferation but promotes migration. (A) MCF-12A cells were transduced with an Adeno-TBX3 Tet-off virus, which allows TBX3 expression to be regulated by 10 µg/ml Doxycyclin (Dox). The efficacy of the system was tested by subjecting protein from the indicated cells to western blot analysis with an antibody specific to human TBX3. p38 was used as a loading control. (B) TBX3 overexpression inhibits cell proliferation. MCF-12A cells from (A) were incubated with 10 µM BrdU for 3 hrs and then processed for immunocytochemistry with an anti-BrdU antibody. The total number of BrdU-positive nuclei was visualized by fluorescence microscopy and expressed as a percentage of the total number of cells from 10 fields of view for each condition (images not shown). The result of one BrdU incorporation assay is shown which is representative of two independent experiments. (C) MCF-12A cells were transduced with adeno-TBX3 virus and doxycycline (Dox) (10 µg/ml) as indicated and the protein harvested was subjected to western blot analysis using antibody specific to human TBX3, TBX2 or p21 and p38 was used as a loading control. (D) TBX3 overexpression promotes migration. MCF-12A cells from (A) were incubated for 48 hrs and subjected to the two-dimensional in vitro scratch assay. Cells were grown to confluence and a linear wound was made by scratching through the monolayer using a sterile 20 µl pipette tip. Mitomycin C (10 µg/ml) was added to prevent cell proliferation and migration measured. The result shown is representative of two independent migration assays and is expressed as an average of 10 fields of view for each condition. A Microsoft Excel student t-test was performed to calculate statistical significance (*$p<0.05$, **$p< 0.001$). Error bars represent standard deviation.

3.3 *TBX3 is a downstream target and mediator of the transforming growth factor β1 (TGF-β1) signalling pathway*

The results above suggest that increased levels of TBX3 inhibit cell proliferation but promote migration of both normal and transformed breast cells. This led to the question as to what are the molecular pathway(s) that up-regulate *TBX3* gene expression. TGF-β1 was considered as a candidate because like TBX3, it plays an important role in mammary morphogenesis and is notoriously activated during breast cancer development (Moses and Barcellos-Hoff, 2011). In addition, it is also well known to inhibit proliferation but promote cell migration (Imamura *et al.*, 2012; Jahn *et al.*, 2012). Furthermore, microarray studies in which normal human breast epithelial cells and keratinocytes were treated with TGF-β1 showed an activation of TBX3 (Kang *et al.*, 2003). This chapter explores the possibility that TGF-β1 may directly activate TBX3 expression to mediate its biological activity.

3.3.1 TGF-β1 transcriptionally activates TBX3 expression in MCF-12A breast epithelial cells and HaCaT keratinocytes

To begin to explore the possibility that TBX3 expression is regulated by TGF-β1, MCF-12A and HaCaT keratinocytes were treated with TGF-β1 or vehicle over a time course spanning 8 hrs to 36 hrs and total protein harvested from the cells was subjected to western blot analyses. The results show that TBX3 levels increased substantially in response to TGF-β1 treatment in both cell lines (**Fig. 3.5A, B**). To confirm the activation of TBX3 levels by TGF-β1, MCF-12A and HaCaT cells were treated with TGF-β1 for 12 hrs and processed for immunofluorescence with an antibody specific to human TBX3 and the cells visualised by fluorescence microscopy. **Figure 3.5C, D** shows that TGF-β1 treated cells have an increase in nuclear TBX3 levels compared to the control cells. Together, these results demonstrate that TGF-β1 upregulates the levels of TBX3 in MCF-12A and HaCaT cells.

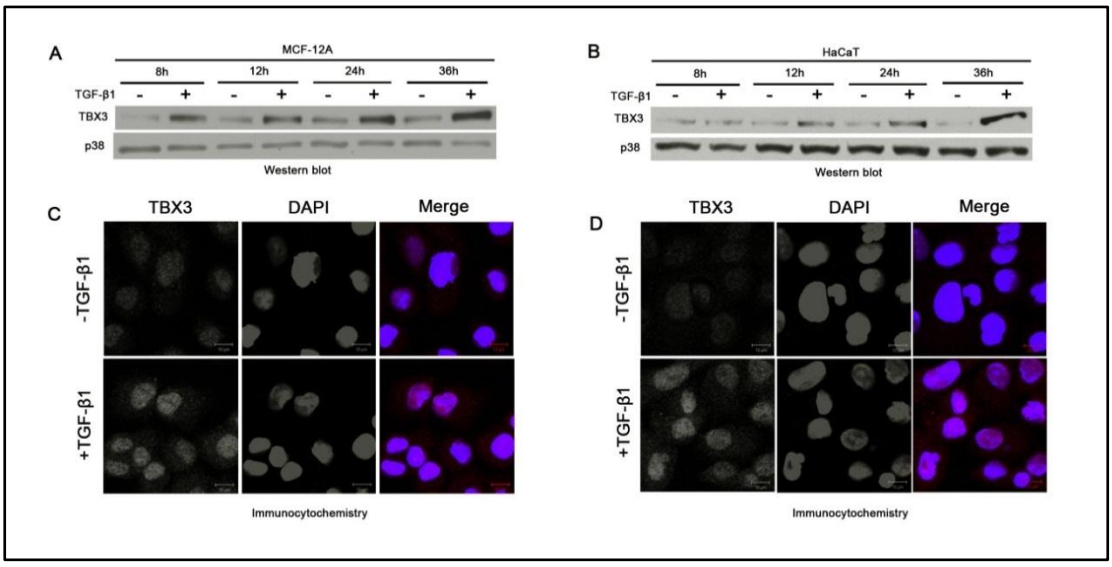

Figure 3.5 TGF-β1 activates TBX3 protein expression. TBX3 protein from MCF-12A cells (A) or HaCaT cells (B) were treated with TGF-β1 (5 ng/ml) for the indicated times and total protein extracted and examined by western blot analysis using an antibody specific to TBX3. p38 was used as a loading control. MCF-12A cells (C) or HaCaT cells (D) were treated with TGF-β1 (5 ng/ml) for 12 hrs and TBX3 levels and subcellular localization were determined by immunocytochemistry using an antibody specific to TBX3. All cells were co-stained with 4',6-diamidino-2-phenylindole (DAPI) to determine the location of the nuclei and in the merged image the red and blue represent TBX3 and DAPI respectively.

To examine the effect of TGF-β1 on TBX3 mRNA levels, quantitative real-time PCR (qRT-PCR) experiments were performed on mRNA extracted from cells treated with TGF-β1 for 3 and 12 hrs. The results demonstrate a 2 and 2.5 fold increase in *TBX3* mRNA levels respectively in MCF-12A cells and 1.4 and 1.8 fold increase respectively in HaCaT cells (**Fig. 3.6A, B**). This corresponded with the results from western blotting and suggested that TGF-β1 may regulate *TBX3* transcriptionally. To confirm this possibility, MCF-12A cells were pre-treated with a transcriptional inhibitor, actinomycin D (AD) before treatment with TGF-β1. The results show that when transcription is inhibited, the TGF-β1-mediated activation of *TBX3* mRNA (**Fig. 3.6C**) and protein (**Fig. 3.6D**) levels were abolished. In summary, these results indicate that TGF-β1 transcriptionally activates TBX3 expression.

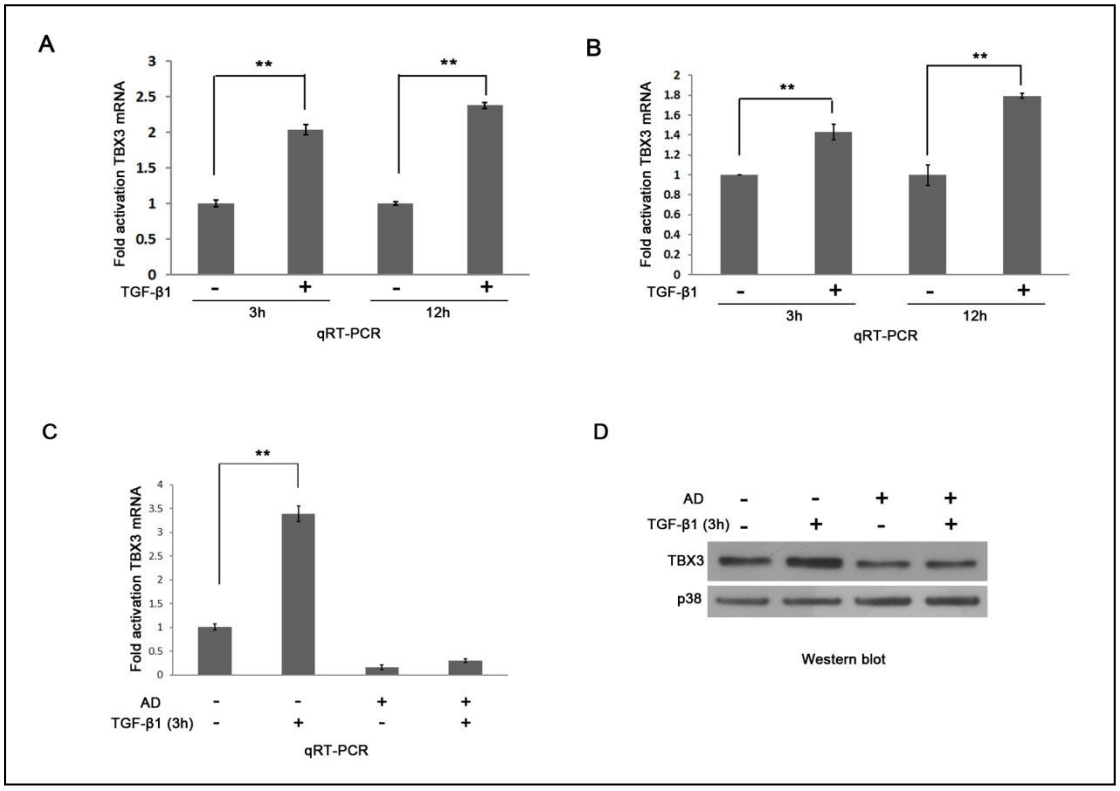

Figure 3.6 TBX3 is transcriptionally activated by TGF-β1. Total RNA extracted from MCF-12A cells (A) or HaCaT cells (B) after 3 or 12 hrs of TGF-β1 treatment was reverse-transcribed and subjected to quantitative real-time PCR (qRT-PCR) using primers specific to *TBX3*. mRNA levels were normalized to *GUSB*. (C, D) MCF-12A cells were pre-treated with vehicle (control) or 5 µg/ml actinomycin D (AD) for 1 hr and treated with TGF-β1 for 3 hrs. RNA and protein were harvested for use in (C) qRT-PCR and (D) western blotting with an antibody specific to human TBX3, respectively. Results from A, B and C are representative of two independent experiments, each performed in duplicate. A Microsoft Excel student t-test was performed to calculate statistical significance (**p< 0.001). Error bars represent standard deviation.

3.3.2 TGF-β1-activated TBX3 expression is mediated by JunB and Smad3/4

The Smad proteins are known to play an important role in the TGF-β1 signalling pathway (Feng and Derynck, 2005) and therefore to identify the mechanism(s) by which TGF-β1 transcriptionally activates TBX3 their possible involvement was considered. To this end, MCF-12A cells were co-transfected with -2186 bp of the *TBX3* promoter driving a firefly luciferase reporter with increasing concentrations of Smad3/4. The results of three independent experiments in which each construct was tested in duplicate, are shown in **figure 3.7A**. Interestingly, at all concentrations tested, Smad3/4 had very little effect on basal *TBX3* promoter activity suggesting that the Smads may require another

co-operating protein to transactivate TBX3 in the TGF-β1 signalling pathway. Based on previous reports, it was speculated that JunB may be a co-factor involved in this regulation (Verrecchia *et al.*, 2001). To test this, MCF-12A cells were treated with 5 ng/ml TGF-β1 over a time course of 0.5 to 4 hours and the levels of JunB and Smad proteins were examined by western blot analysis. The results showed that TGF-β1 treatment led to an increase in JunB and pSmad3 protein levels, which preceded the increase in TBX3 protein levels (**Fig. 3.7B**). As expected, the total levels of Smad2/3, Smad4 and the p38 loading control remained unchanged. These results suggested that JunB and the Smad proteins may be involved in the TGF-β1-induced activation of TBX3.

To confirm the possible in vivo role of JunB and Smad proteins in TGF-β1 regulated TBX3 expression, the MCF-12A cells were transfected with small interfering RNAs (siRNAs) that specifically target and knock down JunB or Smad4. The rationale for knocking down Smad4 was based on reports that it is the nuclear transporter for Smad2/3 (Feng and Derynck, 2005). Briefly, MCF-12A cells were transiently transfected with siJunB or siSmad4 or siControl and untransfected cells (UT) were included as an additional control. Proteins from all cells were harvested after 24 hrs and subjected to western blot analysis. As shown in **figures 3.7C** and **D**, compared to the UT or control siRNA cells, knocking down either JunB or Smad4 did not completely abrogate, but severely compromised, the TGF-β1-induced activation of TBX3 protein and mRNA levels. Together these results provided compelling evidence that both JunB and Smad proteins are important in the regulation of TBX3 by the TGF-β1 pathway.

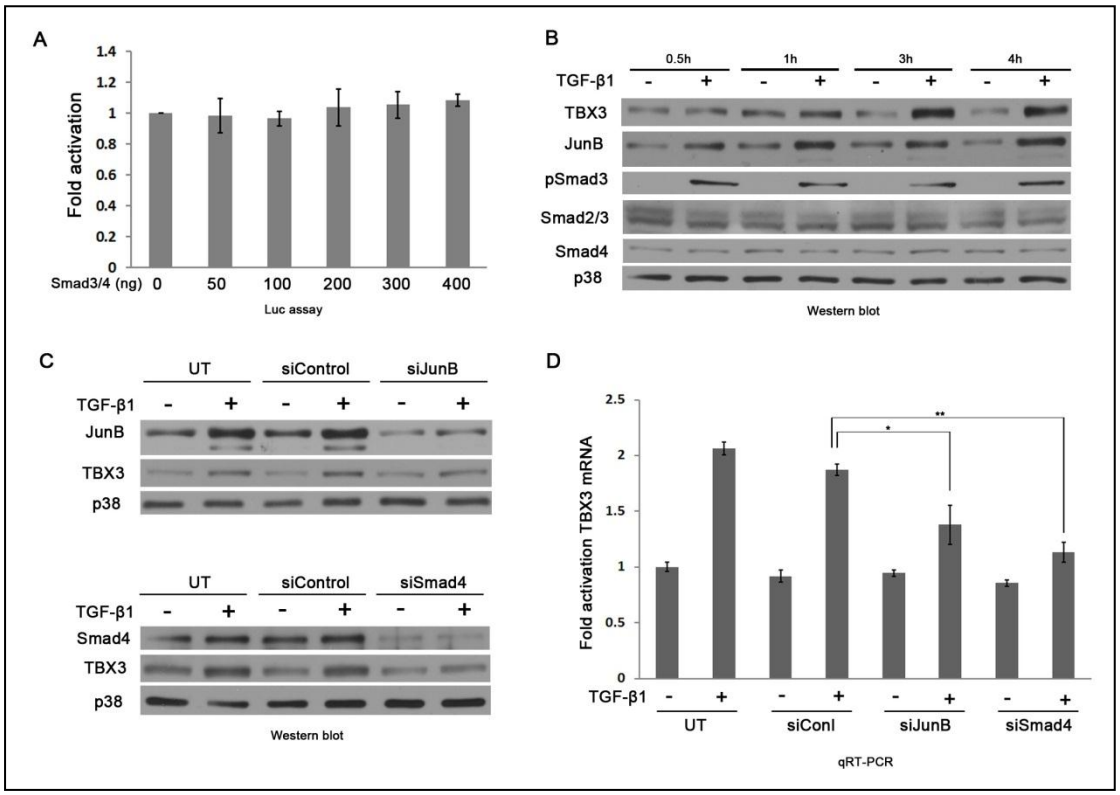

Figure 3.7 JunB and Smad proteins mediate the regulation of TBX3 by TGF-β1. (A) MCF-12A cells were co-transfected with the *TBX3* -2186 bp promoter luciferase reporter (400 ng) and increasing doses of Smad3/4 expression vectors and luciferase activity measured. Mean values (± SD) are presented as fold activity over that of an empty firefly luciferase reporter construct and are representative of at least three independent experiments. (B) MCF-12A cells were serum starved and treated with TGF-β1 at the indicated time points and analysed by western blotting with antibodies specific to TBX3, JunB, pSmad3, Smad2/3 or Smad4. p38 was used as loading control. (C) MCF-12A cells were either untransfected (UT), or transfected with 30 nM siJunB (upper panel) or 50 nM siSmad4 (lower panel) or the equivalent concentration of control siRNA for 24 hrs, followed by 3 hrs of TGF-β1 treatment and subjected to western blotting using antibodies specific to TBX3, JunB or Smad4. p38 was used as loading control. (D) mRNA from (C) was subjected to qRT-PCR analysis. mRNA levels were normalized to *GUSB*. The result of one qRT-PCR experiment is shown which is representative of two independent experiments, each performed in duplicate. A Microsoft Excel student t-test was performed to calculate statistical significance (*p<0.05, **p< 0.001). Error bars represent standard deviation.

3.3.3 JunB and Smad proteins co-operate to activate the *TBX3* promoter at the SBE-67

Having shown that the JunB and Smad proteins play an important role in the TGF-β1-induced activation of TBX3, the next objective was to identify the potential cis-acting regulatory element(s) of JunB and Smad proteins. To this end, the *TBX3* promoter was firstly examined for AP-1 and Smad binding sites. Six putative AP-1 binding

sites (**Fig. 3.8A** *left panel*) and numerous Smad binding elements (SBEs) (not shown) were identified in the -2.1 kb promoter region upstream of the transcription start site. To narrow down the region of the *TBX3* promoter involved in the TGF-β1 mediated activation, MCF-12A cells were co-transfected with a series of 5' deletion constructs of the human *TBX3* promoter and JunB and Smad3/4 expression vectors, and luciferase reporter assays were performed. As shown in **figure 3.8A**, whereas Smad3/4 had no effect on all four constructs, JunB activated all *TBX3* promoter deletion constructs. Interestingly, the co-transfection of JunB and Smad3/4 demonstrated that they co-operate to activate all four promoters.

To identify the site(s) responsible for this activity, putative sites in the shortest TBX3 promoter construct (−141/+38 bp) was used for subsequent analysis, because it maintained a high level of promoter activity. Given that the ability of Smads to co-operate with their co-factors requires their respective binding sites to be in close proximity, the two AP-1 sites at -86 bp and the adjacent SBE (-67 bp) were mutated individually by site-directed mutagenesis (**Fig. 3.8B** *upper panel*). These constructs were compared to the WT -141 bp construct in luciferase reporter assays. Interestingly, as shown in **figure 3.8B** *lower panel*, while the activity of the AP-1 mutant was comparable to that of WT, the SBE mutant significantly dampened the JunB-induced activation and abolished the co-operative effect of JunB and Smad3/4 in response to TGF-β1. This result is consistent with previous reports that in response to signals from TGF-β1 receptors, Smad proteins can co-operate with other sequence-specific transcription factors to regulate transcription of target genes (Poncelet and Schnaper, 2001; Wang *et al.*, 2008b). Together, these data suggest that not only does Smad co-operate with JunB to activate the *TBX3* promoter, but that this activity is mediated by a Smad binding element. The possibility that the TBX3 promoter used in this study does not contain all regulatory elements required for TGF-β1-mediated up-regulation of TBX3 cannot however be ruled out.

3.3.4 TGF-β1 treatment enhances binding of JunB and Smad4 to the *TBX3* promoter

To confirm that JunB and the Smad proteins can bind to the proximal region of the *TBX3* promoter in vivo, a chromatin immunoprecipitation (ChIP) assay was performed. Briefly, MCF-12A cells were fixed with formaldehyde and the cross-linked chromatin was extracted and sheared and the JunB- or Smad4-bound chromatin was immunoprecipitated with an anti-JunB or anti-Smad4 antibody respectively. After reversing the cross-link a set of primers spanning the SBE at -67 bp in the *TBX3* promoter was used to amplify the immunoprecipitated DNA using qRT-PCR analysis. Primers specific to the *GAPDH* coding region were used as a negative control. The results obtained show that compared to the IgG control, JunB and Smad4 were able to bind to the *TBX3* promoter in untreated cells and that in the presence of TGF-β1 this binding was enhanced by a 2.5 fold (JunB) and 5.5 fold (Smad4) increase in signal respectively (**Fig. 3.8C**). These data suggest that JunB and Smad4 directly bind the proximal *TBX3* promoter during basal regulation and that this mechanism is significantly enhanced by TGF-β1 treatment.

To verify that JunB and/or Smad4 specifically bind the SBE -67 site in the *TBX3* promoter, an electromobility-shift assay (EMSA) was performed. Nuclear extract isolated from TGF-β1-treated MCF-12A cells was incubated with a biotin-labelled probe spanning the wild-type (WT) SBE at -67 in the *TBX3* promoter and protein-bound biotinylated DNA run on an acrylamide gel, transferred to a nylon membrane and analysed by chemiluminescence using streptavidin-HRP conjugate. **Figure 3.8D** *left panel* shows there were four complexes observed (lane 2, see arrows) and the lowest two were competed efficiently by non-biotin-labelled homologous WT competitor oligonucleotides (lanes 3, 4, two lower arrows), but not by the oligonucleotide in which the SBE-67 was mutated (MT) (lanes 5, 6). The topmost complex was not competed by either WT or MT competitors suggesting that it may be a non-specific (NS) band or that it represents a complex that binds biotin. Furthermore, the fourth complex was competed by both WT and MT competitors and may thus represent a nuclear factor bound to the probe at a site adjacent to the SBE. To confirm that it was indeed JunB and Smad4 in the nuclear extract

used in **figure 3.8D** that bound the SBE at -67 in the *TBX3* promoter, a DNA affinity immunoblot assay (DAI) was performed. To this end, the same nuclear extracts used for the EMSAs were incubated with biotinylated DNA probes containing either the WT or MT SBE -67 oligos. Protein-bound biotinylated DNA was isolated and analysed by western blotting using antibodies specific to JunB, pSmad3 and Smad4. The results show that in the absence of TGF-β1 stimuli, both JunB and Smad4 but not pSmad3 bound the probes carrying the WT -67. However, when TGF-β1 is present, all three proteins could bind the WT -67 and their binding affinity was greatly decreased when this SBE was mutated (**Fig. 3.8D,** *right panel*). Taken together, these results suggest that in response to TGF-β1, JunB and Smad4 form protein complexes at SBE -67 to directly activate TBX3 expression.

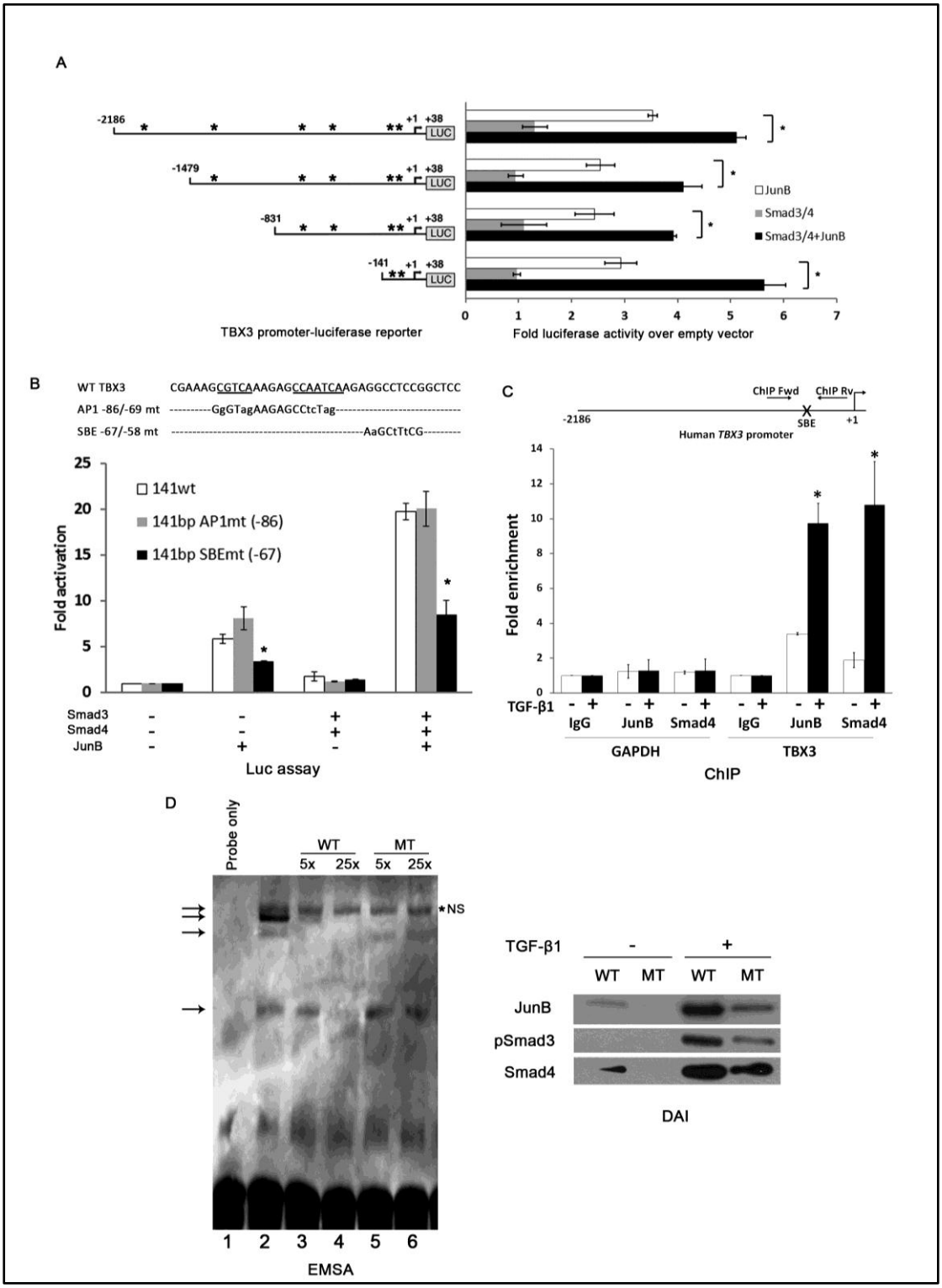

Figure 3.8 TGF-β1 activation of the TBX3 promoter is mediated by a degenerate SBE at −67 base pairs. (A) Schematic illustrations of luciferase reporter constructs containing sequential 5'- deletions of the human *TBX3* promoter (400 ng) which were transiently co-transfected into the MCF-12A cells with vectors expressing human JunB (40 ng) and Smad3/4 (30 ng each). The arrow indicates the transcription start site at +1 and the *

indicates the putative AP-1 binding sites. Mean values (± SD) are presented as fold activity over that of an empty firefly luciferase reporter and are representative of at least three independent experiments. (B) MCF-12A cells were co-transfected with a wild type (WT) *TBX3* -141 bp promoter luciferase reporter (400 ng) or a reporter in which the indicated AP-1 (AP1mt) or Smad-binding-element (SBEmt) was mutated and JunB (40 ng) or Smad3/4 (30 ng each) expression constructs and luciferase activity analysed. The result of one luc assay is shown which is representative of two independent experiments, each performed in triplicate. (C) *Upper panel:* Schematic representation of a region of the human *TBX3* promoter. SBE at position -67 bp is marked with a cross. Forward (ChIP Fwd) and reverse (ChIP Rv) primers are shown according to where they bind, producing a 207 base pair size fragment of the *TBX3* promoter. *Lower panel:* MCF-12A cells were treated with 5 ng/ml TGF-β1 for 3 hrs and chromatin immunoprecipitation assays performed with antibodies against JunB, Smad4 or IgG (negative control). Immunoprecipitated DNA was assayed by qRT-PCR with primers against the *TBX3* promoter or *GAPDH* (negative control). The results of one ChIP experiment is shown which is representative of two independent experiments, each performed in triplicate. Error bars represent standard error of the mean. (D) *Left panel*: For EMSA, biotin-labelled double stranded oligo-nucleotide probes containing the homologous WT SBE −67/−58 site were incubated with nuclear extracts from MCF-12A cells (lanes 2–6). Observed complexes are indicated by arrows on the left. Unspecific complexes are indicated by *NS on the right. Competition analyses were carried out in the presence of 5 x (lanes 3 and 4) or 25 x (lanes 5 and 6) molar excess of unlabelled homologous probes. The complex bands observed for the SBE site are indicated by the two lowest arrows. *Right panel*: Biotinylated DNA probes of the *TBX3* promoter containing the homologous WT or MT SBE were immobilized on streptavidin beads, and incubated with nuclear extracts from MCF-12A cells treated with or without 5 ng/ml TGF-β1 for 3 hrs. The DNA-bound protein complexes were isolated and analysed by western blotting using antibodies to JunB or Smad4. A Microsoft Excel student t-test was performed to calculate statistical significance (*$p < 0.05$). Error bars represent standard deviation.

3.3.5 The anti-proliferative and pro-migratory roles of TGF-β1 are mediated in part by TBX3

TGF-β1 has an anti-proliferative and a pro-migratory role and recent findings from our laboratory have reported similar roles for TBX3 (Peres *et al.*, 2010; Mowla *et al.*, 2011). Having shown that TGF-β1 transcriptionally activates TBX3, it was therefore next speculated that these biological effects of TGF-β1 are mediated in part by TBX3. To test this, an inducible MCF-12A cell line (lenti-MCF-12A) was generated using a lentiviral system. Briefly, the MCF-12A cells were stably transduced with lentiviral infectious particles that contain a GFP-tagged doxycycline (Dox)-inducible shTBX3 that specifically targets and knocks down TBX3. Successfully transduced cells were sorted by fluorescence activated cell sorting (FACS) for GFP expression. The efficacy of the system was confirmed by western blot analysis (**Fig. 3.9A**) that shows that compared to the untreated cells, the addition of 1 μg/ml Dox for as early as 48 hrs led to a significant reduction in TBX3 levels in the lenti-TBX3 cells and this knock down of TBX3 was not observed when the MCF-12A parental cells were treated with Dox under the same conditions.

To examine the role of TBX3 in the TGF-β1-regulated anti-proliferative effect, BrdU incorporation assays were performed where an equal number of cells were plated and pulsed with BrdU for 3 hrs. Results show the total number of BrdU positive cells expressed as a percentage of the total number of cells from 10 fields of view for each condition. When control cells were treated with TGF-β1, TBX3 protein levels increased (**Fig. 3.9B)**, which corresponded with a decrease in proliferation as measured by BrdU incorporation (**Fig. 3.9C**). However, when TBX3 expression was knocked down (**Fig. 3.9B)** there was no statistical difference in the proliferative ability of control and TGF-β1–treated cells (**Fig. 3.9C**), suggesting that TBX3 was required for the inhibitory effect of TGF-β1 on cell proliferation. To measure the impact of TBX3 on the TGF-β1-regulated pro-migratory effect scratch motility assays were performed. **Figure 3.9D** shows that in the Dox^- cells TGF-β1-induced TBX3 upregulation correlated with increased cell migratory ability by approximately 3 fold. However, when TBX3 levels were inhibited by Dox, the

fold change of TGF-β1-induced migration was significantly reduced to approximately less than 1.5 fold. The migration observed when TBX3 was knocked down is probably due to incomplete knock down of TBX3. These results show that TBX3 also plays an important role in mediating the pro-migratory effect of TGF-β1 on these cells.

The above results were reproducible when TBX3 was knocked down in HaCaT cells using a siTBX3 approach (**Fig. 3.9E-G**). Briefly, HaCaT cells were transfected with either 50 nM siControl, which had been validated to have no off-target effects, or 50 nM siTBX3, that specifically target and knock down TBX3 expression. Successful TBX3 knock down was confirmed by western blotting (**Fig. 3.9E**) and the effect of TBX3 knock down on cell proliferation was measured after 30 hrs using the methylthiazol tetrazolium (MTT) assay. While the control cells exhibited reduced proliferation by approximately 1.4 fold in response to TGF-β1, there was no significant difference between the untreated and TGF-β1-treated siTBX3 cells (**Fig. 3.9F**). Similarly, unlike siControl cells, siTBX3 cells failed to respond to TGF-β1-induced pro-migratory stimuli in scratch motility assays (**Fig. 3.9G**). Together, these results suggest that TBX3 is key in mediating the anti-proliferative and pro-migratory roles of TGF-β1 in epithelial cells.

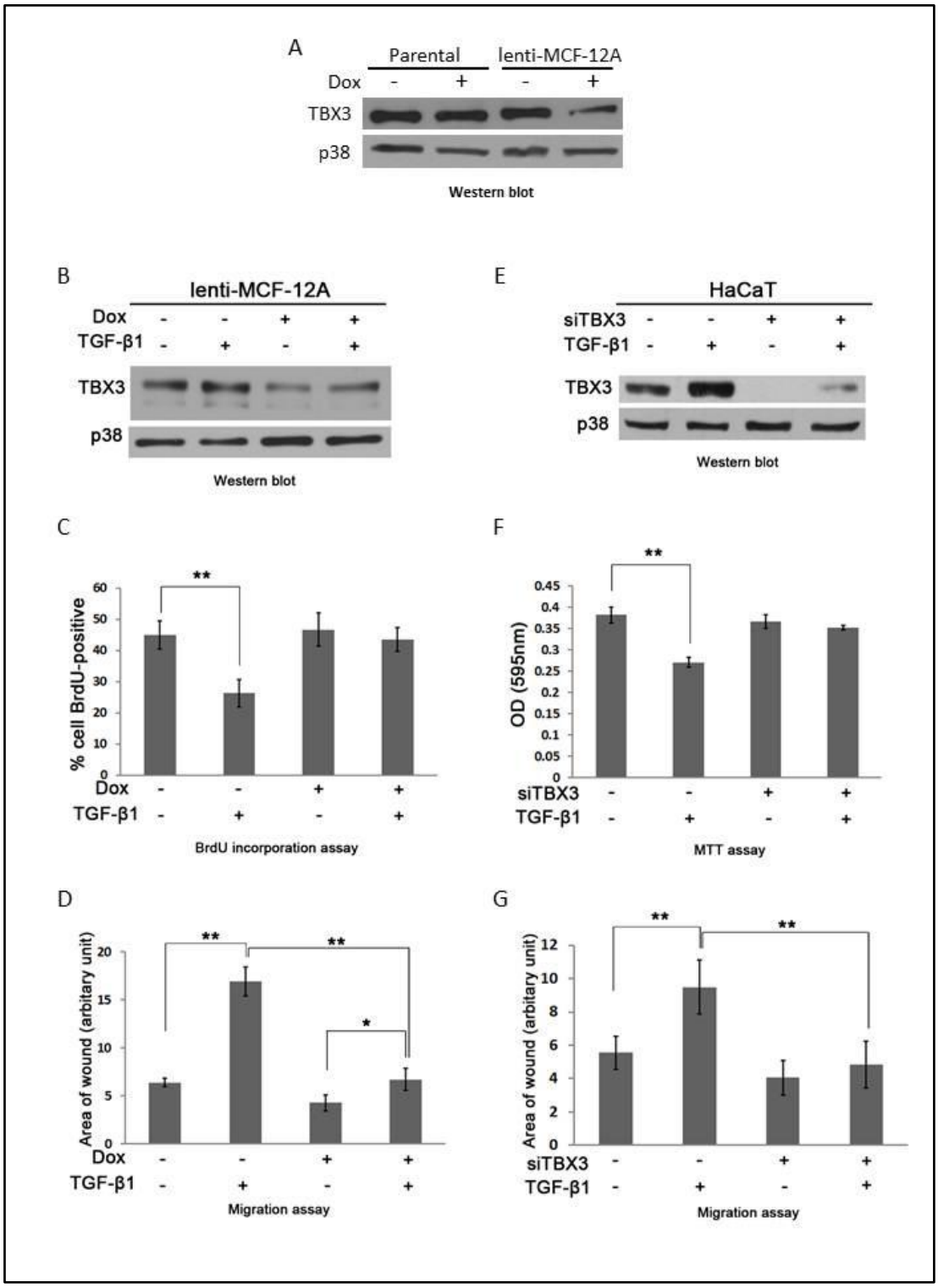

Figure 3.9 TBX3 is a key downstream mediator of TGF-β1 regulated cell proliferation and migration. (A) MCF-12A cells were stably transduced with lentiviral infectious particles containing a GFP-tagged shTBX3 construct and a pure population of shTBX3 cells (lenti-MCF-12A cells) was obtained by fluorescence activated cell sorting (FACS) for GFP expression. Lenti-MCF-12A and parental MCF-12A cells were treated with or without 1 µg/ml Doxycyclin (Dox) for 48 hrs and protein extracts analysed by western blotting using an anti-TBX3 antibody. p38 was used as a loading control. (B, E) Western blot

analyses show the lentiviral shRNA-mediated knock down of TBX3 in MCF-12A cells (B) or siTBX3-mediated knock down in HaCaT cells (E) in the presence or absence of 3 hrs TGF-β1 treatment. p38 was used as a loading control. (C) MCF-12A cells from (B) were incubated with 10 μM BrdU for 3 hrs and harvested for immunocytochemistry using an anti-BrdU antibody. BrdU-positive nuclei were visualized by fluorescence microscopy to measure cell proliferation. The result shown is representative of two independent experiments. (F) Net cell growth of HaCaT cells from (E) was assessed by the methylthiazol tetrazolium (MTT) assay over 30 hrs. The result shown is representative of two independent experiments, each performed in triplicate. (D, G) Cells treated as in (B) and (E) were subjected to a two-dimensional in vitro scratch motility assay as described before. Each result shown is representative of two independent experiments and is expressed as an average of 10 fields of view for each condition. A Microsoft Excel student t-test was performed to calculate statistical significance (*$p<0.05$, **$p< 0.001$). Error bars represent standard deviation.

3.4 *TBX3 represses its homologue TBX2 to execute its anti-proliferative role in the TGF-β1 signalling pathway*

The results above show that TGF-β1 upregulates expression of TBX3 which is key for mediating TGF-β1-induced anti-proliferation and pro-migration of epithelial cells. This raised the question as to which TBX3 target genes are responsible for this. Previous data from our laboratory as well as others showed that TBX2, the homologue of TBX3, functions as a pro-proliferative factor and preliminary reports suggest that TBX3 may be able to repress TBX2 (Jacobs *et al.*, 2000; Vance *et al.*, 2005; Peres *et al.*, 2010; Redmond *et al.*, 2010). It was therefore hypothesized that in response to TGF-β1, TBX3 represses TBX2 in order to inhibit cell proliferation and the following section explores this possibility.

3.4.1 TGF-β1 transcriptionally represses TBX2 expression in MCF-12A breast epithelial and B16 melanoma cells.

To determine if TBX2 is indeed a downstream target of TBX3 in the TGF-β1 anti-proliferative pathway, the effect of TGF-β1 signalling on TBX2 expression was firstly examined. Briefly, MCF-12A breast epithelial and B16 mouse melanoma cells were exposed to TGF-β1 or vehicle over a time course spanning 1 – 36 hours and western blotting performed on extracts from these cells with an antibody to TBX2. Results show that TBX2 levels decrease substantially in response to TGF-β1 treatment in both cell lines from 8 hrs in MCF-12A cells and 4 hrs in B16 cells (**Fig. 3.10A, B**). It is important to note, that this robust repression was also previously observed by an ex-PhD student, Dr Teng, in WI-38 normal human fibroblasts (data not shown). To examine the effect of TGF-β1 on TBX2 mRNA levels, qRT-PCR experiments were performed on mRNA extracted from cells treated with TGF-β1 or vehicle over a time course spanning 1 – 36 hours. The results demonstrate a corresponding decrease in *TBX2* mRNA levels in MCF-12A and B16 cells that precedes the decrease in protein levels (**Fig. 3.10C, D**).

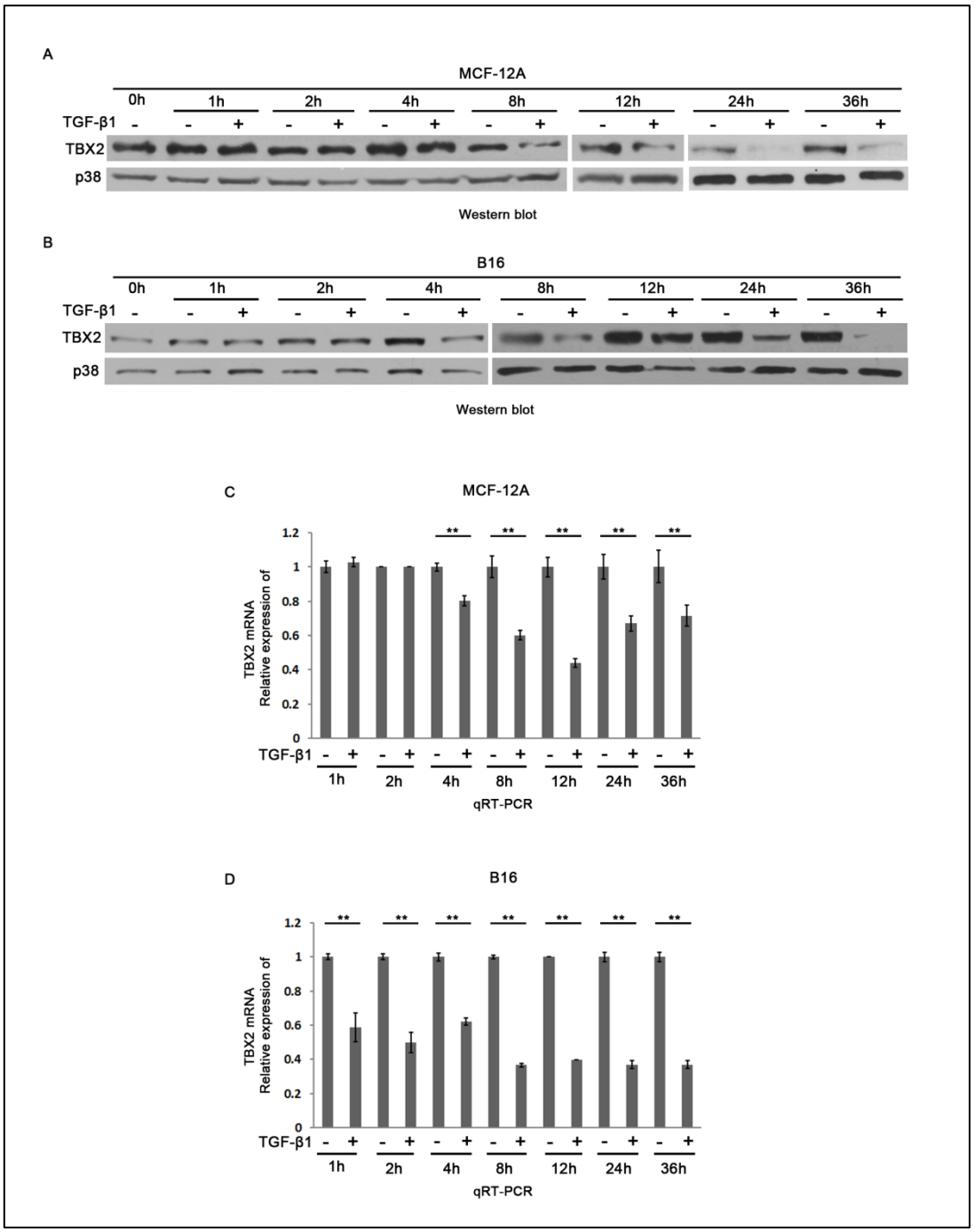

Figure 3.10. TGF-β1 represses TBX2 protein and mRNA expression. TBX2 protein from TGF-β1 (5 ng/ml) treated MCF-12A cells (A) or B16 cells (B) were prepared after the indicated times and was examined by western blot analysis with an antibody specific to human TBX2. p38 was used as a loading control. (C, D) Total RNA extracted from MCF-12A cells (C) or B16 cells (D) after indicated times of TGF-β1 (5 ng/ml) treatment were reverse-transcribed and subjected to qRT-PCR using primers specific to *TBX2*. mRNA levels were normalized to *GUSB*. Each result shown is representative of two independent qRT-PCR experiments, performed in duplicate. A Microsoft Excel student t-test was performed to calculate statistical significance (**p< 0.001). Error bars represent standard deviation.

To investigate if this regulation is transcriptional, a luciferase assay was performed to test whether the *TBX2* promoter is responsive to TGF-β1 treatment. Briefly, MCF-12A cells transfected with the -1604 bp human *TBX2* promoter construct were treated with 5 ng/ml TGF-β1 for 8 hrs, 24 hrs and 36 hrs and the results show a time-dependent decrease in reporter activity in response to TGF-β1 (**Fig. 3.11A**). To distinguish the need for de novo protein synthesis, cells were pre-treated with cycloheximide (CHX), a protein synthesis inhibitor, which abolished the repression of *TBX2* mRNA and protein levels by TGF-β1 (**Fig. 3.11B, C**). Together these results suggest that TGF-β1-mediated repression of TBX2 is transcriptional and that it requires the production of nascent protein.

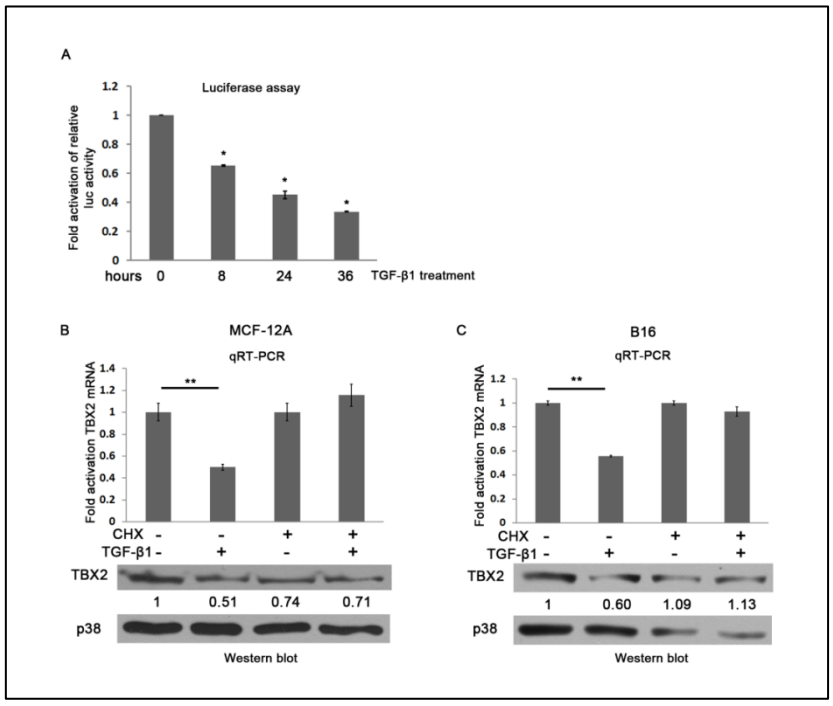

Figure 3.11 TBX2 is transcriptionally regulated by TGF-β1. (A) Luciferase assay using MCF-12A cells which were transfected with a full length human *TBX2* promoter (400 ng) construct and were treated with 5 ng/ml TGF-β1. Mean values (± SD) are presented as fold activity over that of an empty firefly luciferase reporter and are representative of at least three independent experiments. (B, C) MCF-12A (B) and B16 (C) cells were pre-treated with vehicle (control) or 30 µg/ml cycloheximide (CHX) for 1 hr followed by TGF-β1 treatment for 8 hrs for MCF-12A cells and 4 hrs for B16 cells. *Upper panels*: RNA was harvested for use in qRT-PCR using primers specific to *TBX2* and mRNA levels were normalized to *GUSB*. *Lower panels*: Protein was harvested for western blot analysis using an antibody specific to human TBX2 and p38 was used as a loading control. The expression of TBX2 was quantified using UN-SCAN-IT gel 6.1 software and the densitometry values normalised to p38 levels. A Microsoft Excel student t-test was performed to calculate statistical significance (*p<0.05, **p< 0.001). Error bars represent standard deviation.

3.4.2 The downregulation of TBX2 by TGF-β1 is mediated by TBX3 in breast epithelial cells.

To narrow down the region of the *TBX2* promoter mediating its repression by TGF-β1, a series of 5' deletion constructs of the human *TBX2* promoter driving a firefly luciferase reporter were tested in luciferase assays. The results show that the repression of *TBX2* by TGF-β1 treatment is sustained even in the -218 bp *TBX2* promoter construct (**Fig. 3.12A**). Since the primary mediators of canonical TGF-β1 signalling are the Smad proteins it was first investigated whether Smad3 and Smad4 (Smad3/4) are involved in this regulation. To this end, MCF-12A cells were co-transfected with increasing amounts of Smad3/4 expression vectors and the -218 bp *TBX2* promoter luciferase construct and luciferase activity analysed. **Figure 3.12B** shows that Smad3/4 had very little effect on *TBX2* promoter activity suggesting that the regulation of TBX2 by TGF-β1 either requires a Smad co-factor(s) or involves a mechanism that does not directly require the Smads. These experiments were therefore repeated in the presence or absence of the well-known Smad co-factors, JunB or Sp1, but no repression was observed (data not shown). As shown earlier, TGF-β1 activates TBX3 expression to impact negatively on cell proliferation and previous work from Rodriguez et al. (2008) as well as unpublished work from our laboratory indicated that TBX2 and TBX3 may be reciprocally expressed. It was therefore speculated that TBX2 may be downstream of TBX3 in the TGF-β1 pathway. To address this, the -218 bp *TBX2* promoter was screened for T-elements and a T-element which is highly conserved between Tbx2 promoters across several species was identified at -186 bp (**Fig. 3.12C**).

To investigate the possible in vivo role of TBX3 in the repression of TBX2 by TGF-β1, TBX3 was silenced by siRNA and TBX2 protein and mRNA levels determined in TGF-β1 treated cells. Indeed, depleting TBX3 levels in MCF-12A cells diminished the ability of TGF-β1 to repress TBX2 protein and mRNA levels (**Fig. 3.12D, E**). It is worth noting that while the fold repression of TBX2 by TGF-β1 in the siTBX3 cells was still significant, it was lower than that of the control cells and may be due to incomplete knock down of TBX3. Furthermore, knocking down TBX3 in untreated cells resulted in an increase in TBX2

mRNA and protein levels suggesting that TBX3 represses basal and TGF-β1 regulated TBX2 levels.

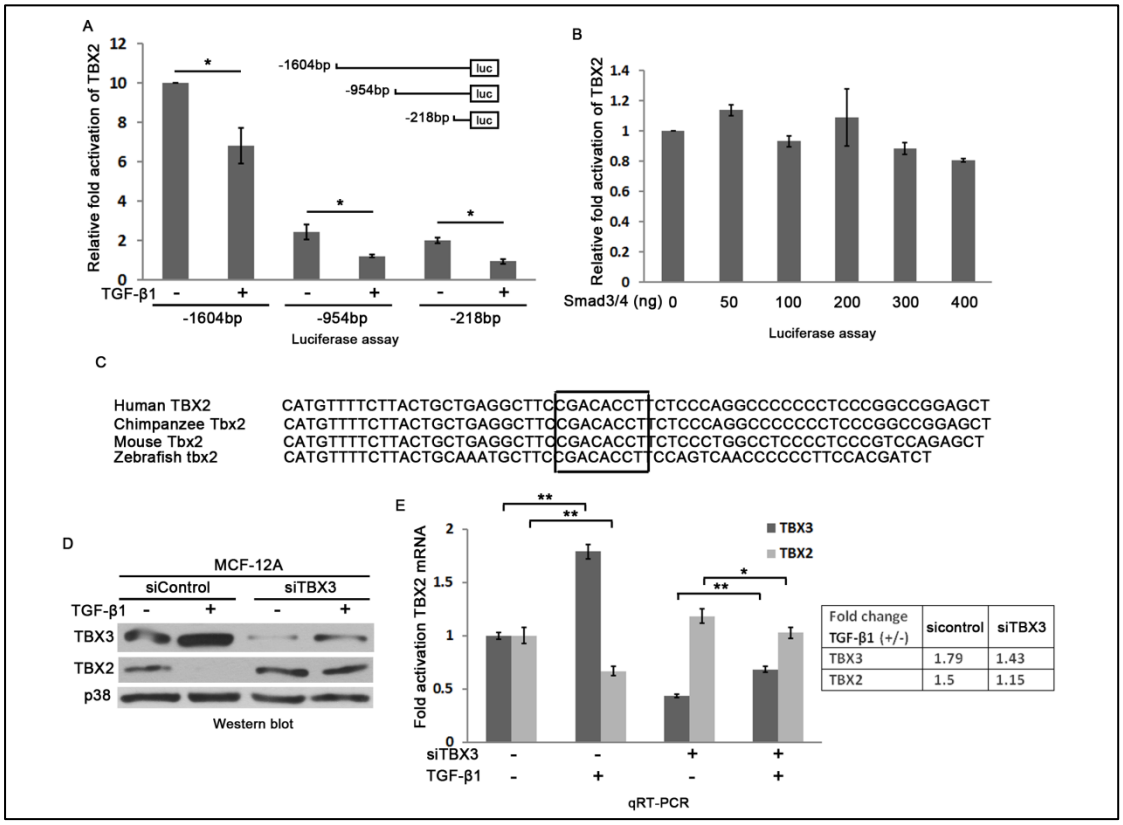

Figure 3.12 The downregulation of TBX2 by TGF-β1 is mediated by TBX3. (A) Luciferase assays of MCF-12A cells transfected with 400 ng of the indicated human *TBX2* 5'-deletion promoter constructs and treated with 5 ng/ml TGF-β1 or vehicle. (B) Luciferase assays of MCF-12A cells co-transfected with increasing amounts of Smad3/4 expression vectors and 400 ng of -218 bp *TBX2* promoter reporter construct. For A-B, mean values (± SD) are presented as fold activity over that of an empty firefly luciferase reporter and are representative of at least three independent experiments. (C) Alignment of the T-element at -186 bp in the human *TBX2* promoter is conserved in chimpanzee, mouse and zebrafish. The box indicates the location of the T-element. (D, E) Serum starved MCF-12A cells were transfected with either 50 nM siControl or siTBX3 for 48 hrs, and the transfection was repeated to maintain the knock down of TBX3 for another two days in which the cells were cultured in 5 ng/ml TGF-β1. The cells were harvested and subjected to (D) western blotting using antibodies specific to TBX3 or TBX2 (p38 was used as loading control) or (E) qRT-PCR analysis with mRNA levels normalized to *GUSB*. The experiment was performed in duplicate. A Microsoft Excel student t-test was performed to calculate statistical significance (*p<0.05, **p< 0.001). Error bars represent standard deviation.

3.4.3 TBX3 binds to the *TBX2* promoter at -186 bp in response to TGF-β1 treatment.

To confirm that TBX3 can directly repress TBX2 in vivo, chromatin immunoprecipitation (ChIP) assays were performed. Briefly, cross-linked chromatin was prepared from TGF-β1-treated and control MCF-12A cells and DNA immunoprecipitated with an antibody to TBX3. After reversing the cross-link a set of primers spanning the -186 bp putative T-element in the *TBX2* promoter was used to amplify the immunoprecipitated DNA using qRT-PCR analysis. Primers specific to the *GAPDH* coding region were used as a negative control. The results obtained show that compared to the untreated control, the binding of TBX3 to the *TBX2* promoter was enhanced by 8.5 fold in the presence of TGF-β1 (**Fig. 3.13A**).

To determine whether TBX3 binds specifically to the -186 bp T-element in the *TBX2* promoter, a DNA affinity immunoblot (DAI) assay was performed. Nuclear extracts isolated from TGF-β1-treated MCF-12A cells were incubated with biotinylated DNA probes containing either the wild type (WT) or mutated T-element (MT) (**Fig. 3.13B** *upper panel*). As an additional control a probe containing a full T-element consensus site was included in these experiments and protein-bound biotinylated DNA was isolated and analysed by western blotting using an anti-TBX3 antibody. The results show that while TBX3 bound strongly to both the consensus and wild-type probes, it displayed a decreased affinity for the probe with the mutated T-element (**Fig. 3.13B** *lower panel*). Together, these results suggest that TBX3 binds the *TBX2* promoter specifically at the T-element at -186 bp.

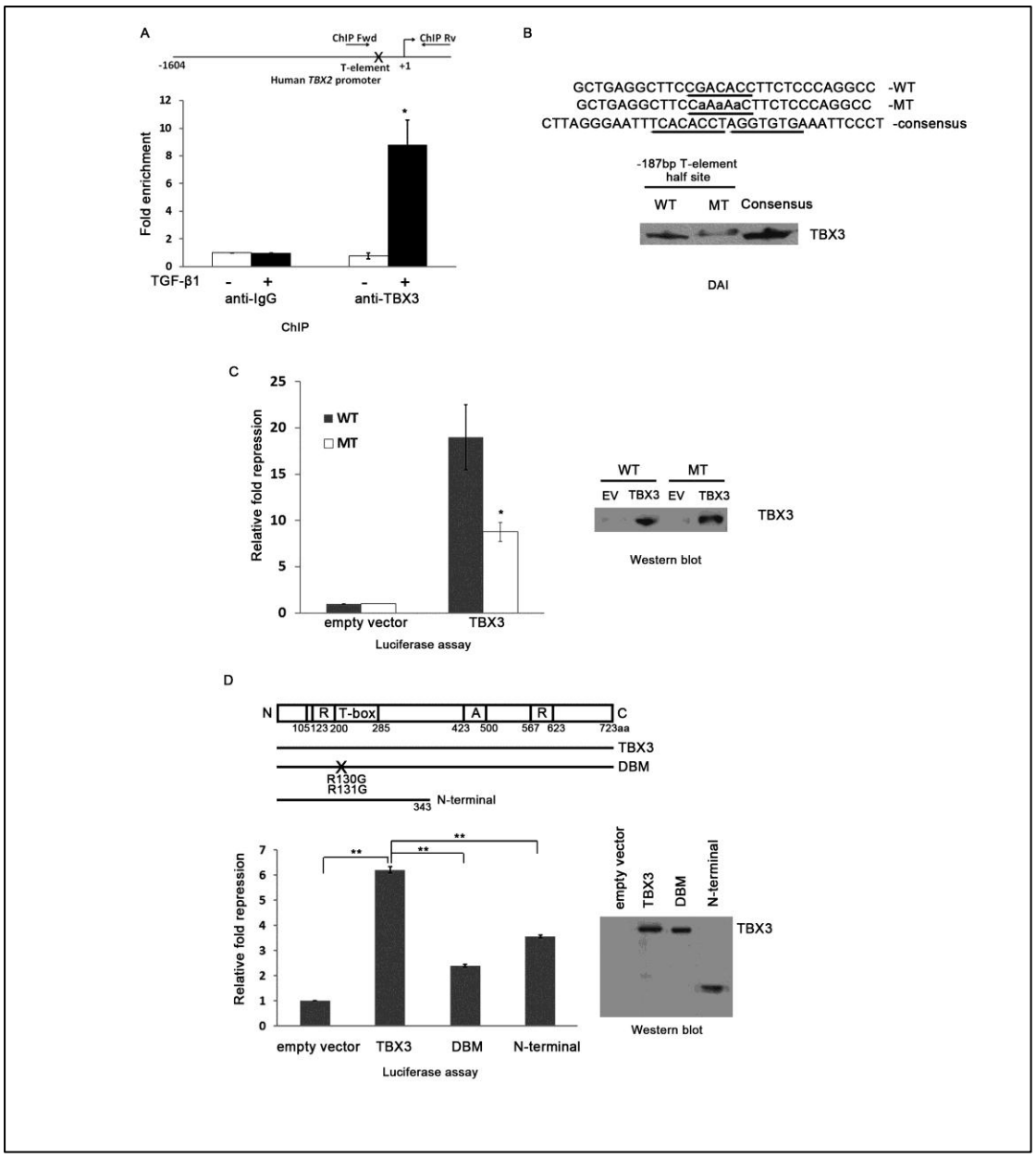

Figure 3.13 TBX3 binds the TBX2 promoter in vivo and in vitro at the T-element at −186 bp. (A) TBX3 binds the *TBX2* promoter in the region of the consensus T-element in vivo. *Upper panel:* Schematic representation of human *TBX2* promoter. T-element at position -186 bp is marked with a cross. Forward (ChIP Fwd) and reverse (ChIP Rv) primers are shown according to where they bind on the *TBX2* promoter. *Lower panel:* MCF-12A cells were treated with 5 ng/ml TGF-β1 for 24 hrs and the cell lysates were used in a ChIP assay performed with antibodies against TBX3 or IgG (negative control). Immunoprecipitated DNA was assayed by qRT-PCR with primers against the *TBX2* promoter or *GAPDH* (negative control). A Microsoft Excel student t-test was performed to calculate statistical significance (*p<0.05). The results of one ChIP experiment is shown which is representative of two independent experiments, each performed in triplicate. Error bars represent standard error of the mean. (B) Biotinylated double stranded oligo-nucleotide probes of the TBX2 promoter containing the WT T-element at -186 bp or MT where this T-element was mutated from CGACACC to CAAAAAC as well as

a probe containing a full consensus T-element were immobilized on streptavidin beads, and incubated with nuclear extracts from MCF-12A cells treated with 5 ng/ml TGF-β1 for 24 hrs. The DNA-bound protein complexes were isolated and analysed by western blotting using antibodies to TBX3. (C) Luciferase assay of MCF-12A cells co-transfected with 100 ng of TBX3 expression vector or empty control vector and 400 ng of either *TBX2* WT or T-element mutant (MT) promoter luciferase reporter. (D) Luciferase assay of MCF-12A cells co-transfected with 400 ng of *TBX2* promoter luciferase reporter and 100 ng of an empty control vector or WT TBX3 or DNA binding domain mutant (DBM) or TBX3 N-terminal truncated expression vector. For (C) and (D), mean values (± SD) are presented as fold activity over that of an empty firefly luciferase reporter and are representative of at least three independent experiments. Western blots (C, D, right) show equal expression of TBX3 protein. Bars, SD. *p < 0.05, ** p<0.001

To test whether TBX3 can repress the *TBX2* promoter and whether the T-element at -186 bp mediates this repression, MCF-12A cells were co-transfected with a TBX3 expression vector and either a wild type -218 bp *TBX2* promoter luciferase construct or a construct in which the T-element was mutated by site-directed mutagenesis. The results show that TBX3 repressed the *TBX2* promoter by approximately 18 fold and that the ability of TBX3 to repress *TBX2* was significantly reduced when the -186 bp T-element was mutated (**Fig. 3.13C**), suggesting that TBX3 represses the *TBX2* promoter via the -186 bp T-element.

To identify the functional domains of the TBX3 protein that are responsible for repressing TBX2, the wild type -218 bp *TBX2* promoter luciferase construct was co-transfected with vectors expressing either a WT TBX3 protein or a TBX3 protein in which the DNA binding domain was mutated or only a N-terminal TBX3 protein lacking the dominant repression domain. The DNA-binding domain (DBD) mutant (DBM) has arginine at position 133 replaced with glycine and was previously shown to disrupt the highly homologous Tbx3 mouse DBD (Habets *et al.*, 2002; Lingbeek *et al.*, 2002). The data obtained indicate that while WT TBX3 represses the *TBX2* promoter by 6 fold, the TBX3 DBM and the N-terminal TBX3 proteins had significantly reduced ability to repress the *TBX2* promoter (**Fig. 3.13D**). These data indicate that the TBX3 DNA binding domain and C-terminus containing a repression domain are important for its ability to repress the *TBX2* promoter. Western blotting confirmed that all three TBX3 constructs were expressed at similar levels and hence loss of the ability of TBX3 DBM and TBX3 N-terminal to repress *TBX2* was not due

to lower levels of expression of these constructs (**Fig. 3.13C, D,** *right panel*).

3.4.4 Ectopic expression of TBX2 is able to rescue TGF-β1 inhibited cell proliferation.

TGF-β1 has been shown to be a potent inhibitor of epithelial cell proliferation (Jahn *et al.*, 2012) and data from section 3.2 above showed that TBX3 plays a key role in mediating this effect in MCF-12A breast epithelial cells. This together with published data showing that TBX2 is a pro-proliferative factor (Jacobs *et al.*, 2000; Vance *et al.*, 2005; Peres *et al.*, 2010; Redmond *et al.*, 2010) led to the hypothesis that the downregulation of TBX2 by TBX3 may contribute to the anti-proliferative effect of TGF-β1. TBX2 was therefore stably overexpressed in the MCF-12A cell line (MCF-12A-TBX2) to investigate whether it could rescue the inhibition of cell proliferation by TGF-β1. Briefly, a pcDNA3.1(+)-TBX2 expression vector or the empty control vector was stably transfected into MCF-12A cells and G418 (400 μg/ml) -resistant clones were pooled after 10 days for subsequent analysis. Western blot analysis confirmed the overexpression of TBX2 (**Fig. 3.14A**) and MCF-12A-TBX2 and control cell lines were cultured in 5 ng/ml TGF-β1 for 4 days and cell numbers were counted using a haemocytometer. The overexpression of TBX2 was not affected by TGF-β1 (**Fig. 3.14A**) and growth curves show that while cell proliferation was significantly reduced by TGF-β1 in the control cells, overexpressing TBX2 was sufficient to rescue this phenotype (**Fig. 3.14B).** The role of TBX2 in this anti-proliferative effect was confirmed by flow cytometry which showed that TGF-β1 treatment induced a significant G1 cell cycle arrest in the control cells but had no effect on the cell cycle profile of the TBX2-overexpressing cells (**Fig. 3.14C**).

The above results correlated with changes in the protein and mRNA levels of the cyclin dependent kinase inhibitor p21 (**Fig. 3.14A, E**), a known mediator of the anti-proliferative function of TGF-β1 and a target gene repressed by TBX2 (Prince *et al.*, 2004a; Jahn *et al.*, 2012). To confirm that TBX2 is upstream of p21 in the TGF-β1 response, TBX2 overexpressing cells were transfected with a p21 expression vector and growth curve analysis performed as before. The results show that the overexpression of p21 in TBX2 overexpressing cells reduced their proliferative ability and that TGF-β1

treatment could not reduce this any further (**Fig. 3.14D**).

Importantly, while TBX2 overexpression abrogated the increase in p21 protein and mRNA levels in TGF-β1 treated cells (**Fig. 3.14A, E**), it failed to have any significant effect on the TGF-β1-induced activation of p15 mRNA levels (**Fig. 3.14F**), another cell cycle inhibitor which has been shown to mediate a G1 arrest in response to TGF-β1 (Reynisdóttir et al, 1995). Together, these data suggested that the anti-proliferative effect of TGF-β1 on MCF-12A cells occurs primarily through upregulation of p21, since the continued repression of p21 in TBX2 overexpressing cells allowed the cells to proliferate even in the presence of TGF-β1 and despite the upregulation of p15. To confirm this, p21 expression was knocked down using a siRNA approach and growth curve analysis performed in the presence and absence of TGF-β1. As expected, cells in which p21 levels were effectively silenced proliferated faster than the control cells in the absence of TGF-β1 (**Fig. 3.14G)**. Importantly, the p21-depleted cells also failed to show a significant decrease in cell proliferation in response to TGF-β1. These data suggest that the down-regulation of TBX2 mediates the anti-proliferative effect of TGF-β1, primarily through allowing upregulation of p21.

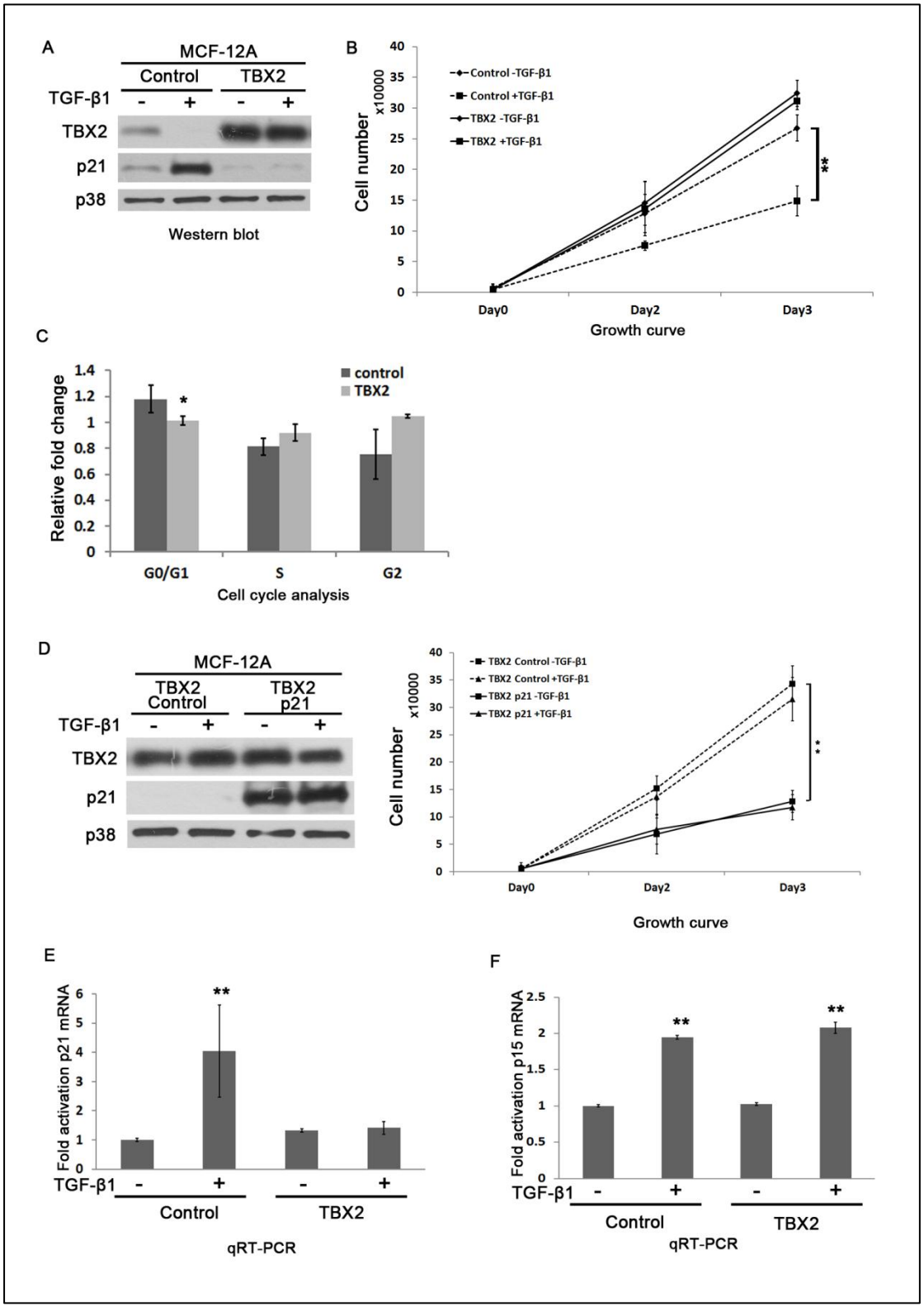
A
MCF-12A
Control
TBX2
TGF-β1
- + - +
TBX2
p21
p38
Western blot
B
Control -TGF-β1
Control +TGF-β1
TBX2 -TGF-β1
TBX2 +TGF-β1
Cell number
x10000
Day0
Day2
Day3
Growth curve
C
control
TBX2
Relative fold change
G0/G1
S
G2
Cell cycle analysis
D
MCF-12A
TBX2 Control
TBX2 p21
TGF-β1
TBX2
p21
p38
TBX2 Control -TGF-β1
TBX2 Control +TGF-β1
TBX2 p21 -TGF-β1
TBX2 p21 +TGF-β1
Cell number
x10000
Growth curve
E
Fold activation p21 mRNA
TGF-β1
Control
TBX2
qRT-PCR
F
Fold activation p15 mRNA
TGF-β1
Control
TBX2
qRT-PCR

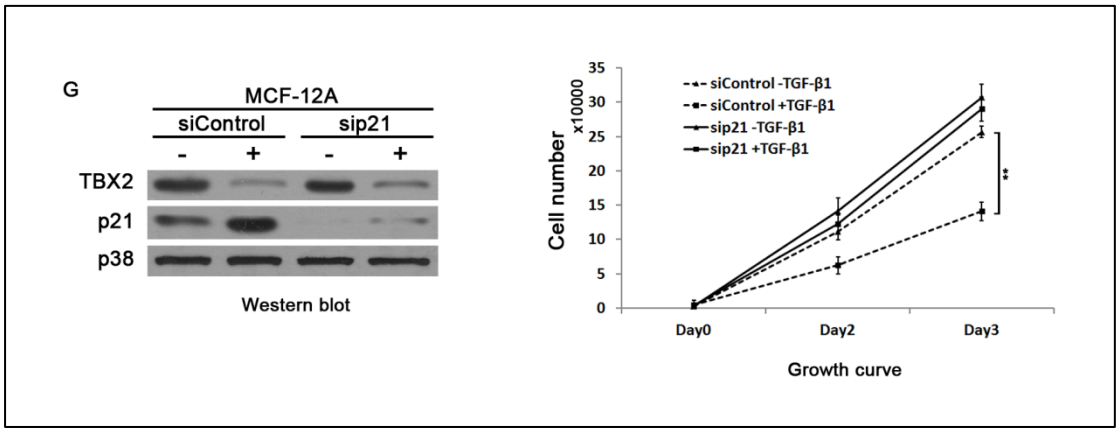

Figure 3.14 Ectopic TBX2 expression rescues TGF-β1-induced growth inhibition through downregulating p21 in breast epithelial cells. (A) MCF-12A cells were stably transfected with 100 ng of either pcDNA3.1(+) (Control) or pcDNA3.1-TBX2 (TBX2) and the clones were pooled. The MCF-12A-Control or -TBX2 cell lines were treated with or without 5 ng/ml TGF-β1 for 3 days and were subjected to western blot analysis using antibodies specific to human TBX2 or p21. p38 was used as a loading control. (B) MCF-12A-Control or -TBX2 cells were seeded in triplicate at a density of 4 X 103 cells per well of a 24-well plate and treated with vehicle or 5 ng/ml TGF-β1 for 3 days. Growth curve assays were performed over a 3 day period and cells harvested by trypsinisation and counted on a haemocytometer. (C) Flow cytometry assays show relative fold change of TGF-β1 treated MCF-12A-Control and -TBX2 cells in G1, S and G2/M phases compared to their corresponding vehicle-treated cells. The result shown is representative of two independent flow cytometries. (D) MCF-12A-TBX2 cells were seeded and treated as in (B). After seeding, cells were transiently transfected with either pRc/CMV (TBX2 Control) or pRc/CMV-p21 (TBX2 p21), treated with TGF-β1 and subjected to growth curve analysis (Right panel). Replicate wells from the growth curve analysis were pooled and protein harvested for western blot analysis (Left panel). (E, F) MCF-12A-Control or -TBX2 cell lines were treated with vehicle or TGF-β1 for 24 hrs and RNA was harvested for use in qRT-PCR analyses to examine the expression of p21 (E) or p15 (F). mRNA levels were normalized to GUSB. Each result shown is representative of two independent experiments, performed in duplicate. (G) MCF-12A cells were seeded as in (B) and were either transfected with 25 nM sip21 (sip21) or the equivalent concentration of control siRNA (siControl) for 12 hrs, followed by 3 days of TGF-β1 treatment and subjected to (Left panel) western blotting and (Right panel) growth curve analysis as described in (D). For all analyses a student t-test was performed to calculate statistical significance (**p< 0.001). Error bars represent standard deviation.

CHAPTER 4

DISCUSSION AND CONCLUDING REMARKS

Breast cancer is the most common malignancy worldwide amongst women and it is estimated that one out of eight women will develop breast cancer in their life time (Cheng *et al.*, 1998; Baselga *et al.*, 2012; Howard and Bland, 2012). Furthermore, the majority of breast cancers are still diagnosed at very late stages in low- and middle-income countries due to inadequate infrastructure and resources and therefore result in a higher mortality compared to the high-income countries (Tfayli *et al.*, 2010). Despite enormous efforts to identify effective breast cancer treatments, there is still limited success with most of the current therapeutic strategies. There is therefore an urgent need to develop novel and effective therapeutic drugs for this disease. The identification of transcription factors which play a key role in breast cancer progression is important because they may represent good targets in the development of novel therapeutic approaches to treat this cancer. The rationale for this is based on the premise that transcription factors are ultimately responsible for controlling gene expression patterns resulting in tumour formation, progression and metastasis. In the last decade, several transcription factors with key roles in breast cancer progression were identified as potential therapeutic targets. Among these was TBX3, a member of the T-box transcription factor family which was found to be overexpressed in a subset of breast cancers (Yarosh et al, 2008; Fan et al, 2004). However, at the start of this study the precise role of this aberrant expression of TBX3 in breast cancer progression was unclear. Furthermore, the mechanism(s) by which TBX3 is upregulated in breast cancer cells and the downstream targets that mediate its roles in this cancer were not known. Using both knockdown and overexpression cell culture models this study reveals that TBX3 is indeed involved in breast cancer progression, particularly contributing to tumour cell migration. Moreover, the Transforming Growth Factor β1 (TGF-β1) pathway, which is frequently deregulated in many cancers including breast cancers, is shown to upregulate TBX3

expression in breast cells. TBX2, a T-box family member which shares a high degree of homology with TBX3 and which is also widely implicated in cancer, is shown to be a direct target of TBX3 in the TGF-β1 pathway. Taken together, these results suggest that the deregulation of TBX3 and its downstream target TBX2 may be causative to breast cancer progression and that they could serve as novel therapeutic targets to treat this disease.

The role of TBX3 in breast cancer progression

TBX3 has been found overexpressed in a subset of breast cancers and at the start of this study it was unclear whether this overexpression contributes to breast cancer progression. This study addresses this by establishing cell culture models in which TBX3 was either (1) stably silenced in an invasive breast ductal carcinoma cell line (MCF-7) which was previously shown to overexpress TBX3 or (2) overexpressed in a normal human breast epithelial cell line (MCF-12A). In both cell culture models the impact of altering TBX3 levels were then examined on key features of the cancer process. The results showed that TBX3 promotes breast cancer cell migration because when it was silenced cell migration was inhibited and the opposite effect was observed when it was overexpressed. These findings are consistent with reports linking TBX3 with cell migration. In 2008, Rodriguez and colleagues showed that TBX3 may contribute to melanoma migration through its ability to directly repress the cell adhesion molecule, E-cadherin. Similarly, TBX3 has a pro-migratory role in human bladder cancer cells and its levels correlated inversely with E-cadherin levels in these cells (Du *et al.*, 2014). Moreover, its role in cancer cell migration and invasion was further highlighted by work performed in head and neck squamous cell carcinoma cell lines in which TBX3 was strongly induced during epithelial-mesenchymal transition which is considered to play a critical role in enhancing cell motility (Humtsoe *et al.*, 2012).

Interestingly, in both knock down and overexpression cell culture models TBX3 was shown to have a negative impact on substrate -dependent and -independent proliferation of breast epithelial cells. While the anti-proliferative and pro-migratory

roles of TBX3 may appear contradictory, they are consistent with previous reports that the proliferation and migration of tumour cells are mutually exclusive and that high proliferative capacity does not necessarily confer metastatic potential (Marshall *et al.*, 2004). Indeed, this phenomenon was observed in numerous in vitro and in vivo studies including in a study by Ma et al. (2009) which showed that the Raf kinase inhibitor protein inhibits cell proliferation but promotes cell migration in rat hepatic stellate cells. (Giese *et al.*, 2003). Furthermore, the TGF-β1 signalling pathway also frequently inhibits epithelial cell proliferation while promoting cell migration (Imamura *et al*, 2012). These functions of TGF-β1 were further demonstrated in a study where an inhibitor of TGF-β1 was shown to promote substrate –dependent and –independent proliferation while inhibiting cell migration (Halder *et al.*, 2005). In summary, it would appear that TBX3 may function as a reciprocal switch between cell proliferation and tumour invasion in cancers where it is overexpressed.

The anti-proliferative function of TBX3 was shown to directly correlate with levels of p53, p21 and p14. This is inconsistent with previous reports showing that TBX3 transcriptionally represses p14 and p21 (Brummelkamp *et al.*, 2002b; Hoogaars *et al.*, 2008). Importantly, when TBX3 levels were overexpressed in the MCF-12A normal human breast epithelial cells, the expression of TBX2, the highly homologous T-box factor to TBX3, was largely reduced. This is interesting because TBX2 is a powerful pro-proliferative factor in melanoma and breast cancer cell lines (Peres et al., 2010; Redmond et al., 2010) and there has been an indication that TBX2 and TBX3 can repress each other (Rodriguez et al., (2008); unpublished data from the Goding and Prince laboratories). The pro-proliferative function of TBX2 was demonstrated to result from its ability to repress both p19/p14ARF and p21 (Jacobs et al., 2000; Lingbeek et al., 2002; Prince et al., 2004) suggesting that the increased levels of p21 in the TBX3 overexpressing cells may be due to an decrease in TBX2 levels. It is however important to note that when TBX3 was knocked down in MCF-7 cells there was no change in TBX2 levels suggesting that in this context the decreased expression of p19/p14ARF and p21 is caused by factors other than TBX2.

It is important to note that contrary to the findings of the current study, a number of studies have shown that TBX3/Tbx3 functions as a pro-proliferative factor (Carlson *et al.*, 2001b; Brummelkamp *et al.*, 2002b; Lingbeek *et al.*, 2002). There is however a precedent for TBX3 functioning as both pro-proliferative and anti-proliferative factor in the context of embryonic development. For example, during heart development Tbx3 functions in an anti-proliferative manner. Ectopic expression of Tbx3 in the highly proliferative tissue of the chamber myocardium resulted in a decrease in cell division, while silencing Tbx3 in the non-chamber myocardium promoted cell proliferation in this region (Ribeiro et al. 2007; Bakker et al. 2008). However, during liver development, Tbx3 acts as a pro-proliferative factor. A study by Suzuki et al (2008) showed that hepatoblasts isolated from the attenuated livers of Tbx3-null mice showed a decrease in proliferative ability and increased p19ARF expression, suggesting that Tbx3 represses p19ARF in these cells to promote liver cell proliferation. Moreover, Peres et al. (2010, 2013) also reported an anti-proliferative role for TBX3 in human radial growth phase and vertical growth phase melanoma cells which correlated with TBX3 activating p19ARF levels. Together with the dual roles described for TBX3 in cancer cell proliferation, these findings suggest that TBX3 may act as a pro- or anti-proliferative factor depending on the cellular context. Together, these findings suggest that the duality of TBX3 in cell proliferation depends on the particular cellular context.

In summary, the results from the knock down and overexpression models generated in this study provide evidence that increased TBX3 levels may contribute to breast cancer progression by enhancing cell migratory ability.

The upregulation of TBX3 by the TGF-β1 signalling pathway in epithelial cells

Having shown that TBX3 inhibits cell proliferation and promotes cell migration, the question arose as to what the mechanisms are that upregulate TBX3 and in particular those involved in regulating its oncogenic activity. This study provides novel data to show that the stimulation of the TGF-β1 signalling pathway results in the upregulation of

TBX3 expression and that TBX3 is a key mediator of its anti-proliferative and pro-migratory roles in epithelial cells.

TGF-β1 is an intercellular ligand that has a well-established anti-proliferative and pro-migratory role in epithelial cells (Massagué, 2012). Based on data from this study that TBX3 similarly promotes migration and invasion while having a negative impact on cell proliferation, it was speculated that TBX3 may be downstream of TGF-β1. Furthermore, microarray studies in which normal human breast epithelial cells and keratinocytes were treated with TGF-β1 showed an activation of TBX3 (Kang et al, 2003). The data presented in this study show that TGF-β1 transcriptionally activates TBX3 leading to an increase in TBX3 mRNA and protein expression in normal human breast epithelial cells and keratinocytes. Using in vitro and in vivo assays this transcriptional activation is shown to be mediated by a co-operation between Smad3/4 and JunB. This is consistent with previous reports that JunB and Smad3 can form a complex in vitro (Verrecchia *et al.*, 2001) and that the transcriptional activity of Smads in the canonical TGF-β1 signalling pathway frequently relies on partner transcription factors such as JunB, Sp1, Egr1, ATF3 and forkhead family members (Chen *et al.*, 1997; Feng *et al.*, 2000; Verrecchia *et al.*, 2001; Kang *et al.*, 2003; Seoane *et al.*, 2004; Fortin and Bernard, 2010). For example, Sp1 has been shown to physically interact with a complex of Smads to mediate TGF-β1 induced $p15^{Ink4B}$ (Feng *et al.*, 2000) and Smad3 cooperatively interacts with either c-Jun or JunB to upregulate expression of the *COL7A1* promoter (Verrecchia *et al.*, 2001).

Identification and characterisation of TBX2 as downstream target of TBX3 in the TGF-β1 signalling pathway

TGF-β1 is a potent inhibitor of cell proliferation, which is thought to result from its ability to induce a G1 cell cycle arrest through the up-regulation of the cyclin dependent kinase inhibitors, p15 and p21 (Reynisdóttir et al, 1995). This study demonstrates that TBX3 is a pivotal player in TGF-β1 mediated anti-proliferation and dissects the interrelated roles of the TBX2 and TBX3 transcription factors in this response.

The current study shows that when the TGF-β1 pathway is stimulated in breast epithelial and melanoma cells, TBX2 expression is repressed through the direct binding of TBX3 to a half T-element in the *TBX2* promoter. Results from this study support evidence for TBX2 being a powerful pro-proliferative factor (Peres *et al.*, 2010; Redmond *et al.*, 2010), and indicate that the downregulation of TBX2 blocks proliferation through the de-repression of the TBX2 target gene, p21, a cdki that initiates the TGF-β1-induced G1 arrest (Yoo *et al.*, 1999). These results are consistent with a recent report that TGF-β1-mediated growth arrest in melanoma cells could be bypassed by ectopic TBX2 expression (Liu *et al.*, 2013). Together these data provide an explanation for how the TGF-β1 pathway exerts its anti-proliferative effect and reveal an upstream mechanism involved in regulating TBX2 and TBX3 in contexts where they are differentially expressed. Moreover, TBX2 overexpression was able to override the anti-proliferative effects of TGF-β1 without affecting p15 levels and knocking down p21 alone abrogated the ability of the cells to respond to the anti-proliferative TGF-β1 signal. Together this suggests that p15 is not required for the effect of TGF-β1 on the proliferative ability of these cells, though it may be involved in other TGF-β1-mediated functions.

TBX2 and TBX3 are highly homologous T-box transcription factors which have distinct roles during embryonic development and in breast cancer and melanoma cell lines where they are both overexpressed (Davenport *et al.*, 2003; Jerome-Majewska *et al.*, 2005; Peres *et al.*, 2010; Douglas and Papaioannou, 2013; Li *et al.*, 2013). Importantly, whereas TBX2 is essential for promoting cell proliferation, the current study and other reports have shown that TBX3 inhibits cell proliferation but is required for cell migration. These results together with data from the current study suggest an interesting interplay between TBX2, TBX3 and TGF-β1 signalling in normal epithelial cells (**Fig. 4.1**). Briefly, in this context TGF-β1 signalling activates TBX3 expression in a Smad/JunB dependent manner and TBX3 then represses *TBX2* transcription which allows for the de-repression of p21 and a G1 cell cycle arrest. Interestingly, malignant cells acquire immortalising mutations that enable them to evade the anti-proliferative effects of TGF-β1 signalling.

For example, one of the mechanisms by which TGF-β1 exerts its anti-proliferative effects is through inhibiting expression of MYC that leads to the de-repression of p21. Many malignant cells however have mutations that result in the constitutive expression of MYC and hence these cells are resistant to the anti-proliferative effects of TGF-β1. It is therefore possible that cancers in which TBX2 is overexpressed will similarly disregard the TGF-β1 anti-proliferative signals. Intriguingly, the TBX3 promoter has a full consensus MYC binding site, raising the possibility that MYC will impact the TBX3-TBX2 axis identified here. The expression of MYC is usually down-regulated by TGF-β1 treatment, and ectopic expression of MYC in mouse keratinocytes desensitized the cells to TGF-β1 mediated growth inhibition (Alexandrow *et al.*, 1995; Feng *et al.*, 2002; Wu *et al.*, 2003). Furthermore, sustained MYC expression in ovarian cancers coincides with resistance to the anti-proliferative effects of TGF-β1 (Baldwin *et al.*, 2003). Although, the precise relationship between MYC and TBX2 and TBX3 expression remains to be determined, there is no doubt that TBX2 and TBX3 are likely to represent key effectors of TGF-β1 signalling in multiple cell types.

In addition to being a potent inhibitor of cell proliferation, TGF-β1 can also stimulate invasiveness by promoting an 'epithelial to mesenchyme transition'. Understanding how TGF-β1 coordinates its effects on the cell cycle and invasion in different cell types is a key issue, both for development and disease. While the TBX3 target genes downstream of the TGF-β1 signalling pathway that promotes migration was not explored in this study it is tempting to speculate that one of them would be E-cadherin, a key epithelial cell adhesion molecule. TBX3 has previously been shown to promote melanoma cell migration by directly repressing E-cadherin (Rodriguez *et al.*, 2008; Boyd *et al.*, 2012) and a study by Vincent et al. (2009) showed that TGF-β1 signalling induces a SNAIL-Smad3/4 complex which negatively regulates E-cadherin in breast epithelial cells. Interestingly, they demonstrated that while knockdown of Smad3/4 significantly rescued the repression of E-cadherin by TGF-β1, knockdown of SNAIL only had a marginal effect suggesting that other transcriptional repressors may also be required for this repression. This study also shows that knocking down TBX3 does not completely abrogate TGF-β1

induced migration. It would therefore be worthwhile to examine the impact of knocking down both TBX3 and SNAIL on E-cadherin levels as well as to determine its effect on TGF-β1 induced breast epithelial cell migration. It is important to note that TBX3 expression has been demonstrated to be upregulated in SNAIL-expressing cells (Humtsoe *et al.*, 2012) and unpublished data from our laboratory show that the expression of SNAIL is reduced in TBX3 knockdown cells. The above observations suggest that TBX3 and SNAIL can positively regulate one another and since they are both able to repress E-cadherin there may be a complex interplay between these three factors.

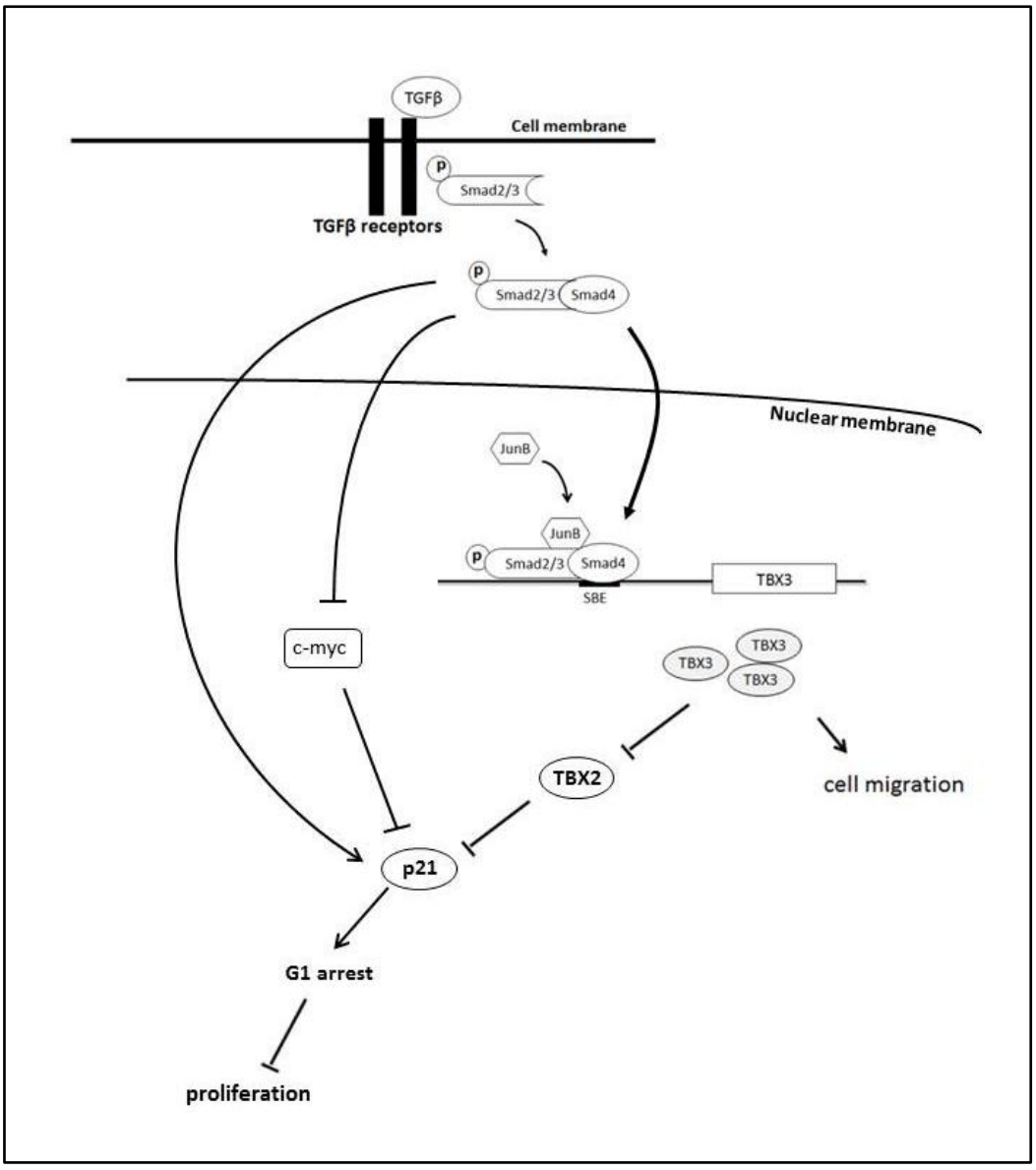

Figure 4.1. Proposed model linking TBX2 and TBX3 to the TGF-β1 signalling pathway.

Concluding remarks

Based on the results generated in this study and the current literature the following model is proposed for the role and regulation of TBX3 in breast epithelial cells (**Fig 6.6**). The complex formed by the binding of TGF-β1 to TGFβRII recruits and phosphorylates the TGFβRI, which in turn phosphorylates Smad2 and Smad3 to release them from the TGFβRI. The phosphorylated Smad2/3 form a complex with Smad4 and translocate to the nucleus where they associate with JunB and bind to the SBE on the *TBX3* promoter and drive the transcription. The activated TBX3 mediates the TGF-β1-regulated anti-proliferative and pro-migratory effect. TBX3 inhibits cell proliferation through repressing *TBX2* transcription which allows for the de-repression of p21 and a G1 cell cycle arrest. The findings of the current study are of great significance as it identifies TBX3 as a potential target for the development of novel breast cancer therapeutics.

CHAPTER 5

BIBLIOGRAPHY

Aagaard, L., Amarzguioui, M., Sun, G., Santos, L. C., Ehsani, A., Prydz, H., and Rossi, J. J. (2007). A facile lentiviral vector system for expression of doxycycline-inducible shRNAs: knockdown of the pre-miRNA processing enzyme Drosha. Mol. Ther. *15*, 938–945.

Abrahams, A., Mowla, S., Parker, M. I., Goding, C. R., and Prince, S. (2008). UV-mediated regulation of the anti-senescence factor Tbx2. J. Biol. Chem. *283*, 2223–2230.

Adams, P. D., Sellers, W. R., Sharma, S. K., Wu, A. D., Nalin, C. M., and Kaelin, W. G. (1996). Identification of a cyclin-cdk2 recognition motif present in substrates and p21-like cyclin-dependent kinase inhibitors. Mol. Cell. Biol. *16*, 6623–6633.

Adem, C. *et al.* (2004). ERBB2, TBX2, RPS6KB1, and MYC alterations in breast tissues of BRCA1 and BRCA2 mutation carriers. Genes. Chromosomes Cancer *41*, 1–11.

Affolter, M., and Basler, K. (2007). The Decapentaplegic morphogen gradient: from pattern formation to growth regulation. Nat. Rev. Genet. *8*, 663–674.

Agulnik, S. I., Garvey, N., Hancock, S., Ruvinsky, I., Chapman, D. L., Agulnik, I., Bollag, R., Papaioannou, V., and Silver, L. M. (1996). Evolution of mouse T-box genes by tandem duplication and cluster dispersion. Genetics *144*, 249–254.

Akiyoshi, S., Inoue, H., Hanai, J., Kusanagi, K., Nemoto, N., Miyazono, K., and Kawabata, M. (1999). c-Ski acts as a transcriptional co-repressor in transforming growth factor-beta signaling through interaction with smads. J. Biol. Chem. *274*, 35269–35277.

Alexandrow, M. G., Kawabata, M., Aakre, M., and Moses, H. L. (1995). Overexpression of the c-Myc oncoprotein blocks the growth-inhibitory response but is required for the mitogenic effects of transforming growth factor beta 1. Proc. Natl. Acad. Sci. U. S. A. *92*, 3239–3243.

Alvarez, A. M. (1996). Apoptosis Induced by Transforming Growth Factor-beta in Fetal Hepatocyte Primary Cultures. J. Biol. Chem. *271*, 7416–7422.

Anscher, M. S., Peters, W. P., Reisenbichler, H., Petros, W. P., and Jirtle, R. L. (1993). Transforming growth factor beta as a predictor of liver and lung fibrosis after

autologous bone marrow transplantation for advanced breast cancer. N. Engl. J. Med. *328*, 1592–1598.

Araki, K., Shimura, T., Suzuki, H., Tsutsumi, S., Wada, W., Yajima, T., Kobayahi, T., Kubo, N., and Kuwano, H. (2011). E/N-cadherin switch mediates cancer progression via TGF-β-induced epithelial-to-mesenchymal transition in extrahepatic cholangiocarcinoma. Br. J. Cancer *105*, 1885–1893.

Arias, J. (1996). Adaptor-mediated Recruitment of RNA Polymerase II to a Signal-dependent Activator. J. Biol. Chem. *271*, 2373–2375.

Atreya, I., Schimanski, C. C., Becker, C., Wirtz, S., Dornhoff, H., Schnürer, E., Berger, M. R., Galle, P. R., Herr, W., and Neurath, M. F. (2007). The T-box transcription factor eomesodermin controls CD8 T cell activity and lymph node metastasis in human colorectal cancer. Gut *56*, 1572–1578.

Baldini, A. (2005). Dissecting contiguous gene defects: TBX1. Curr. Opin. Genet. Dev. *15*, 279–284.

Baldwin, R., Tran, H., and Karlan, B. (2003). of c-myc repression coincides with ovarian cancer resistance to transforming growth factor β growth arrest independent of transforming growth factor β/Smad signaling. Cancer Res.

Ballif, B. C. *et al.* (2010). Identification of a recurrent microdeletion at 17q23.1q23.2 flanked by segmental duplications associated with heart defects and limb abnormalities. Am. J. Hum. Genet. *86*, 454–461.

Ballim, R. D., Mendelsohn, C., Papaioannou, V. E., Prince, S., Deeya, R., and Bronner-fraser, M. (2012). The ulnar-mammary syndrome gene, Tbx3, is a direct target of the retinoic acid signaling pathway, which regulates its expression during mouse limb development. Mol. Biol. Cell *23*, 2362–2372.

Bamshad, M. *et al.* (1997). Mutations in human TBX3 alter limb, apocrine and genital development in ulnar-mammary syndrome. Nat. Genet. *16*, 311–315.

Bamshad, M. *et al.* (1999). The Spectrum of Mutations in TBX3 : Genotype / Phenotype Relationship in Ulnar-Mammary Syndrome. 1550–1562.

Barlat, I., Fesquet, D., Bréchot, C., Henglein, B., Dupuy d'Angeac, A., Vié, A., and Blanchard, J. M. (1993). Loss of the G1-S control of cyclin A expression during tumoral progression of Chinese hamster lung fibroblasts. Cell Growth Differ. *4*, 105–113.

Bärlund, M., Monni, O., Kononen, J., Cornelison, R., Torhorst, J., Sauter, G., Kallioniemi OLLI-P, and Kallioniemi, A. (2000). Multiple genes at 17q23 undergo amplification and overexpression in breast cancer. Cancer Res. *60*, 5340–5344.

Baselga, J. *et al.* (2012). Everolimus in postmenopausal hormone-receptor-positive advanced breast cancer. N. Engl. J. Med. *366*, 520–529.

Basson, C. T. *et al.* (1999). Different TBX5 interactions in heart and limb defined by Holt-Oram syndrome mutations. Proc. Natl. Acad. Sci. U. S. A. *96*, 2919–2924.

Basu, A., Teicher, B. A., and Lazo, J. S. (1990). Involvement of protein kinase C in phorbol ester-induced sensitization of HeLa cells to cis-diamminedichloroplatinum(II). J. Biol. Chem. *265*, 8451–8457.

Bierie, B., and Moses, H. L. (2006). TGF-beta and cancer. Cytokine Growth Factor Rev. *17*, 29–40.

Blokzijl, A., ten Dijke, P., Ibáñez, C. F., Dijke, P., and Iba, C. F. (2002). Physical and functional interaction between GATA-3 and Smad3 allows TGF-beta regulation of GATA target genes. Curr. Biol. *12*, 35–45.

Bollag, R. J., Siegfried, Z., Cebra-Thomas, J. a, Garvey, N., Davison, E. M., and Silver, L. M. (1994). An ancient family of embryonically expressed mouse genes sharing a conserved protein motif with the T locus. Nat. Genet. *7*, 383–389.

Van den Boogaard, M. *et al.* (2012). Genetic variation in T-box binding element functionally affects SCN5A/SCN10A enhancer. J. Clin. Invest. *122*, 2519–2530.

Boogerd, C. J. J., Wong, L. Y. E., van den Boogaard, M., Bakker, M. L., Tessadori, F., Bakkers, J., 't Hoen, P. A. C., Moorman, A. F., Christoffels, V. M., and Barnett, P. (2011). Sox4 mediates Tbx3 transcriptional regulation of the gap junction protein Cx43. Cell. Mol. Life Sci. *68*, 3949–3961.

Boone, B., Haspeslagh, M., and Brochez, L. (2009). Clinical significance of the expression of c-Ski and SnoN, possible mediators in TGF-beta resistance, in primary cutaneous melanoma. J. Dermatol. Sci. *53*, 26–33.

Boskovic, G., and Niles, R. M. (2004). T-box binding protein type two (TBX2) is an immediate early gene target in retinoic-acid-treated B16 murine melanoma cells. Exp. Cell Res. *295*, 281–289.

Bouwman, P., and Jonkers, J. (2012). The effects of deregulated DNA damage signalling on cancer chemotherapy response and resistance. Nat. Rev. Cancer *12*, 587–598.

Boyd, S. C. *et al.* (2012). Oncogenic B-RAF(V600E) Signaling Induces the T-Box3 Transcriptional Repressor to Repress E-Cadherin and Enhance Melanoma Cell Invasion. J. Invest. Dermatol.

Boyer Arnold, N., and Korc, M. (2005). Smad7 abrogates transforming growth factor-beta1-mediated growth inhibition in COLO-357 cells through functional inactivation of the retinoblastoma protein. J. Biol. Chem. *280*, 21858–21866.

Braybrook, C., Doudney, K., Marçano, A. C., Arnason, A., Bjornsson, A., Patton, M. A., Goodfellow, P. J., Moore, G. E., and Stanier, P. (2001). The T-box transcription factor gene TBX22 is mutated in X-linked cleft palate and ankyloglossia. Nat. Genet. *29*, 179–183.

Brummelkamp, T. R., Kortlever, R. M., Lingbeek, M., Trettel, F., Macdonald, M. E., and Lohuizen, M. Van (2002a). TBX-3 , the Gene Mutated in Ulnar-Mammary Syndrome , Is a Negative Regulator of p19 ARF and Inhibits Senescence *. *277*, 6567–6572.

Brummelkamp, T. R., Kortlever, R. M., Lingbeek, M., Trettel, F., MacDonald, M. E., van Lohuizen, M., Bernards, R., and Lohuizen, M. Van (2002b). TBX-3, the gene mutated in Ulnar-Mammary Syndrome, is a negative regulator of p19ARF and inhibits senescence. J. Biol. Chem. *277*, 6567–6572.

Bruneau, B. G., Nemer, G., Schmitt, J. P., Charron, F., Robitaille, L., Caron, S., Conner, D. A., Gessler, M., Nemer, M., and Seidman, C. E. (2001). A Murine Model of Holt-Oram Syndrome Defines Roles of the T-Box Transcription Factor Tbx5 in Cardiogenesis and Disease. Cell *106*, 709–721.

Buess, M., Terracciano, L., Reuter, J., Ballabeni, P., Boulay, J.-L., Laffer, U., Metzger, U., Herrmann, R., and Rochlitz, C. Amplification of SKI is a prognostic marker in early colorectal cancer. Neoplasia *6*, 207–212.

Burgucu, D., Guney, K., Sahinturk, D., Ozbudak, I. H., Ozel, D., Ozbilim, G., and Yavuzer, U. (2012). Tbx3 represses PTEN and is over-expressed in head and neck squamous cell carcinoma. BMC Cancer *12*, 481.

Campbell, C., Goodrich, K., Casey, G., and Beatty, B. (1995). Cloning and mapping of a human gene (TBX2) sharing a highly conserved protein motif with the Drosophila omb gene. Genomics *28*, 255–260.

Carlson, H., Ota, S., Campbell, C. E., and Hurlin, P. J. (2001a). A dominant repression domain in Tbx3 mediates transcriptional repression and cell immortalization: relevance to mutations in Tbx3 that cause ulnar-mammary syndrome. Hum. Mol. Genet. *10*, 2403–2413.

Carlson, H., Ota, S., Campbell, C. E., and Hurlin, P. J. (2001b). A dominant repression domain in Tbx3 mediates transcriptional repression and cell immortalization: relevance to mutations in Tbx3 that cause ulnar-mammary syndrome. Hum. Mol. Genet. *10*, 2403–2413.

Carlson, H., Ota, S., Song, Y., Chen, Y., and Hurlin, P. J. (2002). Tbx3 impinges on the p53 pathway to suppress apoptosis , facilitate cell transformation and block myogenic di erentiation. 3827–3835.

Carney, D. N., Gazdar, A. F., and Minna, J. D. (1980). Positive correlation between histological tumor involvement and generation of tumor cell colonies in agarose in specimens taken directly from patients with small-cell carcinoma of the lung. Cancer Res. *40*, 1820–1823.

Carreira, S., Dexter, T. J., Yavuzer, U., Easty, D. J., and Goding, C. R. (1998). Brachyury-related transcription factor Tbx2 and repression of the melanocyte-specific TRP-1 promoter. Mol. Cell. Biol. *18*, 5099–5108.

Carreira, S., Goodall, J., Denat, L., Rodriguez, M., Nuciforo, P., Hoek, K. S., Testori, A., Larue, L., and Goding, C. R. (2006). Mitf regulation of Dia1 controls melanoma proliferation and invasiveness. Genes Dev. *20*, 3426–3439.

Carreira, S., Liu, B., and Goding, C. R. (2000). The gene encoding the T-box factor Tbx2 is a target for the microphthalmia-associated transcription factor in melanocytes. J. Biol. Chem. *275*, 21920–21927.

Cavallaro, U. (2004). N-cadherin as an invasion promoter: a novel target for antitumor therapy? Curr. Opin. Investig. Drugs *5*, 1274–1278.

Chapman, D. L., Garvey, N., Hancock, S., Alexiou, M., Agulnik, S. I., Gibson-Brown, J. J., Cebra-Thomas, J., Bollag, R. J., Silver, L. M., and Papaioannou, V. E. (1996). Expression of the T-box family genes, Tbx1-Tbx5, during early mouse development. Dev. Dyn. *206*, 379–390.

Chen, C. R., Kang, Y., and Massagué, J. (2001). Defective repression of c-myc in breast cancer cells: A loss at the core of the transforming growth factor beta growth arrest program. Proc. Natl. Acad. Sci. U. S. A. *98*, 992–999.

Chen, C.-R., Kang, Y., Siegel, P. M., Massague, J., and Massagué, J. (2002). E2F4/5 and p107 as Smad cofactors linking the TGFbeta receptor to c-myc repression. Cell *110*, 19–32.

Chen, G., Ghosh, P., Osawa, H., Sasaki, C. Y., Rezanka, L., Yang, J., O'Farrell, T. J., and Longo, D. L. (2007). Resistance to TGF-beta 1 correlates with aberrant expression of TGF-beta receptor II in human B-cell lymphoma cell lines. Blood *109*, 5301–5307.

Chen, H., Fu, T., Suh, W.-K., Tsavachidou, D., Wen, S., Gao, J., Ng Tang, D., He, Q., Sun, J., and Sharma, P. (2013). CD4 T cells require ICOS-mediated PI3K-signaling to increase T-bet expression in the setting of anti-CTLA-4 therapy. Cancer Immunol. Res. *2*, 167–176.

Chen, K. *et al.* (2009). BreakDancer: an algorithm for high-resolution mapping of genomic structural variation. Nat. Methods *6*, 677–681.

Chen, P., Tian, D., and Liu, M. (2008a). The role of Tbx2 in pancreatic cancers and its regulation by Wnt/β-catenin signaling. Chinese-German J. Clin. Oncol. *7*, 404–409.

Chen, R. H., and Chang, T. Y. (1997). Involvement of caspase family proteases in transforming growth factor-beta-induced apoptosis. Cell Growth Differ. *8*, 821–827.

Chen, X. *et al.* (2008b). Integration of external signaling pathways with the core transcriptional network in embryonic stem cells. Cell *133*, 1106–1117.

Chen, X., Weisberg, E., Fridmacher, V., Watanabe, M., Naco, G., and Whitman, M. (1997). Smad4 and FAST-1 in the assembly of activin-responsive factor. Nature *389*, 85–89.

Cheng, H. D., Lui, Y. M., and Freimanis, R. I. (1998). A novel approach to microcalcification detection using fuzzy logic technique. IEEE Trans. Med. Imaging *17*, 442–450.

Cheng, X. *et al.* (2012). Self-Renewing Endodermal Progenitor Lines Generated from Human Pluripotent Stem Cells. Cell Stem Cell *10*, 371–384.

Chesley, P. (1935). Development of the short-tailed mutant in the house mouse. J. Exp. Zool. *70*, 429–459.

Cho, K.-W., Kim, J.-Y., Song, S., Farrell, E., Eblaghie, M. C., Kim, H., Tickle, C., and Jung, H. (2006). Molecular interactions between Tbx3 and Bmp4 and a model for dorsoventral positioning of mammary gland development. Proc. Natl. Acad. Sci. U. S. A. *103*, 16788–16793.

Chowdhury, S., Ammanamanchi, S., and Howell, G. M. (2009). Epigenetic Targeting of Transforming Growth Factor β Receptor II and Implications for Cancer Therapy. Mol. Cell. Pharmacol. *1*, 57–70.

Christoffels, V. M., Hoogaars, W. M. H., Tessari, A., Clout, D. E. W., Moorman, A. F. M., and Campione, M. (2004). T-box transcription factor Tbx2 represses differentiation and formation of the cardiac chambers. Dev. Dyn. *229*, 763–770.

Chu, E. Y., Hens, J., Andl, T., Kairo, A., Yamaguchi, T. P., Brisken, C., Glick, A., Wysolmerski, J. J., and Millar, S. E. (2004). Canonical WNT signaling promotes mammary placode development and is essential for initiation of mammary gland morphogenesis. Development *131*, 4819–4829.

Chung, Y. J., Song, J. M., Lee, J. Y., Jung, Y. T., Seo, E. J., Choi, S. W., and Rhyu, M. G. (1996). Microsatellite instability-associated mutations associate preferentially with the intestinal type of primary gastric carcinomas in a high-risk population. Cancer Res. *56*, 4662–4665.

Chytil, A., Waltner-Law, M., West, R., Friedman, D., Aakre, M., Barker, D., and Law, B. (2004). Construction of a cyclin D1-Cdk2 fusion protein to model the biological functions of cyclin D1-Cdk2 complexes. J. Biol. Chem. *279*, 47688–47698.

Claassen, G. F., and Hann, S. R. (2000). A role for transcriptional repression of p21CIP1 by c-Myc in overcoming transforming growth factor beta -induced cell-cycle arrest. Proc. Natl. Acad. Sci. U. S. A. *97*, 9498–9503.

Coll, M., Seidman, J. G., Mu, C. W., and Cedex, G. (2002). Structure of the DNA-Bound T-Box Domain of Human TBX3 , a Transcription Factor Responsible for Ulnar-Mammary Syndrome. *10*, 343–356.

Conery, A. R., Cao, Y., Thompson, E. A., Townsend, C. M., Ko, T. C., and Luo, K. (2004). Akt interacts directly with Smad3 to regulate the sensitivity to TGF-β-induced apoptosis. Nat. Cell Biol. *6*, 366–372.

Corsino, P., Davis, B., Law, M., Chytil, A., Forrester, E., Nørgaard, P., Teoh, N., and Law, B. (2007). Tumors initiated by constitutive Cdk2 activation exhibit transforming growth factor beta resistance and acquire paracrine mitogenic stimulation during progression. Cancer Res. *67*, 3135–3144.

Courtney, K. D., Corcoran, R. B., and Engelman, J. A. (2010). The PI3K pathway as drug target in human cancer. J. Clin. Oncol. *28*, 1075–1083.

Cowin, P., Wysolmerski, J., Moses, H., Barcellos-hoff, M. H., Visvader, J. E., Smith, G. H., and Piwnica-worms, D. (2010). Molecular mechanisms guiding embryonic mammary gland development. Cold Spring Harb. Perspect. Biol. *2*, a003251.

Cui, W., Fowlis, D. J., Bryson, S., Duffie, E., Ireland, H., Balmain, A., and Akhurst, R. J. (1996). TGFbeta1 inhibits the formation of benign skin tumors, but enhances progression to invasive spindle carcinomas in transgenic mice. Cell *86*, 531–542.

Dan, J., Li, M., Yang, J., Li, J., Okuka, M., Ye, X., and Liu, L. (2013). Roles for Tbx3 in regulation of two-cell state and telomere elongation in mouse ES cells. Sci. Rep. *3*.

Davenport, T. G., Jerome-Majewska, L. A., and Papaioannou, V. E. (2003). Mammary gland, limb and yolk sac defects in mice lacking Tbx3, the gene mutated in human ulnar mammary syndrome. Development *130*, 2263–2273.

Davis, E., Teng, H., Bilican, B., Parker, M. I., Liu, B., Carriera, S., Goding, C. R., and Prince, S. (2008). Ectopic Tbx2 expression results in polyploidy and cisplatin resistance. Oncogene *27*, 976–984.

Deramaudt, T. B. *et al.* (2006). N-cadherin and keratinocyte growth factor receptor mediate the functional interplay between Ki-RASG12V and p53V143A in promoting pancreatic cell migration, invasion, and tissue architecture disruption. Mol. Cell. Biol. *26*, 4185–4200.

Derycke, L. D. M., and Bracke, M. E. (2004). N-cadherin in the spotlight of cell-cell adhesion, differentiation, embryogenesis, invasion and signalling. Int. J. Dev. Biol. *48*, 463–476.

Diamond, M. E., Sun, L., Ottaviano, A. J., Joseph, M. J., and Munshi, H. G. (2008). Differential growth factor regulation of N-cadherin expression and motility in normal and malignant oral epithelium. J. Cell Sci. *121*, 2197–2207.

Douglas, N. C., and Papaioannou, V. E. (2013). The T-box transcription factors TBX2 and TBX3 in mammary gland development and breast cancer. J. Mammary Gland Biol. Neoplasia *18*, 143–147.

Du, H. F., Ou, L. P., Yang, X., Song, X. D., Fan, Y. R., Tan, B., Luo, C. L., and Wu, X. H. (2014). A new PKCα/β/TBX3/E-cadherin pathway is involved in PLCε-regulated invasion and migration in human bladder cancer cells. Cell. Signal. *26*, 580–593.

Duo, S., Tiao-dong, T., Lei, Z., Wei, W., Hong-li, S., and Xian-wei, D. (2009). Expression and Clinical Significance of Tbx2 in Pancreatic Cancer. *10*, 119–122.

Dykxhoorn, D. M., Novina, C. D., and Sharp, P. A. (2003). Killing the messenger: short RNAs that silence gene expression. Nat. Rev. Mol. Cell Biol. *4*, 457–467.

Eblaghie, M. C., Song, S.-J., Kim, J.-Y., Akita, K., Tickle, C., and Jung, H.-S. (2004a). Interactions between FGF and Wnt signals and Tbx3 gene expression in mammary gland initiation in mouse embryos. J. Anat. *205*, 1–13.

Eblaghie, M. C., Song, S.-J. S., Kim, J.-Y. J.-Y., Akita, K., Tickle, C., and Jung, H. H.-S. H.-S. (2004b). Interactions between FGF and Wnt signals and Tbx3 gene expression in mammary gland initiation in mouse embryos. J. Anat. *205*, 1–13.

Elmore, S. (2007). Apoptosis: a review of programmed cell death. Toxicol. Pathol. *35*, 495–516.

Eppert, K. *et al.* (1996). MADR2 maps to 18q21 and encodes a TGFbeta-regulated MAD-related protein that is functionally mutated in colorectal carcinoma. Cell *86*, 543–552.

Etcheverry, A. *et al.* (2010). DNA methylation in glioblastoma: impact on gene expression and clinical outcome.

Ewen, M. E., Sluss, H. K., Whitehouse, L. L., and Livingston, D. M. (1993). TGF beta inhibition of Cdk4 synthesis is linked to cell cycle arrest. Cell *74*, 1009–1020.

Fan, W., Huang, X., Chen, C., Gray, J., and Huang, T. (2004). TBX3 and its isoform TBX3+2a are functionally distinctive in inhibition of senescence and are overexpressed in a subset of breast cancer cell lines. Cancer Res. *64*, 5132–5139.

Fedotov, S., and Iomin, A. (2007). Migration and proliferation dichotomy in tumor-cell invasion. Phys. Rev. Lett. *98*, 118101.

Feng, X. H., Filvaroff, E. H., and Derynck, R. (1995). Transforming growth factor-beta (TGF-beta)-induced down-regulation of cyclin A expression requires a functional TGF-beta receptor complex. Characterization of chimeric and truncated type I and type II receptors. J. Biol. Chem. *270*, 24237–24245.

Feng, X. H., Lin, X., and Derynck, R. (2000). Smad2, Smad3 and Smad4 cooperate with Sp1 to induce p15(Ink4B) transcription in response to TGF-beta. EMBO J. *19*, 5178–5193.

Feng, X.-H., and Derynck, R. (2005). Specificity and versatility in tgf-beta signaling through Smads. Annu. Rev. Cell Dev. Biol. *21*, 659–693.

Feng, X.-H., Liang, Y.-Y., Liang, M., Zhai, W., and Lin, X. (2002). Direct interaction of c-Myc with Smad2 and Smad3 to inhibit TGF-beta-mediated induction of the CDK inhibitor p15(Ink4B). Mol. Cell *9*, 133–143.

Fernando, R. I., Litzinger, M., Trono, P., Hamilton, D. H., Schlom, J., and Palena, C. (2010). The T-box transcription factor Brachyury promotes epithelial-mesenchymal transition in human tumor cells. *120*, 533–544.

Fillmore, C. M., Gupta, P. B., Rudnick, J. a, Caballero, S., Keller, P. J., Lander, E. S., and Kuperwasser, C. (2010). Estrogen expands breast cancer stem-like cells through paracrine FGF/Tbx3 signaling. Proc. Natl. Acad. Sci. U. S. A. *107*, 21737–21742.

Fillmore, C. M., and Kuperwasser, C. (2008). Human breast cancer cell lines contain stem-like cells that self-renew, give rise to phenotypically diverse progeny and survive chemotherapy. Breast Cancer Res. *10*, R25.

Fortin, J., and Bernard, D. J. (2010). SMAD3 and EGR1 physically and functionally interact in promoter-specific fashion. Cell. Signal. *22*, 936–943.

Frank, D. U., Carter, K. L., Thomas, K. R., Burr, R. M., Bakker, M. L., Coetzee, W. A., Tristani-Firouzi, M., Bamshad, M. J., Christoffels, V. M., and Moon, A. M. (2012). Lethal arrhythmias in Tbx3-deficient mice reveal extreme dosage sensitivity of cardiac conduction system function and homeostasis. Proc. Natl. Acad. Sci. U. S. A. *109*, E154–63.

Frank, D. U., Emechebe, U., Thomas, K. R., and Moon, A. M. (2013). Mouse TBX3 mutants suggest novel molecular mechanisms for Ulnar-mammary syndrome. PLoS One *8*, e67841.

Frederick, J. P., Liberati, N. T., Waddell, D. S., Shi, Y., and Wang, X.-F. (2004). Transforming Growth Factor β -Mediated Transcriptional Repression of c- myc Is Dependent on Direct Binding of Smad3 to a Novel Repressive Smad Binding Element

Transforming Growth Factor [illegible] -Mediated Transcriptional Repression of c-myc Is

Dependent on Direc. Mol. Cell. Biol. *24*, 2546–2559.

Fry, M. J. (2001). Phosphoinositide 3-kinase signalling in breast cancer: how big a role might it play? Breast Cancer Res *3*, 304–312.

Fukuchi, M., Nakajima, M., Fukai, Y., Miyazaki, T., Masuda, N., Sohda, M., Manda, R., Tsukada, K., Kato, H., and Kuwano, H. (2004). Increased expression of c-Ski as a co-repressor in transforming growth factor-beta signaling correlates with progression of esophageal squamous cell carcinoma. Int. J. Cancer *108*, 818–824.

Garattini, E., Paroni, G., and Terao, M. (2012). Retinoids and breast cancer: new clues to increase their activity and selectivity. Breast Cancer Res. *14*, 111.

Gibson-Brown, J. J., Agulnik, S. I., Chapman, D. L., Alexiou, M., Garvey, N., Silver, L. M., and Papaioannou, V. E. (1996). Evidence of a role for T-box genes in the evolution of limb morphogenesis and the specification of forelimb/hindlimb identity. Mech. Dev. *56*, 93–101.

Giese, A., Bjerkvig, R., Berens, M. E., and Westphal, M. (2003). Cost of migration: invasion of malignant gliomas and implications for treatment. J. Clin. Oncol. *21*, 1624–1636.

Gluecksohn-Schoenheimer, S. (1938). The Development of Two Tailless Mutants in the House Mouse. Genetics *23*, 573–584.

Gluecksohn-Schoenheimer, S. (1944). The Development of Normal and Homozygous Brachy (T/T) Mouse Embryos in the Extraembryonic Coelom of the Chick. Proc. Natl. Acad. Sci. U. S. A. *30*, 134–140.

Goodall, J., Martinozzi, S., Dexter, T. J., Champeval, D., Carreira, S., Larue, L., and Goding, C. R. (2004). Brn-2 expression controls melanoma proliferation and is directly regulated by beta-catenin. Mol. Cell. Biol. *24*, 2915–2922.

Gordon, K. J., and Blobe, G. C. (2008). Role of transforming growth factor-beta superfamily signaling pathways in human disease. Biochim. Biophys. Acta *1782*, 197–228.

Grady, W. M. *et al.* (1999). Mutational inactivation of transforming growth factor beta receptor type II in microsatellite stable colon cancers. Cancer Res. *59*, 320–324.

Griner, E. M., and Kazanietz, M. G. (2007). Protein kinase C and other diacylglycerol effectors in cancer. Nat. Rev. Cancer *7*, 281–294.

Guarino, M. (2007). Epithelial-mesenchymal transition and tumour invasion. Int. J. Biochem. Cell Biol. *39*, 2153–2160.

Habets, P. E. M. H., Moorman, A. F. M., Clout, D. E. W., van Roon, M. A., Lingbeek, M., van Lohuizen, M., Campione, M., and Christoffels, V. M. (2002). Cooperative action of Tbx2 and Nkx2.5 inhibits ANF expression in the atrioventricular canal: implications for cardiac chamber formation. Genes Dev. *16*, 1234–1246.

Hahn, S. A. *et al.* (1996). DPC4, a candidate tumor suppressor gene at human chromosome 18q21.1. Science *271*, 350–353.

Halder, S. K., Beauchamp, R. D., and Datta, P. K. (2005). A specific inhibitor of TGF-beta receptor kinase, SB-431542, as a potent antitumor agent for human cancers. Neoplasia *7*, 509–521.

Han, J. *et al.* (2010). Tbx3 improves the germ-line competency of induced pluripotent stem cells. Nature *463*, 1096–1100.

Han, S.-U., Kim, H.-T., Seong, D. H., Kim, Y.-S., Park, Y.-S., Bang, Y.-J., Yang, H.-K., and Kim, S.-J. (2004). Loss of the Smad3 expression increases susceptibility to tumorigenicity in human gastric cancer. Oncogene *23*, 1333–1341.

Han, Y., Tu, W.-W., Wen, Y.-G., Yan, D.-W., Qiu, G.-Q., Peng, Z.-H., and Zhou, C.-Z. (2013). Increased expression of TBX2 is a novel independent prognostic biomarker of a worse outcome in colorectal cancer patients after curative surgery and a potential therapeutic target. Med. Oncol. *30*, 688.

Hanahan, D., and Weinberg, R. A. (2000). The hallmarks of cancer. Cell *100*, 57–70.

Hanahan, D., and Weinberg, R. A. (2011). Hallmarks of cancer: the next generation. Cell *144*, 646–674.

Hanahan, D., Weinberg, R. A., and Francisco, S. (2000). The Hallmarks of Cancer Review University of California at San Francisco. *100*, 57–70.

Hanna, J., Cheng, A. W., Saha, K., Kim, J., Lengner, C. J., Soldner, F., Cassady, J. P., Muffat, J., Carey, B. W., and Jaenisch, R. (2010). Human embryonic stem cells with biological and epigenetic characteristics similar to those of mouse ESCs. Proc. Natl. Acad. Sci. U. S. A. *107*, 9222–9227.

Hannon, G. J. (2002). RNA interference. Nature *418*, 244–251.

Hansel, D. E., Rahman, A., House, M., Ashfaq, R., Berg, K., Yeo, C. J., and Maitra, A. (2004). Met proto-oncogene and insulin-like growth factor binding protein 3 overexpression correlates with metastatic ability in well-differentiated pancreatic endocrine neoplasms. Clin. Cancer Res. *10*, 6152–6158.

Harrelson, Z., Kelly, R. G., Goldin, S. N., Gibson-Brown, J. J., Bollag, R. J., Silver, L. M., and Papaioannou, V. E. (2004). Tbx2 is essential for patterning the atrioventricular canal and for morphogenesis of the outflow tract during heart development. Development *131*, 5041–5052.

Hayashi, H. *et al.* (1997). The MAD-Related Protein Smad7 Associates with the TGFβ Receptor and Functions as an Antagonist of TGFβ Signaling. Cell *89*, 1165–1173.

Hazan, R. B., Phillips, G. R., Qiao, R. F., Norton, L., and Aaronson, S. A. (2000). Exogenous expression of N-cadherin in breast cancer cells induces cell migration, invasion, and metastasis. J. Cell Biol. *148*, 779–790.

He, M. l, Wen, L., Campbell, C. E., Wu, J. Y., and Rao, Y. (1999). Transcription repression by Xenopus ET and its human ortholog TBX3, a gene involved in ulnar-mammary syndrome. Proc. Natl. Acad. Sci. U. S. A. *96*, 10212–10217.

Heldin, C., Vanlandewijck, M., and Moustakas, A. (2012). Regulation of EMT by TGFβ in cancer. FEBS Lett. *586*, 1959–1970.

Hemmings, B. A., and Restuccia, D. F. (2012). PI3K-PKB/Akt pathway. Cold Spring Harb. Perspect. Biol. *4*, a011189.

Herrmann, B. G., Labeit, S., Poustka, A., King, T. R., and Lehrach, H. (1990). Cloning of the T gene required in mesoderm formation in the mouse. Nature *343*, 617–622.

Hinshelwood, R. A. *et al.* (2007). Concordant epigenetic silencing of transforming growth factor-beta signaling pathway genes occurs early in breast carcinogenesis. Cancer Res. *67*, 11517–11527.

Hirai, H., Karian, P., and Kikyo, N. (2011). Regulation of embryonic stem cell self-renewal and pluripotency by leukaemia inhibitory factor. Biochem. J. *438*, 11–23.

Hiroi, Y., Kudoh, S., Monzen, K., Ikeda, Y., Yazaki, Y., Nagai, R., and Komuro, I. (2001). Tbx5 associates with Nkx2-5 and synergistically promotes cardiomyocyte differentiation. Nat. Genet. *28*, 276–280.

Hoek, K. *et al.* (2004). Expression Profiling Reveals Novel Pathways in the Transformation of Melanocytes to Melanomas. *165*, 5270–5282.

Hoogaars, W. M. H. *et al.* (2007). Tbx3 controls the sinoatrial node gene program and imposes pacemaker function on the atria. Genes Dev. *21*, 1098–1112.

Hoogaars, W. M. H., Barnett, P., Rodriguez, M., Clout, D. E., Moorman, A. F. M., Goding, C. R., and Christoffels, V. M. (2008). TBX3 and its splice variant TBX3 + exon 2a are functionally similar. Pigment Cell Melanoma Res. *21*, 379–387.

Howard, J. H., and Bland, K. I. (2012). Current management and treatment strategies for breast cancer. Curr. Opin. Obstet. Gynecol. *24*, 44–48.

Hu, X., Cui, D., Moscinski, L. C., Zhang, X., Maccachero, V., and Zuckerman, K. S. (2007). TGFbeta regulates the expression and activities of G2 checkpoint kinases in human myeloid leukemia cells. Cytokine *37*, 155–162.

Huber, M. A., Azoitei, N., Baumann, B., Grünert, S., Sommer, A., Pehamberger, H., Kraut, N., Beug, H., and Wirth, T. (2004). NF-kappaB is essential for epithelial-mesenchymal transition and metastasis in a model of breast cancer progression. J. Clin. Invest. *114*, 569–581.

Humtsoe, J. O., Koya, E., Pham, E., Aramoto, T., Zuo, J., Ishikawa, T., and Kramer, R. H. (2012). Transcriptional profiling identifies upregulated genes following induction of epithelial-mesenchymal transition in squamous carcinoma cells. Exp. Cell Res. *318*, 379–390.

Imamura, T., Hikita, A., and Inoue, Y. (2012). The roles of TGF-β signaling in carcinogenesis and breast cancer metastasis. Breast Cancer *19*, 118–124.

Inagawa, S., Itabashi, M., Adachi, S., Kawamoto, T., Hori, M., Shimazaki, J., Yoshimi, F., and Fukao, K. (2002). Expression and prognostic roles of beta-catenin in

hepatocellular carcinoma: correlation with tumor progression and postoperative survival. Clin. Cancer Res. *8*, 450–456.

Ismail, A., and Bateman, A. (2009). Expression of TBX2 promotes anchorage-independent growth and survival in the p53-negative SW13 adrenocortical carcinoma. CANCER Lett., 1–11.

Ito, A., Asamoto, M., Hokaiwado, N., Takahashi, S., and Shirai, T. (2005). Tbx3 expression is related to apoptosis and cell proliferation in rat bladder both hyperplastic epithelial cells and carcinoma cells. Cancer Lett. *219*, 105–112.

Ivanova, N., Dobrin, R., Lu, R., Kotenko, I., Levorse, J., DeCoste, C., Schafer, X., Lun, Y., and Lemischka, I. R. (2006). Dissecting self-renewal in stem cells with RNA interference. Nature *442*, 533–538.

Izumoto, S., Arita, N., Ohnishi, T., Hiraga, S., Taki, T., Tomita, N., Ohue, M., and Hayakawa, T. (1997). Microsatellite instability and mutated type II transforming growth factor-beta receptor gene in gliomas. Cancer Lett. *112*, 251–256.

Jackson, D., Zheng, Y., Lyo, D., Shen, Y., Nakayama, K., Nakayama, K. I., Humphries, M. J., Reyland, M. E., and Foster, D. A. (2005). Suppression of cell migration by protein kinase Cdelta. Oncogene *24*, 3067–3072.

Jacobs, J. J. *et al.* (2000). Senescence bypass screen identifies TBX2, which represses Cdkn2a (p19(ARF)) and is amplified in a subset of human breast cancers. Nat. Genet. *26*, 291–299.

Jahn, S. C., Law, M. E., Corsino, P. E., and Law, B. K. (2012). TGF-beta antiproliferative effects in tumor suppression. Front. Biosci. (Schol. Ed). *4*, 749–766.

Jakowlew, S. B. (2006). Transforming growth factor-beta in cancer and metastasis. Cancer Metastasis Rev. *25*, 435–457.

Jang, C.-W., Chen, C.-H., Chen, C.-C., Chen, J., Su, Y.-H., and Chen, R.-H. (2002). TGF-beta induces apoptosis through Smad-mediated expression of DAP-kinase. Nat. Cell Biol. *4*, 51–58.

Jawhari, A., Jordan, S., Poole, S., Browne, P., Pignatelli, M., and Farthing, M. (1997). Abnormal immunoreactivity of the E-cadherin-catenin complex in gastric carcinoma: Relationship with patient survival. Gastroenterology *112*, 46–54.

Jerome, L. A., and Papaioannou, V. E. (2001). DiGeorge syndrome phenotype in mice mutant for the T-box gene, Tbx1. Nat. Genet. *27*, 286–291.

Jerome-Majewska, L. A., Jenkins, G. P., Ernstoff, E., Zindy, F., Sherr, C. J., and Papaioannou, V. E. (2005). Tbx3, the ulnar-mammary syndrome gene, and Tbx2 interact in mammary gland development through a p19Arf/p53-independent pathway. Dev. Dyn. *234*, 922–933.

Jong, H.-S., Lee, H. S., Kim, T. Y., Im, Y.-H., Park, J.-W., Kim, N. K., and Bang, Y.-J. (2002). Attenuation of transforming growth factor beta-induced growth inhibition in human hepatocellular carcinoma cell lines by cyclin D1 overexpression. Biochem. Biophys. Res. Commun. *292*, 383–389.

Jonk, L. J. C. (1998). Identification and Functional Characterization of a Smad Binding Element (SBE) in the JunB Promoter That Acts as a Transforming Growth Factor-beta , Activin, and Bone Morphogenetic Protein-inducible Enhancer. J. Biol. Chem. *273*, 21145–21152.

Joo, Y.-E., Rew, J.-S., Park, C.-S., and Kim, S.-J. (2002). Expression of E-cadherin, alpha- and beta-catenins in patients with pancreatic adenocarcinoma. Pancreatology *2*, 129–137.

Kallergi, G., Papadaki, M. A., Politaki, E., Mavroudis, D., Georgoulias, V., and Agelaki, S. (2011). Epithelial to mesenchymal transition markers expressed in circulating tumour cells of early and metastatic breast cancer patients. Breast Cancer Res. *13*, R59.

Kalluri, R., and Weinberg, R. A. (2009). The basics of epithelial-mesenchymal transition. *119*.

Kandimalla, R., van Tilborg, A. a G., Kompier, L. C., Stumpel, D. J. P. M., Stam, R. W., Bangma, C. H., and Zwarthoff, E. C. (2012). Genome-wide analysis of CpG island methylation in bladder cancer identified TBX2, TBX3, GATA2, and ZIC4 as pTa-specific prognostic markers. Eur. Urol. *61*, 1245–1256.

Kang, J. S., Alliston, T., Delston, R., and Derynck, R. (2005). Repression of Runx2 function by TGF-beta through recruitment of class II histone deacetylases by Smad3. EMBO J. *24*, 2543–2555.

Kang, Y., Chen, C.-R., Massague, J., and Massagué, J. (2003). A self-enabling TGFbeta response coupled to stress signaling: Smad engages stress response factor ATF3 for Id1 repression in epithelial cells. Mol. Cell *11*, 915–926.

Karatzas, G., Karayiannakis, A. J., Syrigos, K. N., Chatzigianni, E., Papanikolaou, S., Riza, F., and Papanikolaou, D. (1999). E-cadherin expression correlates with tumor differentiation in colorectal cancer. Hepatogastroenterology. *46*, 232–235.

Karayiannakis, A. J., Syrigos, K. N., Polychronidis, A., and Simopoulos, C. (2001). Expression patterns of alpha-, beta- and gamma-catenin in pancreatic cancer: correlation with E-cadherin expression, pathological features and prognosis. Anticancer Res. *21*, 4127–4134.

Kartikasari, A. E. R., Zhou, J. X., Kanji, M. S., Chan, D. N., Sinha, A., Grapin-Botton, A., Magnuson, M. A., Lowry, W. E., and Bhushan, A. (2013). The histone demethylase Jmjd3 sequentially associates with the transcription factors Tbx3 and Eomes to drive endoderm differentiation. EMBO J. *32*, 1393–1408.

Kato, Y., Habas, R., Katsuyama, Y., Näär, A. M., and He, X. (2002). A component of the ARC/Mediator complex required for TGF beta/Nodal signalling. Nature *418*, 641–646.

Kawakami, Y. *et al.* (2007). Tbx2 and Tbx3 regulate the dynamics of cell proliferation during heart remodeling. PLoS One *2*, e398.

Kawamura, A., Koshida, S., and Takada, S. (2008). Activator-to-repressor conversion of T-box transcription factors by the Ripply family of Groucho/TLE-associated mediators. Mol. Cell. Biol. *28*, 3236–3244.

Kim, S. G., Jong, H.-S., Kim, T.-Y., Lee, J. W., Kim, N. K., Hong, S. H., and Bang, Y.-J. (2004). Transforming growth factor-beta 1 induces apoptosis through Fas ligand-independent activation of the Fas death pathway in human gastric SNU-620 carcinoma cells. Mol. Biol. Cell *15*, 420–434.

Kispert, a, Koschorz, B., and Herrmann, B. G. (1995a). The T protein encoded by Brachyury is a tissue-specific transcription factor. EMBO J. *14*, 4763–4772.

Kispert, A., and Herrmann, B. G. (1993). The Brachyury protein novel DNA binding. *12*, 3211–3220.

Kispert, A., Ortner, H., Cooke, J., and Herrmann, B. G. (1995b). The chick Brachyury gene: developmental expression pattern and response to axial induction by localized activin. Dev. Biol. *168*, 406–415.

Kleeff, J., Ishiwata, T., Maruyama, H., Friess, H., Truong, P., Büchler, M. W., Falb, D., and Korc, M. (1999). The TGF-beta signaling inhibitor Smad7 enhances tumorigenicity in pancreatic cancer. Oncogene *18*, 5363–5372.

Klymkowsky, M. W., and Savagner, P. (2009). Epithelial-mesenchymal transition: a cancer researcher's conceptual friend and foe. Am. J. Pathol. *174*, 1588–1593.

Ko, T. C., Sheng, H. M., Reisman, D., Thompson, E. A., and Beauchamp, R. D. (1995). Transforming growth factor-beta 1 inhibits cyclin D1 expression in intestinal epithelial cells. Oncogene *10*, 177–184.

Koinuma, D., Tsutsumi, S., Kamimura, N., Taniguchi, H., Miyazawa, K., Sunamura, M., Imamura, T., Miyazono, K., and Aburatani, H. (2009). Chromatin immunoprecipitation on microarray analysis of Smad2/3 binding sites reveals roles of ETS1 and TFAP2A in transforming growth factor beta signaling. Mol. Cell. Biol. *29*, 172–186.

Kondo, Y., Kanai, Y., Sakamoto, M., Genda, T., Mizokami, M., Ueda, R., and Hirohashi, S. (1999). Beta-catenin accumulation and mutation of exon 3 of the beta-catenin gene in hepatocellular carcinoma. Jpn. J. Cancer Res. *90*, 1301–1309.

Larisch, S. *et al.* (2000). A novel mitochondrial septin-like protein, ARTS, mediates apoptosis dependent on its P-loop motif. Nat. Cell Biol. *2*, 915–921.

Law, D. J., Gebuhr, T., Garvey, N., Agulnik, S. I., and Silver, L. M. (1995). Identification, characterization, and localization to chromosome 17q21-22 of the human TBX2 homolog, member of a conserved developmental gene family. Mamm. Genome *6*, 793–797.

Lee, H.-J., Yun, C.-H., Lim, S. H., Kim, B.-C., Baik, K. G., Kim, J.-M., Kim, W.-H., and Kim, S.-J. (2007). SRF is a nuclear repressor of Smad3-mediated TGF-beta signaling. Oncogene *26*, 173–185.

Levy, L., and Hill, C. S. (2006). Alterations in components of the TGF-beta superfamily signaling pathways in human cancer. Cytokine Growth Factor Rev. *17*, 41–58.

Li, J., Weinberg, M. S., Zerbini, L., and Prince, S. (2013). The oncogenic TBX3 is a downstream target and mediator of the TGF-β1 signaling pathway. Mol. Biol. Cell.

Li, J.-R., Li, J.-G., Deng, G.-H., Zhao, W.-L., Dan, Y.-J., Wang, Y.-M., and Chen, S. (2011). A common promoter variant of TBX21 is associated with allele specific binding to Yin-Yang 1 and reduced gene expression. Scand. J. Immunol. *73*, 449–458.

Liang, Y.-Y., Brunicardi, F. C., and Lin, X. (2009). Smad3 mediates immediate early induction of Id1 by TGF-beta. Cell Res. *19*, 140–148.

Liberati, N. T., Datto, M. B., Frederick, J. P., Shen, X., Wong, C., Rougier-Chapman, E. M., and Wang, X. F. (1999). Smads bind directly to the Jun family of AP-1 transcription factors. Proc. Natl. Acad. Sci. U. S. A. *96*, 4844–4849.

Liberatore, C. M., Searcy-Schrick, R. D., and Yutzey, K. E. (2000). Ventricular expression of tbx5 inhibits normal heart chamber development. Dev. Biol. *223*, 169–180.

Lingbeek, M. E., Jacobs, J. J. L., and van Lohuizen, M. (2002). The T-box repressors TBX2 and TBX3 specifically regulate the tumor suppressor gene p14ARF via a variant T-site in the initiator. J. Biol. Chem. *277*, 26120–26127.

Liu, D., Black, B. L., and Derynck, R. (2001a). TGF-beta inhibits muscle differentiation through functional repression of myogenic transcription factors by Smad3. Genes Dev. *15*, 2950–2966.

Liu, F., Cao, J., Lv, J., Dong, L., Pier, E., Xu, G. X., Wang, R., Xu, Z., Goding, C., and Cui, R. (2013). TBX2 expression is regulated by PAX3 in the melanocyte lineage. Pigment Cell Melanoma Res. *26*, 67–77.

Liu, J., Lin, C., Gleiberman, A., Ohgi, K. A., Herman, T., Huang, H. P., Tsai, M. J., and Rosenfeld, M. G. (2001b). Tbx19, a tissue-selective regulator of POMC gene expression. Proc. Natl. Acad. Sci. U. S. A. *98*, 8674–8679.

Liu, W.-K., Jiang, X.-Y., and Zhang, Z.-X. (2010). Expression of PSCA, PIWIL1, and TBX2 in endometrial adenocarcinoma. Onkologie *33*, 241–245.

Logan, C. Y., and Nusse, R. (2004). The Wnt signaling pathway in development and disease. Annu. Rev. Cell Dev. Biol. *20*, 781–810.

Lomnytska, M., Dubrovska, A., Hellman, U., Volodko, N., and Souchelnytskyi, S. (2006). Increased expression of cSHMT, Tbx3 and utrophin in plasma of ovarian and breast cancer patients. Int. J. Cancer *118*, 412–421.

Lu, R., Yang, A., and Jin, Y. (2011). Dual functions of T-box 3 (Tbx3) in the control of self-renewal and extraembryonic endoderm differentiation in mouse embryonic stem cells. J. Biol. Chem. *286*, 8425–8436.

Lyng, H., Brøvig, R. S., Svendsrud, D. H., Holm, R., Kaalhus, O., Knutstad, K., Oksefjell, H., Sundfør, K., Kristensen, G. B., and Stokke, T. (2006). Gene expressions and copy numbers associated with metastatic phenotypes of uterine cervical cancer. BMC Genomics *7*, 268.

Ma, J., Li, F., Liu, L., Cui, D., Wu, X., Jiang, X., and Jiang, H. (2009). Raf kinase inhibitor protein inhibits cell proliferation but promotes cell migration in rat hepatic stellate cells. Liver Int. *29*, 567–574.

Macfarlan, T. S., Gifford, W. D., Driscoll, S., Lettieri, K., Rowe, H. M., Bonanomi, D., Firth, A., Singer, O., Trono, D., and Pfaff, S. L. (2012). Embryonic stem cell potency fluctuates with endogenous retrovirus activity. Nature *487*, 57–63.

MacMurray, A., and Shin, H. S. (1988). The antimorphic nature of the Tc allele at the mouse T locus. Genetics *120*, 545–550.

Mahlamäki, E. H., Bärlund, M., Tanner, M., Gorunova, L., Höglund, M., Karhu, R., and Kallioniemi, A. (2002). Frequent amplification of 8q24, 11q, 17q, and 20q-specific genes in pancreatic cancer. Genes. Chromosomes Cancer *35*, 353–358.

Marengo, B., De Ciucis, C., Ricciarelli, R., Pronzato, M., Marinari, U., and Domenicotti, C. (2011). Protein Kinase C: An Attractive Target for Cancer Therapy. Cancers (Basel). *3*, 531–567.

Markowitz, S., Wang, J., Myeroff, L., Parsons, R., Sun, L., Lutterbaugh, J., Fan, R. S., Zborowska, E., Kinzler, K. W., and Vogelstein, B. (1995). Inactivation of the type II TGF-beta receptor in colon cancer cells with microsatellite instability. Science *268*, 1336–1338.

Marshall, J.-C., Caissie, A. L., Callejo, S. A., Antecka, E., and Burnier Jr, M. N. (2004). Cell proliferation profile of five human uveal melanoma cell lines of different metastatic potential. Pathobiology *71*, 241–245.

Martinez, L. A., Chen, Y., Pavone, A., Fischer, S. M., and Conti, C. J. (2000). Deregulated expression of cyclin D1 overrides antimitogenic signals. Oncogene *19*, 315–322.

Massagué, J. (2012). TGFβ signalling in context. Nat. Rev. Mol. Cell Biol. *13*, 616–630.

Massagué, J., Seoane, J., and Wotton, D. (2005). Smad transcription factors. Genes Dev. *19*, 2783–2810.

McCune, K., Bhat-Nakshatri, P., Thorat, M. A., Nephew, K. P., Badve, S., and Nakshatri, H. (2010). Prognosis of hormone-dependent breast cancers: implications of the presence of dysfunctional transcriptional networks activated by insulin via the immune transcription factor T-bet. Cancer Res. *70*, 685–696.

Meneghini, V., Odent, S., Platonova, N., Egeo, A., and Merlo, G. R. (2006). Novel TBX3 mutation data in families with ulnar-mammary syndrome indicate a genotype-phenotype relationship: mutations that do not disrupt the T-domain are associated with less severe limb defects. Eur. J. Med. Genet. *49*, 151–158.

Mesbah, K., Harrelson, Z., Théveniau-Ruissy, M., Papaioannou, V. E., Kelly, R. G., The, M., and Virginia, E. (2008). Tbx3 is required for outflow tract development. Circ. Res. *103*, 743–750.

Minguillon, C., and Logan, M. (2003). The comparative genomics of T-box genes. Brief. Funct. Genomic. Proteomic. *2*, 224–233.

Miyazono, K. (2009). Transforming growth factor-β signaling in epithelial-mesenchymal transition and progression of cancer. Proc. Japan Acad. Ser. B *85*, 314–323.

Mizutani, C. M., and Bier, E. (2008). EvoD/Vo: the origins of BMP signalling in the neuroectoderm. Nat. Rev. Genet. *9*, 663–677.

Morikawa, M., Koinuma, D., Tsutsumi, S., Vasilaki, E., Kanki, Y., Heldin, C.-H., Aburatani, H., and Miyazono, K. (2011). ChIP-seq reveals cell type-specific binding patterns of BMP-specific Smads and a novel binding motif. Nucleic Acids Res. *39*, 8712–8727.

Moses, H., and Barcellos-Hoff, M. H. (2011). TGF-beta biology in mammary development and breast cancer. Cold Spring Harb. Perspect. Biol. *3*, a003277.

Mowla, S., Pinnock, R., Leaner, V. D., Goding, C. R., and Prince, S. (2011). PMA-induced up-regulation of TBX3 is mediated by AP-1 and contributes to breast cancer cell migration. Biochem. J. *433*, 145–153.

Mullen, A. C., Orlando, D. A., Newman, J. J., Lovén, J., Kumar, R. M., Bilodeau, S., Reddy, J., Guenther, M. G., DeKoter, R. P., and Young, R. A. (2011). Master transcription factors determine cell-type-specific responses to TGF-β signaling. Cell *147*, 565–576.

Naiche, L. a, Harrelson, Z., Kelly, R. G., and Papaioannou, V. E. (2005). T-box genes in vertebrate development. Annu. Rev. Genet. *39*, 219–239.

Nakajima, S. *et al.* (2004). N-cadherin expression and epithelial-mesenchymal transition in pancreatic carcinoma. Clin. Cancer Res. *10*, 4125–4133.

Nimmakayalu, M., Major, H., Sheffield, V., Solomon, D. H., Smith, R. J., Patil, S. R., and Shchelochkov, O. A. (2011). Microdeletion of 17q22q23.2 encompassing TBX2 and TBX4 in a patient with congenital microcephaly, thyroid duct cyst, sensorineural hearing loss, and pulmonary hypertension. Am. J. Med. Genet. A *155A*, 418–423.

Niwa, H., Ogawa, K., Shimosato, D., and Adachi, K. (2009). A parallel circuit of LIF signalling pathways maintains pluripotency of mouse ES cells. Nature *460*, 118–122.

Onder, T. T., Gupta, P. B., Mani, S. A., Yang, J., Lander, E. S., and Weinberg, R. A. (2008). Loss of E-cadherin promotes metastasis via multiple downstream transcriptional pathways. Cancer Res. *68*, 3645–3654.

Osada, H., Tatematsu, Y., Sugito, N., Horio, Y., and Takahashi, T. (2005). Histone modification in the TGFbetaRII gene promoter and its significance for responsiveness to HDAC inhibitor in lung cancer cell lines. Mol. Carcinog. *44*, 233–241.

Osaki, M., Oshimura, M., and Ito, H. (2004). PI3K-Akt pathway: its functions and alterations in human cancer. Apoptosis *9*, 667–676.

Papaioannou, V. E. (2001). T-box genes in development: from hydra to humans. Int. Rev. Cytol. *207*, 1–70.

Papaioannou, V. E., and Silver, L. M. (1998). The T-box gene family. Bioessays *20*, 9–19.

Pardali, K., Kurisaki, a, Morén, a, ten Dijke, P., Kardassis, D., and Moustakas, a (2000). Role of Smad proteins and transcription factor Sp1 in p21(Waf1/Cip1) regulation by transforming growth factor-beta. J. Biol. Chem. *275*, 29244–29256.

Parekh, T. V, Gama, P., Wen, X., Demopoulos, R., Munger, J. S., Carcangiu, M.-L., Reiss, M., and Gold, L. I. (2002). Transforming growth factor beta signaling is disabled early in human endometrial carcinogenesis concomitant with loss of growth inhibition. Cancer Res. *62*, 2778–2790.

Park, I.-K. *et al.* (2002). Differential gene expression profiling of adult murine hematopoietic stem cells. Blood *99*, 488–498.

Park, J. C., Chae, Y. K., Son, C. H., Kim, M. S., Lee, J., Ostrow, K., Sidransky, D., Hoque, M. O., and Moon, C. (2008). Epigenetic silencing of human T (brachyury homologue) gene in non-small-cell lung cancer. Biochem. Biophys. Res. Commun. *365*, 221–226.

Parker, J., Daniel, L. W., and Waite, M. (1987). Evidence of protein kinase C involvement in phorbol diester-stimulated arachidonic acid release and prostaglandin synthesis. J. Biol. Chem. *262*, 5385–5393.

Parsons, R., Myeroff, L. L., Liu, B., Willson, J. K., Markowitz, S. D., Kinzler, K. W., and Vogelstein, B. (1995). Microsatellite instability and mutations of the transforming growth factor beta type II receptor gene in colorectal cancer. Cancer Res. *55*, 5548–5550.

Paxton, C., Zhao, H., Chin, Y., Langner, K., and Reecy, J. (2002). Murine Tbx2 contains domains that activate and repress gene transcription. *283*, 117–124.

Peinado, H., Quintanilla, M. growth factor beta-1 induces snail transcription factor in epithelial cell lines: mechanisms for epithelial mesenchymal transitions., and Cano, A. (2003). Transforming growth factor beta-1 induces snail transcription factor in epithelial cell lines: mechanisms for epithelial mesenchymal transitions. J. Biol. Chem. *278*, 21113–21123.

Pera, M. F., and Tam, P. P. L. (2010). Extrinsic regulation of pluripotent stem cells. *465*.

Peres, J., Davis, E., Mowla, S., Bennett, D. C., Li, J. a., Wansleben, S., and Prince, S. (2010). The Highly Homologous T-Box Transcription Factors, TBX2 and TBX3, Have Distinct Roles in the Oncogenic Process. Genes Cancer *1*, 272–282.

Peres, J., and Prince, S. (2013). The T-box transcription factor, TBX3, is sufficient to promote melanoma formation and invasion. Mol. Cancer *12*, 117.

Perlman, R., Schiemann, W. P., Brooks, M. W., Lodish, H. F., and Weinberg, R. A. (2001). TGF-beta-induced apoptosis is mediated by the adapter protein Daxx that facilitates JNK activation. Nat. Cell Biol. *3*, 708–714.

Pflugfelder, G. O., Roth, H., and Poeck, B. (1992). A homology domain shared between Drosophila optomotor-blind and mouse Brachyury is involved in DNA binding. Biochem. Biophys. Res. Commun. *186*, 918–925.

Pierce, D. F., Johnson, M. D., Matsui, Y., Robinson, S. D., Gold, L. I., Purchio, A. F., Daniel, C. W., Hogan, B. L., and Moses, H. L. (1993). Inhibition of mammary duct development but not alveolar outgrowth during pregnancy in transgenic mice expressing active TGF-beta 1. Genes Dev. *7*, 2308–2317.

Platonova, N., Scotti, M., Babich, P., Bertoli, G., Mento, E., Meneghini, V., Egeo, A., Zucchi, I., and Merlo, G. R. (2007). TBX3, the gene mutated in ulnar-mammary syndrome, promotes growth of mammary epithelial cells via repression of p19ARF, independently of p53. Cell Tissue Res. *328*, 301–316.

Poncelet, a C., and Schnaper, H. W. (2001). Sp1 and Smad proteins cooperate to mediate transforming growth factor-beta 1-induced alpha 2(I) collagen expression in human glomerular mesangial cells. J. Biol. Chem. *276*, 6983–6992.

Postigo, A. A. (2003). Opposing functions of ZEB proteins in the regulation of the TGFbeta/BMP signaling pathway. EMBO J. *22*, 2443–2452.

Price, F. D., Yin, H., Jones, A., van Ijcken, W., Grosveld, F., and Rudnicki, M. A. (2013). Canonical Wnt signaling induces a primitive endoderm metastable state in mouse embryonic stem cells. Stem Cells *31*, 752–764.

Prince, S., Carreira, S., Vance, K. W., Abrahams, A., and Goding, C. R. (2004a). Tbx2 Directly Represses the Expression of the p21 WAF1 Cyclin-Dependent Kinase Inhibitor Kinase Inhibitor. Cancer Res. *64*, 1669–1674.

Prince, S., Carreira, S., Vance, K. W., Abrahams, A., and Goding, C. R. (2004b). Tbx2 directly represses the expression of the p21(WAF1) cyclin-dependent kinase inhibitor. Cancer Res. *64*, 1669–1674.

Prince, S., Wiggins, T., Hulley, P. A., and Kidson, S. H. (2003). Stimulation of Melanogenesis by Tetradecanoylphorbol 13-acetate (TPA) in Mouse Melanocytes and Neural Crest Cells. Pigment Cell Res. *16*, 26–34.

Qi, T., Han, J., Cui, Y., Zong, M., Liu, X., and Zhu, B. (2008). Comparative proteomic analysis for the detection of biomarkers in pancreatic ductal adenocarcinomas. J. Clin. Pathol. *61*, 49–58.

Raingeaud, J., Gupta, S., Rogers, J. S., Dickens, M., Han, J., Ulevitch, R. J., and Davis, R. J. (1995). Pro-inflammatory cytokines and environmental stress cause p38 mitogen-activated protein kinase activation by dual phosphorylation on tyrosine and threonine. J. Biol. Chem. *270*, 7420–7426.

Ralph, D., McClelland, M., and Welsh, J. (1993). RNA fingerprinting using arbitrarily primed PCR identifies differentially regulated RNAs in mink lung (Mv1Lu) cells growth arrested by transforming growth factor beta 1. Proc. Natl. Acad. Sci. *90*, 10710–10714.

Rashbass, P., Cooke, L. A., Herrmann, B. G., and Beddington, R. S. (1991). A cell autonomous function of Brachyury in T/T embryonic stem cell chimaeras. Nature *353*, 348–351.

Reddy, K. B., Hocevar, B. A., and Howe, P. H. (1994). Inhibition of G1 phase cyclin dependent kinases by transforming growth factor beta 1. J. Cell. Biochem. *56*, 418–425.

Redmond, K. L. *et al.* (2010). T-box 2 represses NDRG1 through an EGR1-dependent mechanism to drive the proliferation of breast cancer cells. Oncogene *29*, 3252–3262.

Remy, I., Montmarquette, A., and Michnick, S. W. (2004). PKB/Akt modulates TGF-beta signalling through a direct interaction with Smad3. Nat. Cell Biol. *6*, 358–365.

Renard, C.-A. *et al.* (2007). Tbx3 is a downstream target of the Wnt/beta-catenin pathway and a critical mediator of beta-catenin survival functions in liver cancer. Cancer Res. *67*, 901–910.

Reynisdóttir, I., Polyak, K., Iavarone, A., and Massagué, J. (1995). Kip/Cip and Ink4 Cdk inhibitors cooperate to induce cell cycle arrest in response to TGF-beta. Genes Dev. *9*, 1831–1845.

Richmond, P. J., Karayiannakis, A. J., Nagafuchi, A., Kaisary, A. V, and Pignatelli, M. (1997). Aberrant E-cadherin and alpha-catenin expression in prostate cancer: correlation with patient survival. Cancer Res. *57*, 3189–3193.

Roberts, C., Ivins, S. M., James, C. T., and Scambler, P. J. (2005). Retinoic acid down-regulates Tbx1 expression in vivo and in vitro. Dev. Dyn. *232*, 928–938.

Robinson, G. W. (2007). Cooperation of signalling pathways in embryonic mammary gland development. Nat. Rev. Genet. *8*, 963–972.

Robson, C. N., Gnanapragasam, V., Byrne, R. L., Collins, A. T., and Neal, D. E. (1999). Transforming growth factor-beta1 up-regulates p15, p21 and p27 and blocks cell cycling in G1 in human prostate epithelium. J. Endocrinol. *160*, 257–266.

Rock, J. R., Onaitis, M. W., Rawlins, E. L., Lu, Y., Clark, C. P., Xue, Y., Randell, S. H., and Hogan, B. L. M. (2009). Basal cells as stem cells of the mouse trachea and human airway epithelium. Proc. Natl. Acad. Sci. U. S. A. *106*, 12771–12775.

Rodriguez, M., Aladowicz, E., Lanfrancone, L., and Goding, C. R. (2008). Tbx3 represses E-cadherin expression and enhances melanoma invasiveness. Cancer Res. *68*, 7872–7881.

Rowley, M., Grothey, E., and Couch, F. J. (2004). The Role of Tbx2 and Tbx3 in Mammary Development and Tumorigenesis. J. Mammary Gland Biol. Neoplasia *9*, 109–118.

Roymans, D., and Slegers, H. (2001). Phosphatidylinositol 3-kinases in tumor progression. Eur. J. Biochem. *268*, 487–498.

Sakabe, M., Kokubo, H., Nakajima, Y., and Saga, Y. (2012). Ectopic retinoic acid signaling affects outflow tract cushion development through suppression of the myocardial Tbx2-Tgfβ2 pathway. Development *139*, 385–395.

Saltzman, A., Munro, R., Searfoss, G., Franks, C., Jaye, M., and Ivashchenko, Y. (1998). Transforming growth factor-beta-mediated apoptosis in the Ramos B-lymphoma cell line is accompanied by caspase activation and Bcl-XL downregulation. Exp. Cell Res. *242*, 244–254.

Sasaki, G., Ogata, T., Ishii, T., Hasegawa, T., Sato, S., and Matsuo, N. (2002). Novel mutation of TBX3 in a Japanese family with ulnar-mammary syndrome: implication for impaired sex development. Am. J. Med. Genet. *110*, 365–369.

Satterwhite, D. J., Aakre, M. E., Gorska, A. E., and Moses, H. L. (1994). Inhibition of cell growth by TGF beta 1 is associated with inhibition of B-myb and cyclin A in both BALB/MK and Mv1Lu cells. Cell Growth Differ. *5*, 789–799.

Sawada, K. *et al.* (2008). Loss of E-cadherin promotes ovarian cancer metastasis via alpha 5-integrin, which is a therapeutic target. Cancer Res. *68*, 2329–2339.

Schier, A. F. (2009). Nodal morphogens. Cold Spring Harb. Perspect. Biol. *1*, a003459.

Schiffer, M., Bitzer, M., Roberts, I. S., Kopp, J. B., ten Dijke, P., Mundel, P., and Böttinger, E. P. (2001). Apoptosis in podocytes induced by TGF-beta and Smad7. J. Clin. Invest. *108*, 807–816.

Schulte-Merker, S., Ho, R. K., Herrmann, B. G., and Nüsslein-Volhard, C. (1992). The protein product of the zebrafish homologue of the mouse T gene is expressed in nuclei of the germ ring and the notochord of the early embryo. Development *116*, 1021–1032.

Seoane, J., Le, H.-V., Shen, L., Anderson, S. a, and Massagué, J. (2004). Integration of Smad and forkhead pathways in the control of neuroepithelial and glioblastoma cell proliferation. Cell *117*, 211–223.

Seoane, J., Pouponnot, C., Staller, P., Schader, M., Eilers, M., and Massagué, J. (2001). TGFbeta influences Myc, Miz-1 and Smad to control the CDK inhibitor p15INK4b. Nat. Cell Biol. *3*, 400–408.

Sgambato, A., Doki, Y., Schieren, I., and Weinstein, I. B. (1997). Effects of cyclin E overexpression on cell growth and response to transforming growth factor beta depend on cell context and p27Kip1 expression. Cell Growth Differ. *8*, 393–405.

Shi, Y., Wang, Y. F., Jayaraman, L., Yang, H., Massagué, J., and Pavletich, N. P. (1998). Crystal structure of a Smad MH1 domain bound to DNA: insights on DNA binding in TGF-beta signaling. Cell *94*, 585–594.

Showell, C., Binder, O., and Conlon, F. L. (2006). NIH Public Access. *229*, 201–218.

Sinclair, C. S. *et al.* (2002). TBX2 is preferentially amplified in BRCA1- and BRCA2-related breast tumors. Cancer Res. *62*, 3587–3591.

Singh, R. *et al.* (2012). Tbx2 and Tbx3 induce atrioventricular myocardial development and endocardial cushion formation. Cell. Mol. Life Sci. *69*, 1377–1389.

Sinha, S., Abraham, S., Gronostajski, R. M., and Campbell, C. E. (2000). Differential DNA binding and transcription modulation by three. *258*, 15–29.

Smith, J. C., Price, B. M., Green, J. B., Weigel, D., and Herrmann, B. G. (1991). Expression of a Xenopus homolog of Brachyury (T) is an immediate-early response to mesoderm induction. Cell *67*, 79–87.

Smith, J., Mowla, S., and Prince, S. (2011). Basal transcription of the human TBX3 gene , a key developmental regulator which is overexpressed in several cancers , requires functional NF-Y and Sp1 sites. Gene *486*, 41–46.

Soutourina, J., Wydau, S., Ambroise, Y., Boschiero, C., and Werner, M. (2011). Direct interaction of RNA polymerase II and mediator required for transcription in vivo. Science *331*, 1451–1454.

Staller, P. *et al.* (2001). Repression of p15INK4b expression by Myc through association with Miz-1. Nat. Cell Biol. *3*, 392–399.

Stennard, F. A. *et al.* (2005). Murine T-box transcription factor Tbx20 acts as a repressor during heart development, and is essential for adult heart integrity, function and adaptation. Development *132*, 2451–2462.

Stephens, P. J. *et al.* (2012). The landscape of cancer genes and mutational processes in breast cancer. Nature *486*, 400–404.

Stoicov, C., Fan, X., Liu, J. H., Bowen, G., Whary, M., Kurt-Jones, E., and Houghton, J. (2009). T-bet knockout prevents Helicobacter felis-induced gastric cancer. J. Immunol. *183*, 642–649.

Stott, D., Kispert, a, and Herrmann, B. G. (1993). Rescue of the tail defect of Brachyury mice. Genes Dev. *7*, 197–203.

Stroschein, S. L. (1999). Negative Feedback Regulation of TGF- Signaling by the SnoN Oncoprotein. Science (80-.). *286*, 771–774.

Sulzer, M. A., Leers, M. P., van Noord, J. A., Bollen, E. C., and Theunissen, P. H. (1998). Reduced E-cadherin expression is associated with increased lymph node metastasis and unfavorable prognosis in non-small cell lung cancer. Am. J. Respir. Crit. Care Med. *157*, 1319–1323.

Sun, Y., Liu, X., Eaton, E. N., Lane, W. S., Lodish, H. F., and Weinberg, R. A. (1999). Interaction of the Ski oncoprotein with Smad3 regulates TGF-beta signaling. Mol. Cell *4*, 499–509.

Surani, A., and Tischler, J. (2012). Stem cells: a sporadic super state. Nature *487*, 43–45.

Tada, M., and Smith, J. C. (2001). T-targets : Clues to understanding the functions of T-box proteins. 1–11.

Takabatake, Y., Takabatake, T., Sasagawa, S., and Takeshima, K. (2002). Conserved expression control and shared activity between cognate T-box genes Tbx2 and Tbx3 in connection with Sonic hedgehog signaling during Xenopus eye development. Dev. Growth Differ. *44*, 257–271.

Takanami, I., Tanaka, F., Hashizume, T., and Kodaira, S. (1997). Roles of the transforming growth factor beta 1 and its type I and II receptors in the development of a pulmonary adenocarcinoma: results of an immunohistochemical study. J. Surg. Oncol. *64*, 262–267.

Talbot, L. J., Bhattacharya, S. D., and Kuo, P. C. (2012). Epithelial-mesenchymal transition, the tumor microenvironment, and metastatic behavior of epithelial malignancies. Int. J. Biochem. Mol. Biol. *3*, 117–136.

Tan, E.-J., Thuault, S., Caja, L., Carletti, T., Heldin, C.-H., and Moustakas, A. (2012). Regulation of transcription factor Twist expression by the DNA architectural protein high mobility group A2 during epithelial-to-mesenchymal transition. J. Biol. Chem. *287*, 7134–7145.

Tang, X.-H., and Gudas, L. J. (2011). Retinoids, retinoic acid receptors, and cancer. Annu. Rev. Pathol. *6*, 345–364.

Teng, H., Ballim, R. D., Mowla, S., and Prince, S. (2009). Phosphorylation of Histone H3 by Protein Kinase C Signaling Plays a Critical Role in the Regulation of the Developmentally Important TBX2 Gene *. J. Biol. Chem. *284*, 26368–26376.

Teng, H., Parker, M. I., and Prince, S. (2008). Functional characterization of cis-acting elements involved in basal transcription of the human Tbx2 gene: a new insight into the role of Sp1 in transcriptional regulation. Gene *423*, 8–13.

Tesar, P. J., Chenoweth, J. G., Brook, F. A., Davies, T. J., Evans, E. P., Mack, D. L., Gardner, R. L., and McKay, R. D. G. (2007). New cell lines from mouse epiblast share defining features with human embryonic stem cells. Nature *448*, 196–199.

Tfayli, A., Temraz, S., Abou Mrad, R., and Shamseddine, A. (2010). Breast cancer in low- and middle-income countries: an emerging and challenging epidemic. J. Oncol. *2010*, 490631.

Thiagalingam, S. *et al.* (1996). Evaluation of candidate tumour suppressor genes on chromosome 18 in colorectal cancers. Nat. Genet. *13*, 343–346.

Thiery, J. P. (2002). Epithelial-mesenchymal transitions in tumour progression. Nat. Rev. Cancer *2*, 442–454.

Thiery, J. P., Acloque, H., Huang, R. Y. J., and Nieto, M. A. (2009). Epithelial-mesenchymal transitions in development and disease. Cell *139*, 871–890.

Thorgeirsson, S. S., and Grisham, J. W. (2002). Molecular pathogenesis of human hepatocellular carcinoma. Nat. Genet. *31*, 339–346.

Thuault, S., Tan, E.-J., Peinado, H., Cano, A., Heldin, C.-H., and Moustakas, A. (2008). HMGA2 and Smads co-regulate SNAIL1 expression during induction of epithelial-to-mesenchymal transition. J. Biol. Chem. *283*, 33437–33446.

Thuault, S., Valcourt, U., Petersen, M., Manfioletti, G., Heldin, C.-H., and Moustakas, A. (2006). Transforming growth factor-beta employs HMGA2 to elicit epithelial-mesenchymal transition. J. Cell Biol. *174*, 175–183.

Thun, M. J., DeLancey, J. O., Center, M. M., Jemal, A., and Ward, E. M. (2010). The global burden of cancer: priorities for prevention. Carcinogenesis *31*, 100–110.

Tótth, A., Sebestyén, A., Barna, G., Nagy, K., Göndör, A., Bocsi, J., Mihalik, R., Peták, I., Houghton, J., and Kopper, L. (2001). TGF beta 1 induces caspase-dependent but death-receptor independent apoptosis in lymphoid cells. Anticancer Res. *21*, 1207–1212.

Trempus, C. S. *et al.* (2011). A novel role for the T-box transcription factor Tbx1 as a negative regulator of tumor cell growth in mice. Mol. Carcinog. *50*, 981–991.

Valderrama-Carvajal, H., Cocolakis, E., Lacerte, A., Lee, E.-H., Krystal, G., Ali, S., and Lebrun, J.-J. (2002). Activin/TGF-beta induce apoptosis through Smad-dependent expression of the lipid phosphatase SHIP. Nat. Cell Biol. *4*, 963–969.

Vance, K. W., Carreira, S., Brosch, G., and Goding, C. R. (2005). Tbx2 is overexpressed and plays an important role in maintaining proliferation and suppression of senescence in melanomas. Cancer Res. *65*, 2260–2268.

Veltmaat, J. M. *et al.* (2006). Gli3-mediated somitic Fgf10 expression gradients are required for the induction and patterning of mammary epithelium along the embryonic axes. *2335*, 2325–2335.

Veltmaat, J. M., Veelen, W. Van, Thiery, J. P., and Bellusci, S. (2004). Identification of the Mammary Line in Mouse by Wnt10b Expression. 349–356.

Verrecchia, F., Vindevoghel, L., Lechleider, R. J., Uitto, J., Roberts, a B., and Mauviel, a (2001). Smad3/AP-1 interactions control transcriptional responses to TGF-beta in a promoter-specific manner. Oncogene *20*, 3332–3340.

Vincent, T. *et al.* (2009). A SNAIL1-SMAD3/4 transcriptional repressor complex promotes TGF-beta mediated epithelial-mesenchymal transition. Nat. Cell Biol. *11*, 943–950.

Wang, B., Lindley, L. E., Fernandez-vega, V., Rieger, M. E., Sims, A. H., and Briegel, K. J. (2012). The T box transcription factor TBX2 promotes epithelial-mesenchymal transition and invasion of normal and malignant breast epithelial cells. PLoS One *7*, e41355.

Wang, C., and Youle, R. J. (2009). The Role of Mitochondria in Apoptosis*. Annu. Rev. Genet. *43*, 95–118.

Wang, D., Long, J., Dai, F., Liang, M., Feng, X.-H., and Lin, X. (2008a). BCL6 represses Smad signaling in transforming growth factor-beta resistance. Cancer Res. *68*, 783–789.

Wang, J. *et al.* (2013). Tbx3 and Nr5α2 play important roles in pig pluripotent stem cells. Stem Cell Rev. *9*, 700–708.

Wang, Y., Lamba, P., Bonomi, M., Persani, L., Roberson, M. S., Bernard, D. J., and Fortin, J. (2008b). Activator protein-1 and smad proteins synergistically regulate human follicle-stimulating hormone beta-promoter activity. Endocrinology *149*, 5577–5591.

Wansleben, S., Davis, E., Peres, J., and Prince, S. (2013). A novel role for the anti-senescence factor TBX2 in DNA repair and cisplatin resistance. Cell Death Dis. *4*, e846.

Weeks, B. H., He, W., Olson, K. L., and Wang, X. J. (2001). Inducible expression of transforming growth factor beta1 in papillomas causes rapid metastasis. Cancer Res. *61*, 7435–7443.

Weidgang, C. E. *et al.* (2013). TBX3 Directs Cell-Fate Decision toward Mesendoderm. Stem Cell Reports *1*, 248–265.

Weiss, A., and Attisano, L. (2012). The TGFbeta Superfamily signaling pathway 2012.pdf.

De Wever, O., Westbroek, W., Verloes, A., Bloemen, N., Bracke, M., Gespach, C., Bruyneel, E., and Mareel, M. (2004). Critical role of N-cadherin in myofibroblast

invasion and migration in vitro stimulated by colon-cancer-cell-derived TGF-beta or wounding. J. Cell Sci. *117*, 4691–4703.

Wildey, G. M., Patil, S., and Howe, P. H. (2003). Smad3 potentiates transforming growth factor beta (TGFbeta)-induced apoptosis and expression of the BH3-only protein Bim in WEHI 231 B lymphocytes. J. Biol. Chem. *278*, 18069–18077.

Wilson, V., and Conlon, F. L. (2002). The T -box family. 1–7.

Wilson, V., Manson, L., Skarnes, W., and Beddington, R. (1995). The T gene is necessary for normal mesodermal morphogenetic cell movements during gastrulation. Development *121*, 877–886.

Wilson, V., Rashbass, P., and Beddington, R. (1993). Chimeric analysis of T (Brachyury) gene function. Development *117*, 1321–1331.

Wolfraim, L. A. *et al.* (2004). Loss of Smad3 in acute T-cell lymphoblastic leukemia. N. Engl. J. Med. *351*, 552–559.

Wollnik, B., Kayserili, H., Uyguner, O., Tukel, T., and Yuksel-Apak, M. (2002). Haploinsufficiency of TBX3 causes ulnar-mammary syndrome in a large Turkish family. Ann. Génétique *45*, 213–217.

Wong, C., Rougier-Chapman, E. M., Frederick, J. P., Datto, M. B., Liberati, N. T., Li, J. M., Wang, X. F., and Joshua, P. (1999). Smad3-Smad4 and AP-1 complexes synergize in transcriptional activation of the c-Jun promoter by transforming growth factor beta. Mol. Cell. Biol. *19*, 1821–1830.

Wu, M. Y., and Hill, C. S. (2009). Tgf-beta superfamily signaling in embryonic development and homeostasis. Dev. Cell *16*, 329–343.

Wu, S., Cetinkaya, C., Munoz-Alonso, M. J., von der Lehr, N., Bahram, F., Beuger, V., Eilers, M., Leon, J., and Larsson, L.-G. (2003). Myc represses differentiation-induced p21CIP1 expression via Miz-1-dependent interaction with the p21 core promoter. Oncogene *22*, 351–360.

Xie, L., Law, B. K., Aakre, M. E., Edgerton, M., Shyr, Y., Bhowmick, N. A., and Moses, H. L. (2003). Transforming growth factor beta-regulated gene expression in a mouse mammary gland epithelial cell line. Breast Cancer Res. *5*, R187–98.

Yagi, K., Furuhashi, M., Aoki, H., Goto, D., Kuwano, H., Sugamura, K., Miyazono, K., and Kato, M. (2002). c-myc is a downstream target of the Smad pathway. J. Biol. Chem. *277*, 854–861.

Yamamoto, M., Fukuda, K., Miura, N., Suzuki, R., Kido, T., and Komatsu, Y. (1998). Inhibition by dexamethasone of transforming growth factor beta1-induced apoptosis in rat hepatoma cells: a possible association with Bcl-xL induction. Hepatology *27*, 959–966.

Yamamura, Y., Hua, X., Bergelson, S., and Lodish, H. F. (2000). Critical role of Smads and AP-1 complex in transforming growth factor-beta -dependent apoptosis. J. Biol. Chem. *275*, 36295–36302.

Yamashita, S., Takahashi, S., McDonell, N., Watanabe, N., Niwa, T., Hosoya, K., Tsujino, Y., Shirai, T., and Ushijima, T. (2008). Methylation silencing of transforming growth factor-beta receptor type II in rat prostate cancers. Cancer Res. *68*, 2112–2121.

Yamashita, S., Tsujino, Y., Moriguchi, K., Tatematsu, M., and Ushijima, T. (2006). Chemical genomic screening for methylation-silenced genes in gastric cancer cell lines using 5-aza-2'-deoxycytidine treatment and oligonucleotide microarray. Cancer Sci. *97*, 64–71.

Yanagisawa, K. O. (1990). Does the T gene determine the anteroposterior axis of a mouse embryo? Jpn. J. Genet. *65*, 287–297.

Yarosh, W., Barrientos, T., Esmailpour, T., Lin, L., Carpenter, P. M., Osann, K., Anton-culver, H., and Huang, T. (2008). TBX3 is overexpressed in breast cancer and represses p14 ARF by interacting with histone deacetylases. Cancer Res. *68*, 693–699.

Yasuo, H., and Satoh, N. (1993). Function of vertebrate T gene. Nature *364*, 582–583.

Yasuo, H., and Satoh, N. (1994). An Ascidian Homolog of the Mouse Brachyury (T) Gene is Expressed Exclusively in Notochord Cells at the Fate Restricted Stage. (Ascidians/T (Brachyury) gene/sequence conservation/notochord cells/transient expression). Dev. Growth Differ. *36*, 9–18.

Yin, X., Wolford, C. C., Chang, Y.-S., McConoughey, S. J., Ramsey, S. A., Aderem, A., and Hai, T. (2010). ATF3, an adaptive-response gene, enhances TGF{beta} signaling and cancer-initiating cell features in breast cancer cells. J. Cell Sci. *123*, 3558–3565.

Yoo, J., Ghiassi, M., Jirmanova, L., Balliet, A. G., Hoffman, B., Fornace, A. J., Liebermann, D. A., Bottinger, E. P., and Roberts, A. B. (2003). Transforming growth factor-beta-induced apoptosis is mediated by Smad-dependent expression of GADD45b through p38 activation. J. Biol. Chem. *278*, 43001–43007.

Yoo, Y. D., Choi, J. Y., Lee, S. J., Kim, J. S., Min, B. R., Lee, Y. I., and Kang, Y. K. (1999). TGF-beta-induced cell-cycle arrest through the p21(WAF1/CIP1)-G1 cyclin/Cdks-p130 pathway in gastric-carcinoma cells. Int. J. Cancer *83*, 512–517.

Yu, J. *et al.* (2010). Epigenetic inactivation of T-box transcription factor 5, a novel tumor suppressor gene, is associated with colon cancer. Oncogene *29*, 6464–6474.

Zakin, L., and De Robertis, E. M. (2010). Extracellular regulation of BMP signaling. Curr. Biol. *20*, R89–92.

Zhang, J., He, M., Qi Dong, Xie, W., Chen, Y., Lin, M. C. M., Leung, P., Zhang, Y., and Kung, H. (2011). Aqueous extracts of Fructus Ligustri Lucidi enhance the sensitivity of human colorectal carcinoma DLD-1 cells to doxorubicin-induced apoptosis via Tbx3 suppression. Integr. Cancer Ther. *10*, 85–91.

Zhang, L.-H., Li, Q., Li, P., Zhu, S.-T., Wang, J., Yang, H.-L., Xu, C.-Q., and Guo, X.-H. (2012). Association between gastric cancer and -1993 polymorphism of TBX21 gene. World J. Gastroenterol. *18*, 1117–1122.

Zhang, Y., Feng, X. H., and Derynck, R. (1998). Smad3 and Smad4 cooperate with c-Jun/c-Fos to mediate TGF-beta-induced transcription. Nature *394*, 909–913.

Zhao, D., Wu, Y., and Chen, K. (2014). Tbx3 isoforms are involved in pluripotency maintaining through distinct regulation of Nanog transcriptional activity. Biochem. Biophys. Res. Commun. *444*, 411–414.

Zhu, Y., Ju, S., Chen, E., Dai, S., Li, C., Morel, P., Liu, L., Zhang, X., and Lu, B. (2010). T-bet and eomesodermin are required for T cell-mediated antitumor immune responses. J. Immunol. *185*, 3174–3183.

Zong, M., Meng, M., and Li, L. (2011). Low Expression of TBX4 Predicts Poor Prognosis in Patients with Stage II Pancreatic Ductal Adenocarcinoma. Int. J. Mol. Sci. *12*, 4953–4963.

CHAPTER 6

APPENDIX

6.1 Luria Broth (LB)

10g Bacto-tryptone
5g Bacto-yeast
10g NaCl
pH 7

6.2 Mycoplasma Test

Mounting fluid

20 mM Citric acid
55 mM $Na_2HPO_4.2H_2O$
50% Glycerol
pH to 5.5 and store at 4°C

6.3 Vector map of pTIG

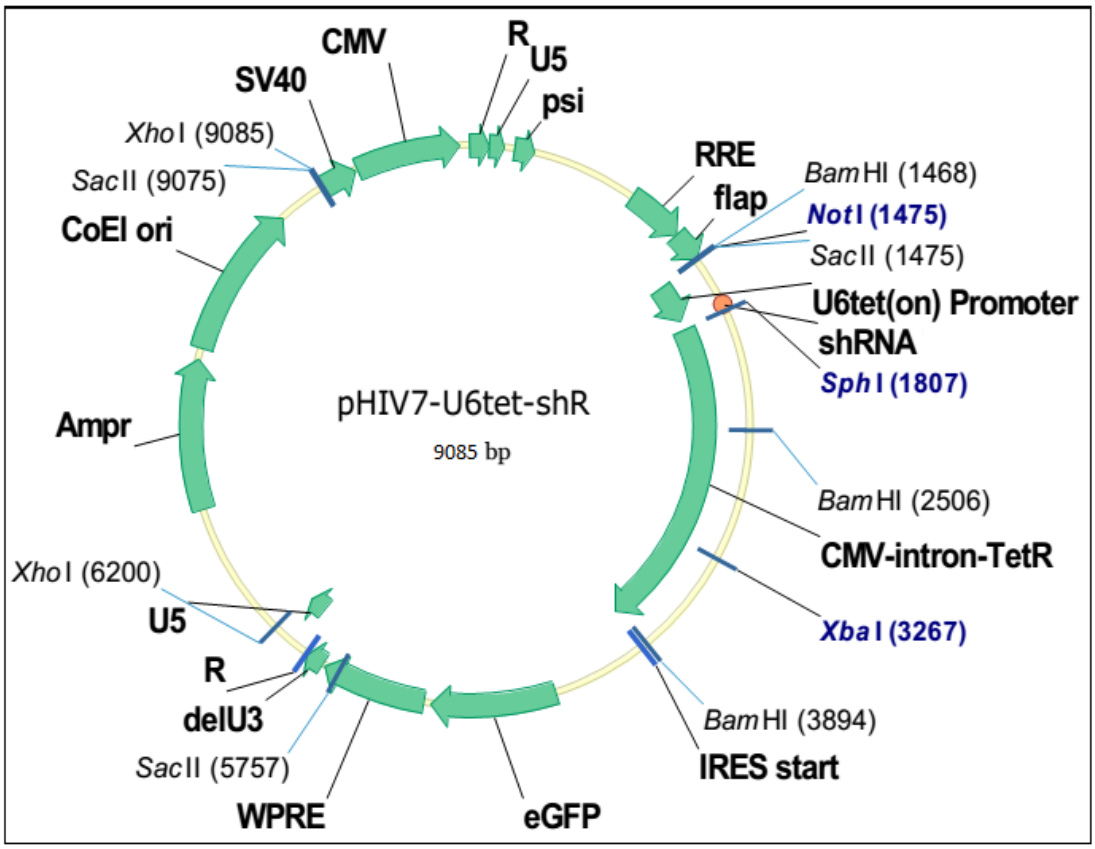

Figure 6.1 Vector map for pTIG-shRNA.

6.4 Stable TBX3 knockdown using a lentiviral delivery system

HBS2X

280 mM NaCl
100 mM Hepes
1.5 mM Na_2HPO_4 (pH between 7.11 - 7.13)
Filter sterilise and store at -20^{o}C

6.5 Western Blot analysis

RIPA

150 mM NaCl
1% Triton X-100
0.1% SDS
20 mM Tris (pH 7.5)
1% deoxycholate
Protease inhibitors added prior to harvesting: 1X complete protease inhibitor tablets (Roche, Germany), aprotinin (1 μg/ml), pepstatin (1 μg/ml), phenylmethanesulphonyl fluoride (PMSF) (0.5 mM)

Sodium Dodecyl Sulphate (SDS)-polyacrylamide gels

Resolving gel:

Acryl-bisacryl-amide mix (30:08) (percentage depending on size of protein of interest)
0.375 M Tris (pH 8.8)
0.1% SDS
0.1% TEMED
0.1% Ammonium persulphate

Stacking gel:

5% Acryl-bisacryl-amide mix (30:08)
0.192 M Tris (pH6.8)
0.1% SDS
0.1% TEMED
0.1% Ammonium persulphate

Acryl-bisacryl-amide mix (30:08):

29 g acrylamide
1 g N,N`-methylenebisacrylamide
Make up to 100 ml, heating at 37°C to dissolve chemicals. Store at 4°C, protected from light

Running buffer:

1 g SDS
3.03 g Tris
14.41 g Glycine
Make up to 1 litre

Transfer buffer:
2.9 g Glycine
5.8 g Tris
0.37 g SDS
200 ml isopropanol
Make up to 1 litere and store at 4°C.

Phosphate buffered saline (PBS)/Tween
10X PBS:
8 g NaCl
1.45 g $Na_2HPO_4.12H_2O$
0.2 g KCl
0.2 g KH_2PO_4
Make up to 1 litre, pH to 7.4

PBS/Tween:
For membrane washes, add 0.1% Tween to 1X PBS

Stripping buffer
62.5 mM Tris-HCl (pH6.7)
2% SDS
100 mM β-mercaptoethanol

6.6 Assessment of proliferation/senescence
5-bromo-2-deoxyuridine (BrdU) incorporation assay
Carnoy's Fixative
1 : 3 acetic acid : methanol

Borate buffer (0.1 M)
3.8 g sodium borate (borax)
Make up to 100 ml, pH to 8.5

Senescence Associated beta-Galactosidase assay
Staining solution
5 mM potassium ferrocyanide
5 mM potassium ferricyanide
2 mM Mg_2Cl_2
1 mg/ml x-gal
PBS pH 6

6.7 Chromatin immunoprecipitation (ChIP) assay
Buffer 1
10 mM EDTA
0.5 mM EGTA

10 mM Hepes,
0.25% Triton X-100

Buffer 2
1 mM EDTA
0.5 mM EGTA
10 mM Hepes
200 mM NaCl

Lysis buffer
10 mM EDTA
50 mM Tris-Cl pH 8.1
0.5% Nonidet P-40
1% SDS

Immunoprecipitation Buffer
2 mM EDTA
150 mM NaCl
20 mM Tris-Cl pH 8.1
1% Triton X-100

Wash buffer 1
2 mM EDTA
20 mM Tris-Cl pH 8.1
0.1% SDS
1% Triton X-100
150 mM NaCl

Wash buffer 2
2 mM EDTA
20 mM Tris-Cl pH 8.1
0.1% SDS
1% Triton X-100
500 mM NaCl

Wash buffer 3
1 mM EDTA
10 mM Tris-Cl pH 8.1
250 mM LiCl
1% sodium deoxycholate
1% Nonidet P-40

Wash buffer 4
1 mM EDTA

10 mM Tris-Cl pH 8.1

Extraction buffer
100 mM $NaHCO_3$
1% SDS

6.8 Non-radioactive Electromobility Shift Assay

Buffer 1
10mM Tris pH7.5
10mM NaCl
2mM $MgCl_2$

Buffer 2
20mM HEPES pH 7.9
420mM NaCl
1.5mM MgCl2
0.2mM EDTA pH8
25% glycerol

5x Incubation Buffer
100 mM HEPES pH 7.9
250 mM KCl
2.5 mM DTT
10 mM EDTA
5 mM $MgCl_2$
20% Ficoll 400

6.9 DNA affinity immunoblot (DAI) assay

Binding buffer
20 mM Tris-HCl pH 7.6
50 mM NaCl
1 mM $MgCl_2$
0.2 mM EDTA
0.5 mM dithiothreitol
5% glycerol
10 ng/µl poly(dI-dC))

Protein loading buffer
125 mM Tris-HCl, pH 6.5
0.4% SDS
10% β-mercaptoethanol
20% glycerol

6.10Flow Cytometry

Propidium Iodide solution

2 mM $MgCl_2$

10 mM Pipes buffer

0.1 M NaCl

0.1% Triton X-100

0.01 mg/ml Propidium iodide